TECHNISCHE UNIVERSITÄT WIEN
Vienna University of Technology

D I P L O M A R B E I T

Sleepstageing with heart rate variability

Thema

Ausgeführt am Institut für

E354 – Institute of Electrodynamics, Microwave and Circuit Engineering

der Technischen Universität Wien

unter der Anleitung von Ao. Univ. Prof. Dipl.-Ing. Dr. techn. Eugenijus Kaniusas

durch

Carsten Stastny
Name

Dorfmeistergasse 47, 1120 Wien
Anschrift

Datum

Unterschrift (Student)

Table of Contents

Abbreviations

AF	Atrial fibrillation
AMI	Acute myocardial infaction
ANS	Autonomic nervous system
ApEn	Approximate entropy
ASCII	American Standard Code for Information Interchange
AV	Atrioventricular
bpm	Beats per minute
CAD	Coronary artery disease
CAN	Cardiac autonomic neuropathy
Ca^{2+}	Calcium
CBT	Cognitive behavior therapy
CCM	Complex correlation measure
CHD	Coronary heart disease
CHF	Congestive heart failure
DCM	Dilated cardiomypathy
DFA	Detrended fluctuation analysis
ECG	Electrocardiography, Electrocardiogram
EDF	European Data Format
EEG	Electroencephalography
EMG	Electromyography
EOG	Electrooculography
f	Frequency
$f^{\mathrm{t}}_{\mathrm{Winv,rel}}$	$f^{\mathrm{t}}_{\mathrm{Winv}}$ in relative units
$f_{\max}$	Upper bound of the relevant frequency
$f_{\min}$	Lower bound of the relevant frequency
f_{W}	Spectrum weighted frequencies
$f^{\mathrm{h}}_{\mathrm{W}}$	Spectrum weighted frequencies of humoral spectrum of HRV
$f^{\mathrm{t}}_{\mathrm{Winv}}$	Inversion of $f^{\mathrm{t}}_{\mathrm{W}}$
$f^{\mathrm{p}}_{\mathrm{W}}$	Spectrum weighted frequencies of parasympathetic spectrum of HRV
$f^{\mathrm{s}}_{\mathrm{W}}$	Spectrum weighted frequencies of sympathetic spectrum of HRV
$f^{\mathrm{t}}_{\mathrm{W}}$	Spectrum weighted frequencies of total spectrum of HRV
fir1	Finite impulse response filter design
FM	Fibromyalgia
HF	High frequency
HR	Heart rate
HRV	Heart rate variability
Hz	Hertz
K^+	Potassium
LE	Lyapunov exponent
LF	Low frequency
LLE	Largest lyapunov exponent
LVE	Left ventricular enlargement
MI	Myocardial infarction
MOD	Method of delays
ms	Milliseconds

mV	Millivolt
MSE	Multiscale entropy
N	Filter order
Na^+	Sodium
OSA	Obstructive sleep apnea
PSD, p	Power spectral density
PSG	Polysomnography
PSP	Parasympathetic
r	Cross-correlation coefficient
RA	Rheumatoid arthritis
RBD	REM sleep behavior disorder
REM	Rapid eye movement
RF	Renal failure
RMSE	Refined multiscale entropy
RMSSD	Root mean square of successive beat to beat differences
R-peak	R-peak of the QRS complex of an ECG
RR-interval	Interval between two R-peaks of ECG
S1	Sleep stage NREM-1
S2	Sleep stage NREM-2
S3	Sleep stage NREM-3
S4	Sleep stage NREM-4
SA	Sinoatrial
SampEn	Sample entropy
SD1	Short-term heart rate variability
SD2	Long-term heard rate variability
SDLE	Scale dependent lyapunov exponent
SDNN,SDRR	Standard deviation of the RR intervals
SDSD	Standard deviation of successive differences
SICU	Surgical intensive care unit
SP	Sympathetic
TINN	Triangular interpolation of RR-interval histogram
Var	Variance
VLF	Very low frequency
Wn	Cut-off frequency
µV	Microvolt

Acknowledgements

I would like to express my deepest gratitude to Prof. Eugenijus Kaniusas for his patience, excellent guidance, full support and expertise. There are a lot of things in the fields of scientific work and scientific writing which I would not have known without him. Because of his dedication to his scientific work and to his students I could not have wished for a better advisor and mentor. Without him this thesis would not have been possible.

This thesis was part of a project supported by the company Heartbalance. Therefore I am very thankful to MMag. Peter Hauschild, CEO of Heartbalance, for giving me the opportunity to do scientific research on this very interesting topic.

I would like to especially thank my parents Friedrich Stastny and Ursula Golubich for always believing in me, for their support and their continuous encouragement throughout this thesis and my whole studies. My parents were always there for me, no matter how hard it was or how long it took and I could always count on them.

Last but not least I would like to thank my friends and my girlfriend for giving me the time it took to write my thesis and for supporting me. Everybody was very understanding when I did not have that much time for them throughout the last year and that really helped me a lot.

Abstract

Sleep is an important topic in the lives of human beings because it is necessary for survival. Other than its general known function of revitalizing the human body sleep can also be associated with various pathologic conditions. Therefore sleep has been subject of studies for many of years. It can be analyzed using Polysomnography (PSG). In PSG multiple instruments (including electroencephalography, electromyography, electrooculography and electrocardiography (ECG)) are required to record various biosignals in order to identify and analyze different sleep phases and sleep stages. Additionally the recorded signals have to be assessed visually by an expert. It is desirable to reduce the amount of instrumentation required for the analysis of sleep quality. During sleep the autonomous nervous system (ANS) regulates various bodily functions. Besides for example respiration, digestion, vasomotor activity and reflex actions the ANS also effects cardiac regulation. There is close relation between autonomic control of heart rate and the central nervous system, especially during sleep when ambient factors do not dominate [1].

The variation in time intervals of consecutive heart beats is called heart rate variability (HRV) and reflects the activity of the ANS. Therefore it might be possible to analyze sleep quality using HRV. Our objective was to assess a new method to identify sleep stages by using HRV in order to evaluate sleep without the use of multiple devices required by traditional PSG. There are various linear and nonlinear methods to analyze HRV. Each method has its advantages, disadvantages and limitations.

We used spectrum weighted mean frequencies of the total HRV spectrum ($f_{\mathrm{W}}^{\mathrm{t}}$) of the power spectral density (PSD) to identify different sleep stages and assessed how they correlate to somnograms recorded by multiple devices of PSG. The correlation was analyzed by calculating corresponding cross correlation coefficients. For our analysis we acquired 22 datasets of raw ECG signals from a sleep laboratory and their somnograms recorded by conventional PSG. Because of baseline drift and noise, preprocessing of the ECG signals was necessary in order to ensure a good R-peak detection. Because of their effect on PSD, outliers originating from ectopic beats and falsely identified R-peaks had to be corrected. We used different options (Removal of sleep stages of short periods of time, combination of sleep stages, different inversion methods and different filter options) to analyze and improve calculated cross correlation coefficients.

Our results showed that some somnograms, especially those from healthy subjects, had a high correlation with our HRV based sleep estimation. Semi-periodic somnograms provide better results in terms of the HRV-based sleep prediction than fragmented somnograms. The combination of sleep stages (Wake + Rapid eye Movement, S1 + S2, S3 + S4) seems to improve the HRV-based estimation of somnograms, whereas the combination of only S3+S4 seems to weaken this estimation in most cases. The removal of sleep stages with the duration of only a few minutes does not seem to alter our results significantly. We found that the negation of the weighted mean frequency ($-f_{\mathrm{W}}^{\mathrm{t}}$) tends to yield better sleep prediction than its inversion ($1/f_{\mathrm{W}}^{\mathrm{t}}$). The preprocessing methods we used did not significantly influence our results.

We conclude that HRV can be used to assess sleep quality in many cases, especially in rather healthy somnograms. However, further research is needed to improve sleep prediction in fragmented somnograms.

Abstrakt

Schlaf ist notwendig um zu überleben und deshalb ein wichtiges Thema und Forschungsgebiet der Menschheit. Zusätzlich zur Funktion der Revitalisierung des menschlichen Körper wird Schlaf auch mit unterschiedlichen Erkrankungen in Verbindung gebracht. Unteranderem deshalb ist Schlafforschung wichtig und wird bereits seit längerem verfolgt. Die Standardmethode um Schlaf zu erforschen ist die sogenannte Polysomnographie (PSG). Bei der PSG werden mehrere Geräte (Elektroenzephalographie, Elektromyographie, Elektrookulographie und Elektrokardiographie (EKG)) dazu verwendet, verschiedene Biosignale aufzuzeichnen um unterschiedliche Schlafstadien zu identifizieren und zu analysieren. Zusätzlich müssen die Signale von einem Experten visuell ausgewertet werden. Es ist wünschenswert die Anzahl der verwendeten Geräte zu verringern um die Analyse der Qualität des Schlafes zu vereinfachen. Das autonome Nervensystem (ANS) steuert verschiedene Körperfunktionen während des Schlafes. Neben Atmung, Verdauung, vasomotorischen Aktivitäten und Reflexen beeinflusst das ANS auch unseren Herzrhythmus. Es besteht eine enge Verbindung zwischen unserem zentralen Nervensystem und der autonomen Kontrolle unserer Herzrate, vor allem während des Schlafens, wenn äußere Einflüsse minimal sind.

Die Variation der Länge der Intervalle zwischen den einzelnen Herzschlägen nennt man Herzratenvariabilität (HRV). HRV reflektiert die Aktivität des ANS und deshalb kann es möglich sein Schlafqualität mit Hilfe der HRV zu analysieren. Unser Ziel war die Anwendung und Beurteilung einer neuen Methode um Schlaf durch HRV zu evaluieren, um die Anzahl der benötigten Gerätschaften die bei der traditionellen PSG zum Einsatz kommen zu verringern. Es gibt einige lineare und nichtlineare Methoden um HRV zu analysieren. Jede einzelne Methode hat seine Stärken, Schwächen und Limits.

Für unsere Analyse verglichen wir gewichtete mittlere Frequenzen der spektralen Leistungsdichte (PSD) des gesamten HRV-Spektrums ($f_{\mathrm{W}}^{\mathrm{t}}$) mit Somnogrammen, die mit Hilfe verschiedener Geräte der PSG aufgenommen und erstellt wurden. Dazu errechneten wir die jeweiligen Kreuzkorrelationskoeffizienten. Für unsere Arbeit erhielten wir 22 EKG Datensätze und deren Somnogramme, aufgenommen mit konventioneller PSG, von einem Schlaflabor. Da die EKG-Signale verrauscht und von Basisliniendrifts durchzogen waren mussten sie zuerst vorverarbeitet werden um die verschiedenen R-Zacken des EKGs optimal detektieren zu können. Ausreißer aufgrund von Extrasystolen und falsch erkannte R-Zacken wurden manuell entfernt da sie die PSD sehr stark beeinflussen können. Um die errechneten Kreuzkorrelationskoeffizienten zu analysieren und zu verbessern, verwendeten wir verschiedene Optionen (Kurze Schlafphasen entfernen, Schlafphasen kombinieren, unterschiedliche Inversionsmethoden und unterschiedliche Filteroptionen).

Unsere Ergebnisse zeigen, dass eine hohe Korrelation zwischen manchen Somnogrammen (vor allem von gesunden Personen) und unserer HRV basierenden Schlafschätzung besteht. Semiperiodische Somnogramme korrelierten besser als fragmentierte Somnogramme. Die Kombination von Schlafphasen (Wach + Schnelle Augenbewegungen, S1 + S2, S3 + S4) verbesserte die Schlafschätzung, während die Kombination von nur S3 + S4 sie in den meisten Fällen schwächte. Die Entfernung von kurzen Schlafphasen schien unsere Resultate nicht signifikant zu beeinflussen. Wir stellten fest, dass die negation der gewichtenten mittleren Frequenz ($-f_{\mathrm{w}}^{\mathrm{t}}$) eine bessere Schlafvorhersage darstellte als ihre Inversion ($1/f_{\mathrm{W}}^{\mathrm{t}}$). Verwendete Vorverarbeitungsmethoden der EKG Signale beeinflussten unsere Ergebnisse nicht signifikant.

Wir schließen daraus, dass HRV dazu verwendet werden kann Schlafqualität in vielen Fällen, vor allem in gesunden Somnogrammen, zu beurteilen. Um Schlafvorhersage in fragmentierten Somnogrammen zu verbessern ist noch weitere Forschung notwendig.

1. Introduction

Sleep is an important topic in the lives of human beings because it is necessary for survival. Other than its general known function of revitalizing the human body sleep can also be associated with various pathologic conditions. Therefore sleep has been subject of studies for many of years. It can be analyzed using Polysomnography (PSG). In PSG multiple instruments (including electroencephalography (EEG), electromyography (EMG), electrooculography (EOG) and electrocardiography (ECG)) are required to record various biosignals in order to identify and analyze different sleep phases and sleep stages. Additionally the recorded signals have to be assessed visually by an expert. It is desirable to reduce the amount of instrumentation required for the analysis of sleep quality. During sleep the autonomous nervous system (ANS) regulates various bodily functions. Besides for example respiration, digestion, vasomotor activity and reflex actions it also effects cardiac regulation. There is close relation between autonomic control of heart rate and the central nervous system, especially during sleep when ambient factors do not dominate [1].

The variation in time intervals of consecutive heart beats is called heart rate variability (HRV) and reflects the activity of the ANS. Therefore it might be possible to analyze sleep quality using HRV. It has been suggested by Kaniusas et al. [2] that spectrum weighted mean frequencies f_W of HRV can be used to assess the sleep structure using only ECG (as a single biosignal). ECG is available from portable devices, which would facilitate an easy sleep assessment. It could be useful for people in remote areas, people who are traveling a lot (businessmen, sportsmen,…) as well as for elderly people or people with limited mobility. The resulting HRV data could be analyzed locally or remotely to get an instant assessment of the night's sleep right after waking up. It could also be useful for assessment of different kinds or different doses of sleep medication.

This thesis covers the basics of electrical biosignals, linear and nonlinear analysis methods of HRV, sleep and HRV based sleep estimation by comparing weighted mean frequencies of PSD to somnograms, recorded by conventional PSG.

1.1. Genesis of electrical biosignals

To understand how electrical biosignals are generated we have to start by looking at them at a cell basis. There are cells in the human body which can create electrical activity (pacemaker or action potentials) without any external stimulation. These cells are called pacemaker cells. Pacemaker cells maintain a rhythmic pacemaker potential instead of a constant resting membrane potential (Figure 1.1). A slow membrane depolarization occurs in these cells towards their threshold level in order to generate an action potential by opening voltage-gated channels for Na^+ (Sodium) and K^+ (Potassium) ions. The inflow of Na^+ ions predominates the outflow of K^+ ions, which leads to depolarization until the threshold is reached. As soon as the threshold is reached, voltage-gated Ca^{2+} (Calcium) channels in the membrane open, which leads to an accelerated depolarization and to the creation of an action potential. In response to the rapid depolarization, K^+ channels are opened allowing an outflow of K^+ ions and thus a repolarization of the cell membrane until the K^+ channels close again. After a certain period of hyperpolarization, the voltage gated K^+ and Na^+ channels open again and a new period of the rhythmic pacemaker potential begins.

The inflow and outflow of ions can be influenced by parasympathetic and sympathetic axons of the ANS. Parasympathetic axons can slow the rate of the diastolic depolarization by facilitating an outflow of K^+ ions of pacemaker cells while sympathetic axons can accelerate the heart rate by increasing an inflow of Ca^{2+} ions into pacemaker cells.

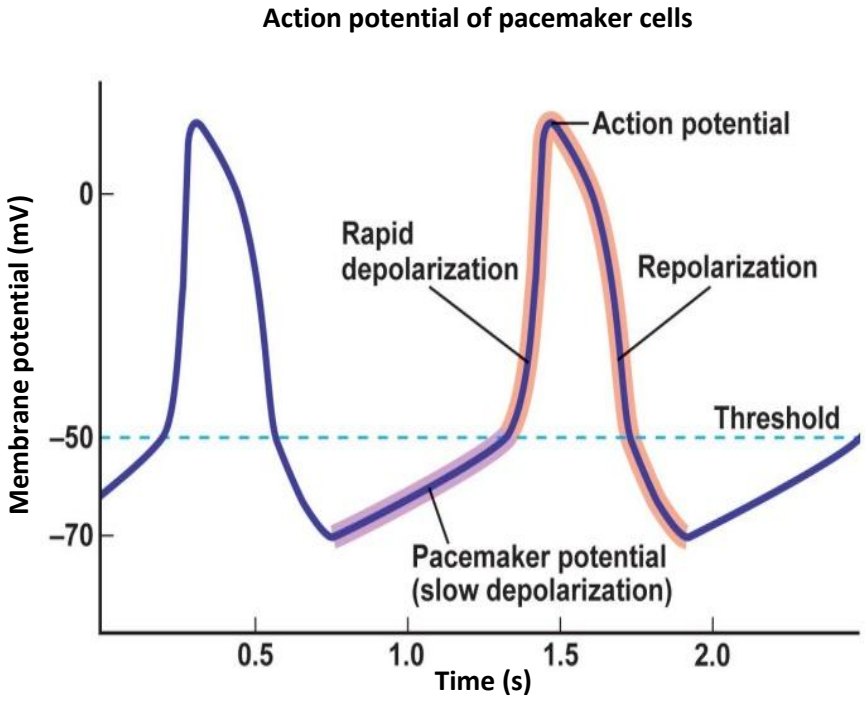

Figure 1.1: Action potential of a pacemaker cell including depolarization phases and Repolarization phases in millivolts over time in seconds. [3]

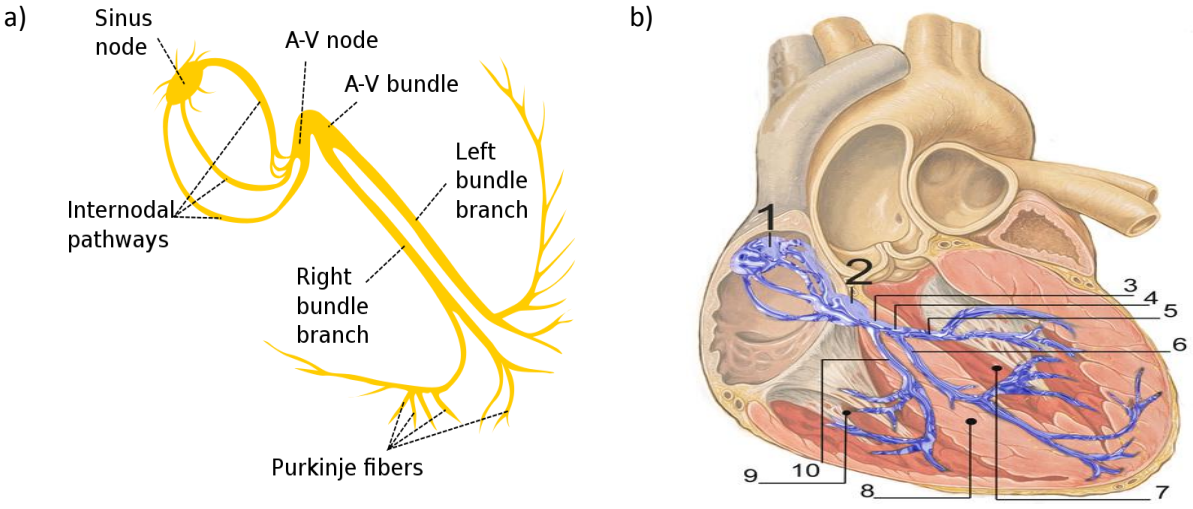

Figure 1.2: a) Schematic drawing of electrical conduction system of the heart consisting of different nodes and in internodal pathways. b) Schematic drawing of how the electrical conduction system is situated in the heart. 1. Sinoatrial node, 2. AV node,3. Bundle of His, 4. Left bundle branch, 5. Left posterior fascicle, 6. Left-anterior fascicle, 7. Left ventricle, 8. Ventricular septum, 9. Right ventricle, 10. Right bundle branch [4]

These cells are concentrated in different nodes of the human heart. Together with internodal pathways they form the electrical conduction system of the heart (Figure 1.2a-b) which is responsible for the generation and propagation of action potentials. The Sinoatrial node (SA node or Sinus node) acts as the spontaneous primary pacemaker, whereas the Atrioventricular node (AV node), the Bundle of His and the Purkinje fibers act as secondary pacemakers. The conduction system coordinates the pumping action of each of the heart's chambers so that the heart can efficiently pump blood through the pulmonary circulation loop (blood gets oxygenated) and the systemic circulation loop (oxygenated blood gets provided to the rest of the body).

The different nodes create action potentials with different firing rates which can be measured in beats per minute (bpm):

SA node	**AV node**	**Bundle of His and Purkinje fibers**
about 70 bpm	about 50 bpm	about 30 bpm

Table 1.1: Firing rates of different nodes of the heart

Besides pacemaker cells the heart also contains cardiac muscle cells or cardiomyocytes. Cardiomyocytes are short branched, elastic cells which are interconnected with each other at the end of each cell via numerous mechanical and electrical gap junctions. The potentials created and propagated by the heart's electrical conduction system then spread to cardiac muscle cells causing them to depolarize and therefore contract (Figure 1.3). The rapid depolarization happens because of an influx of Na^+ ions through voltage-gated channels in the membrane of cardiomyocytes (Phase 0). After depolarization, Na^+ channels close and additional K^+ channels open to allow the outflow of K^+ ions resulting in a slight repolarization (Phase 1). Following Phase 1, Ca^{2+} starts leaking in. The balance between the outflow of K^+ ions and the inflow of Ca^{2+} ions creates a "plateau" like phase

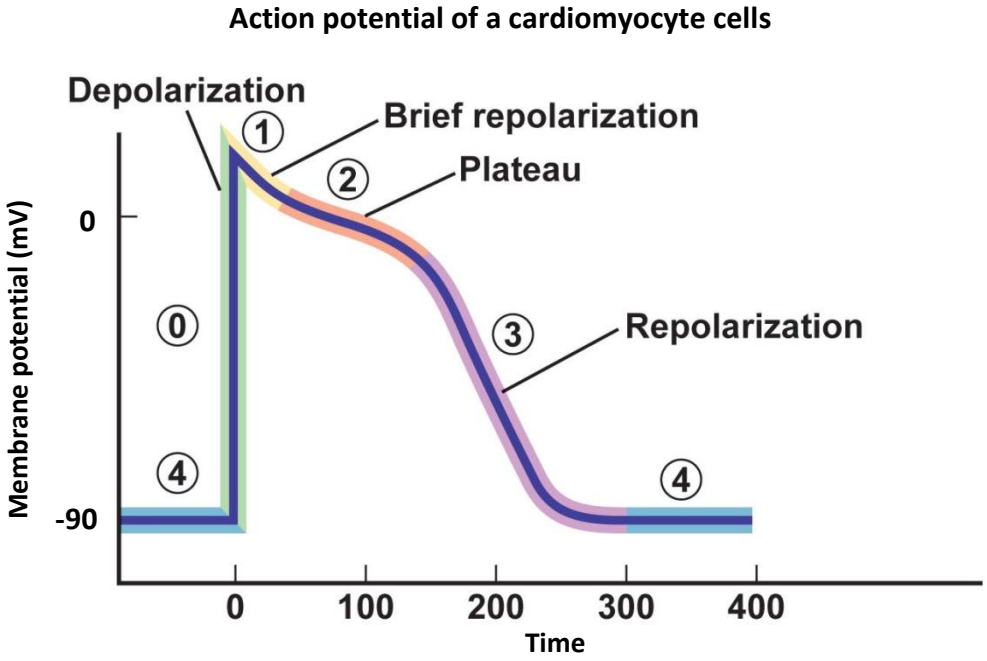

Figure 1.3: Schematic drawing of the action potential of a cardiomyocyte cell and their depolarization and repolarization phases. [3]

(Phase 2). After a certain amount of time Ca^{2+}channels close while there is still an outflow of K^{+} ions leading to a repolarization (Phase 3). The cells then have a resting membrane potential until they are stimulated again (Phase 4).

ECG can register electrical excitation of cardiac muscle. It uses electrodes attached to the surface of the skin to measure and record depolarization and repolarization of hearts muscle by detecting and amplifying small potential differences on the skin. The spread of depolarization and repolarization determines the waveform of the ECG. ECG is a non-invasive method. One way to measure electrical excitation of the heart muscle is called Einthoven derivation. One electrode is attached to the left arm, one to the right arm and one to the left leg (Figure 1.4). The depolarization of the cardiac muscle can be detected as rise and downfall of Voltage between two electrodes. The output from each pair of electrodes is known as a lead.

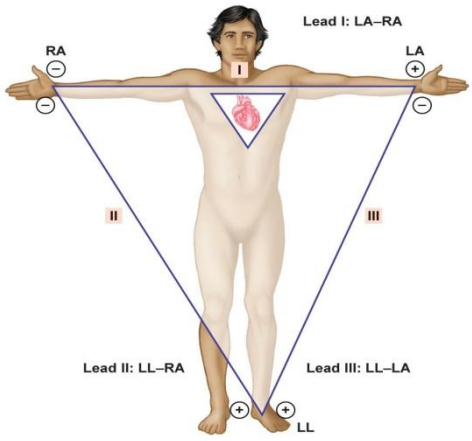

Figure 1.4: Einthoven derivation with one electrode attached to each arm and one attached to the left leg forming different leads. [3]

In a healthy heart each beat begins in the right atrium with an action potential from the SA node. The signal spreads across the right and left atria causing the muscle cells to depolarize and contract. (P-wave). After the signal leaves the Atrium it enters the ventricles through the AV node. It then propagates through the Bundle of His and down the Purkinje fibers, which causes both ventricles to contract. (QRS-complex). When the action potential leaves the ventricles the ventricular walls start to relax and repolarize (T-wave). A schematic drawing of a normal sinus rhythm of the human heart can be seen in figure 1.5.

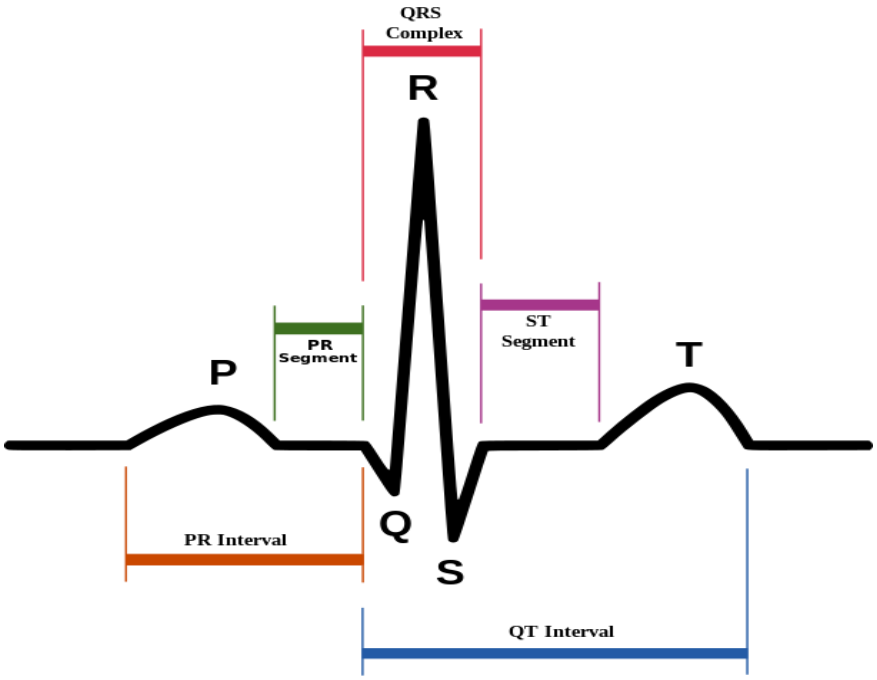

Figure 1.5: Schematic drawing of a normal Sinus rhythm of a human heart consisting of a P-wave, the QRS-complex, the T-wave and different segments between them [5]

1.2. Heart rate variability

Heart rate variability describes the variation in time intervals of consecutive heart beats. It is measured in milliseconds (ms). For practical and signal processing reasons the intervals get measured from one R-peak to the following one. The signals gained from the ECG's R-peaks (Figure 1.6a) are called RR-interval series or RR-intervals (RR) and can then be used for analysis of HRV (Figure 1.6b). The analysis of HRV has been found to be a powerful tool to identify healthy conditions [1] and particular pathological conditions. [6] [7] There are various linear and nonlinear methods to analyze HRV. It has been proposed that HRV can be better described through nonlinear analysis rather than linear analysis due to missing signal stationarity and diverse conditioning requirements. [8] The HRV signal analysis is influenced by a lot of different factors such as time and amplitude resolution of the ECG recordings, duration of the recordings, stationarity of the recording, present trends, ectopic beats, arrhythmias, and noise. [9] Therefore the method of HRV analysis and their parameters have to be chosen very carefully.

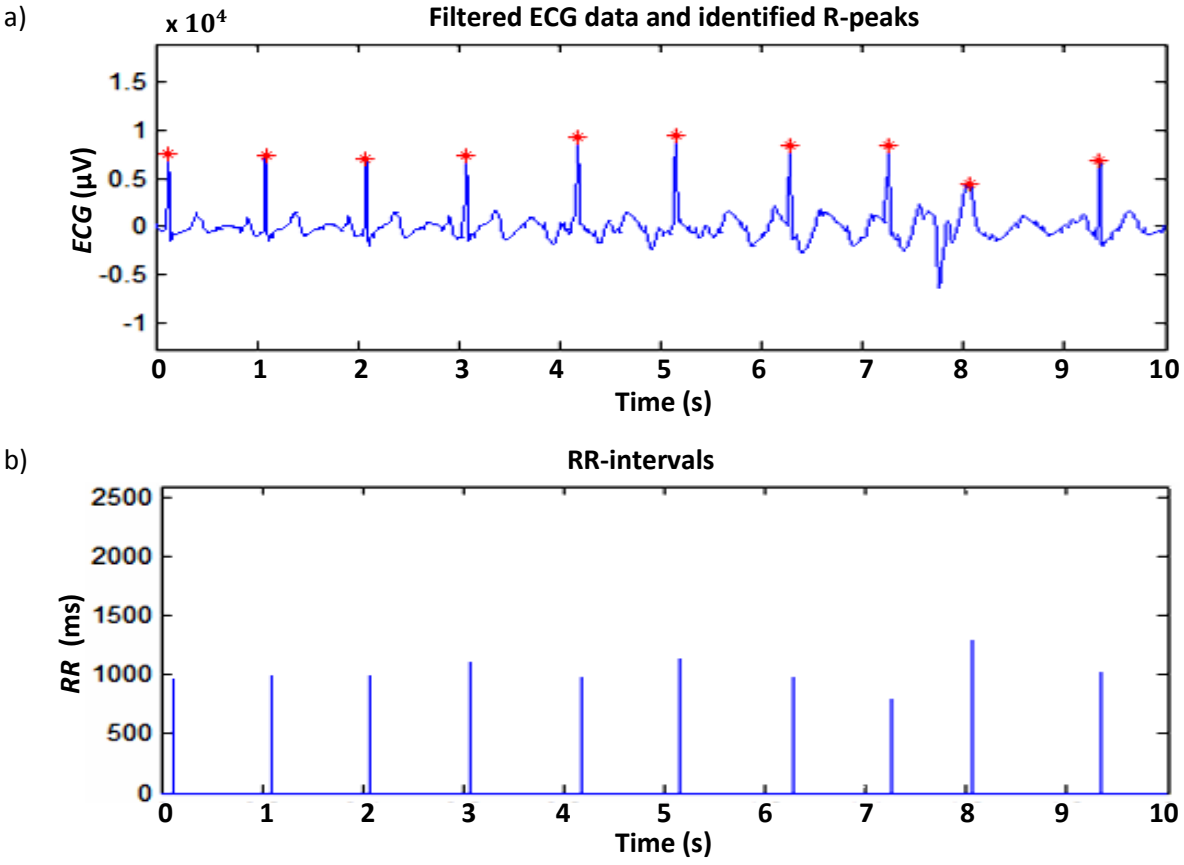

Figure 1.6: ECG data and RR corresponding RR-interval series. a) Filtered ECG data and identified R-peaks over time in seconds (s). b) RR-intervals (ms) over time in seconds (s)

Another way of visualizing RR-interval series are so called rhythmograms (or tachograms) which also show the different lengths of RR-intervals. (Figure 1.7)

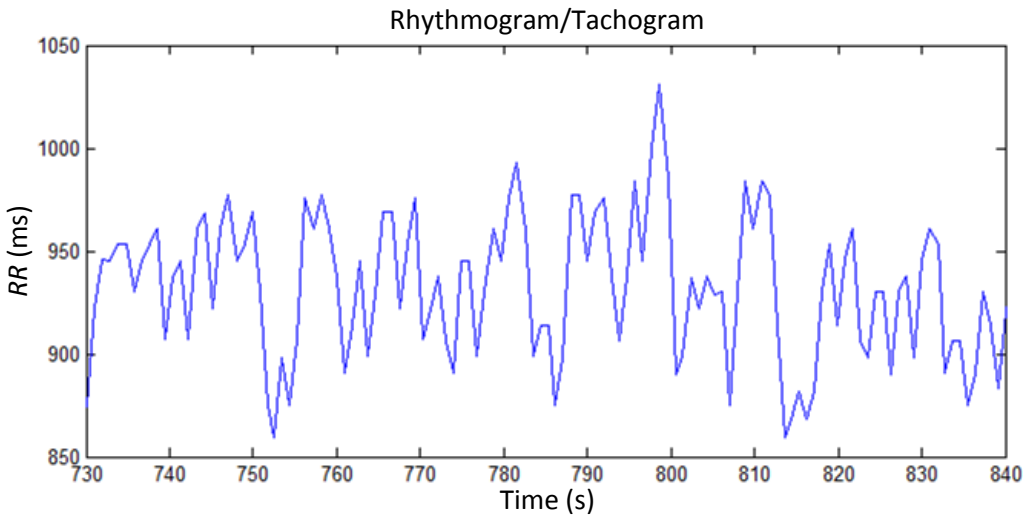

Figure 1.7: Rhythmogram/Tachogram. RR-intervals in milliseconds (ms) over time in seconds (s)

1.2.1. Linear analysis

Linear analysis methods of HRV can be grouped into various categories. There are time domain methods, frequency domain methods, geometric methods, time frequency methods and methods derived from fractal geometry. This chapter includes a short summary of chosen methods of linear analysis. Since there are so many different methods this thesis cannot cover them all and we had to focus on a couple of well known and widely used ones. The summaries include a basic description of the method, stability and improvements and applications. We chose following methods, each having its advantages and disadvantages:

	Advantages	**Disadvantages**
Time domain analysis		
Standard deviation of RR-intervals (SDNN)	Simple to calculate [10]	SDNN is not a well defined statistical quantity because of its dependence of length of the signal [10]. Time domain measures in general do not reliably distinguish between distinct biological signals. There are many different data series with identical means and standard deviations, but with different underlying rhythms. [11]. Sensitive to artifacts (e.g. stationarity of the signal) [11]
Root mean square of successive differences of RR-intervals (RMSSD)		Can be affected by artifacts and outliers [12]
Frequency domain analysis		
Power spectral density (PSD)	Useful to evaluate relationship to mechanisms [11]	Requires periodicity and stationarity [11]. Altered by posture, sleep, activity [13]. Sensitive to artifacts [11].
Geometric analysis		
HRV triangular index and triangular interpolation of the RR interval histogram (TINN)	Insensitivity to analytical quality of RR-interval series [10]. Simple measure of HRV [14]	Need reasonable number of RR intervals. (recordings which last at least 20 minutes, preferably 24 hours) [10]
Poincare plots	Poincare Plots are a simple visualization tool of HRV [15]. Outlier (ectopic beats or artifacts) can be easily identified [16]. Possible insights into short-term and long-term variability [15]	Derived statistics are not independent from other classical time domain measures [17]

Table 1.2: Methods of linear analysis of HRV plus their advantages and disadvantages

Standard deviation of RR-intervals (SDNN)

SDNN is the standard deviation of normal to normal RR intervals. It is a measurement of variability or dispersion of a data set that can be calculated very easily. SDNN reflects all the cyclic components responsible for variability and can be seen as global marker of HRV. [18]

Method:

First we calculate the arithmetic mean of the RR values:

$$\overline{RR} = \frac{1}{N}\sum_{i=1}^{N} RR_{\mathrm{i}} \tag{1.1}$$

The standard deviation of a discrete random variable is the root mean square of its values from the mean:

$$SDNN = \sqrt{\frac{1}{N}\sum_{i=1}^{N}(RR_{\mathrm{i}} - \overline{RR})^2} \tag{1.2}$$

Where $\overline{RR}$ is the arithmetic mean of RR-intervals (RR_{i}) and N denotes the number of RR_{i}. The index i ranges from 1 to N.

Applications:

SDNN as predictive value of mortality within one year after acute myocardial infarction (AMI) [18]**:**

Balanescu et al. concluded that the SDNN has a prognostic value independent from left ventricular ejection fraction and spontaneous ventricular arrhythmias one year after acute myocardial infarction and that the reduction of mortality risk by reperfusion therapy does not decrease the prognostic value of HRV after AMI.

Heart rate variability as marker of subclinical inflammation of middle aged and elderly subjects [19]**:**

Sajadieh et al. assessed HRV as a marker for subclinical inflammation in patients without prior history of cardiovascular disease or strokes. They found that HRV was negatively associated with smoking, C-reactive protein, white blood cell count, blood sugar, triglyceride concentration, female gender and diabetes. In contrast, physical activity was strongly associated with higher HRV. They concluded that reduced HRV was associated with subclinical inflammation in healthy middle-aged and elderly subjects.

Association of depression with reduced heart rate variability in coronary artery disease (CAD) [20]**:**

Carney et al. tested if depressed patients with CAD have decreased HRV compared with non-depressed CAD patients. The depression patients were compared according to age, sex and smoking status. They found that the SDNN was significantly lower in depressed than in non-depressed patients and concluded that decreased HRV may help explain the increased risk for cardiac mortality and morbidity in depressed CAD patients.

Stability and improvements:

Since the SDNN value changes with signal length it is not possible to compare signals with different signal lengths. Therefore the Task Force of The European Society of Cardiology and The North American Society of Pacing and Electrophysiology have suggested to use recordings of same lengths (e.g. 5 minutes or 24 hours). [10]

Root mean square of successive differences of RR-intervals (RMSSD)

RMSSD is the root mean square of successive differences of RR-intervals. It can be used to evaluate components that have a short-term effect on HRV, corresponding to parasympathetic activity. [18]

Method:

As shown by Chamchad et al. [21]:

$$RMSSD = \sqrt{\frac{1}{N-1}\sum_{i=1}^{N-1}(RR_{\mathrm{i+1}} - \mathrm{RR_i})^2} \tag{1.3}$$

RR_i are RR-intervals with an index i ranging from 1 to the total number (N) of RR-intervals minus 1.

Applications:

Detection of irregular pulses in patients with Atrial fibrillation (AF) [22] **:**

McManus et al. tested the hypothesis that a smart phone based application could detect an irregular pulse from AF using RMSSD and Shannon entropy as analysis methods. RMSSD and Shannon entropy were significantly higher in participants in AF than they were in normal sinus rhythm. They concluded that their method accurately distinguished pulse recordings during AF from sinus rhythm.

Change of HRV during treatment for depression in patients with coronary heart disease [23]**:**

Carney et al. tried to determine whether treatment for depression with cognitive behavior therapy (CBT) is associated with increased HRV. They classified mildly to severely depressed patients, and compared them to a control group. They found that RMSSD (reflecting mostly parasympathetic activity) improved significantly in the severely depressed patients, but remained unchanged in the mildly depressed and the control patients. Carney et al. concluded that treating depression with CBT may increase short-term HRV and thus it may have a beneficial effect on a risk factor for mortality in depressed patients with coronary heart disease.

Assessment of HRV in fibromyalgia patients [24]**:**

Mork et al. investigated HRV in fibromyalgia (FM) patients and healthy control subjects during different sleep stages to examine the association with pain and sleep quality. Their results showed that RMSSD was lower in patients with FM compared to the control group during NREM-2 sleep and during REM sleep. RMSSD showed modes positive correlations with sleep quality and modes negative correlations with neck/shoulder pain. They concluded that RMSSD is attenuated in FM patients compared to the control group during NREM-2 and REM sleep.

Stability and improvements:

All time domain HRV indices can be affected by artifacts and outliers (e.g. ectopic beats) and therefore require clean datasets. [12]

Power spectral density (PSD)

The power spectral density gives a visual and quantitative representation of how contributing frequencies to an underlying signal are distributed. The spectral ranges of HRV (Table 1.3) can be observed between 0.01 Hz and 0.5 Hz with different frequencies in between corresponding to particular physiological activity or sleep states [2]:

Very low frequency (VLF) **Humoral activity**	**Low frequency (LF)** **Sympathetic activity**	**High frequency (HF)** **Parasympathetic activity**
0.01-0.06 Hz	0.06-0.15 Hz	0.15-0.4 Hz

Table 1.3: Frequency ranges of HRV

In case or RR-intervals which have a physical unit of 1 millisecond, the spectral density has the unit of $1\ \mathrm{ms}^2/\mathrm{Hz}$. (Figure 1.8)

Method:

As shown by Rieke et al. [25]:

Calculation of truncated Fourier transform $\hat{x}_T(\omega)$:

$$\hat{x}_{\mathrm{T}}(\omega) = \frac{1}{\sqrt{T}} \int_0^T RR(t) e^{-i\omega t} dt \tag{1.4}$$

Where $RR(t)$, the RR-interval series over time (t), is integrated in the finite interval $[0, T]$ and ω denotes the angular frequency.

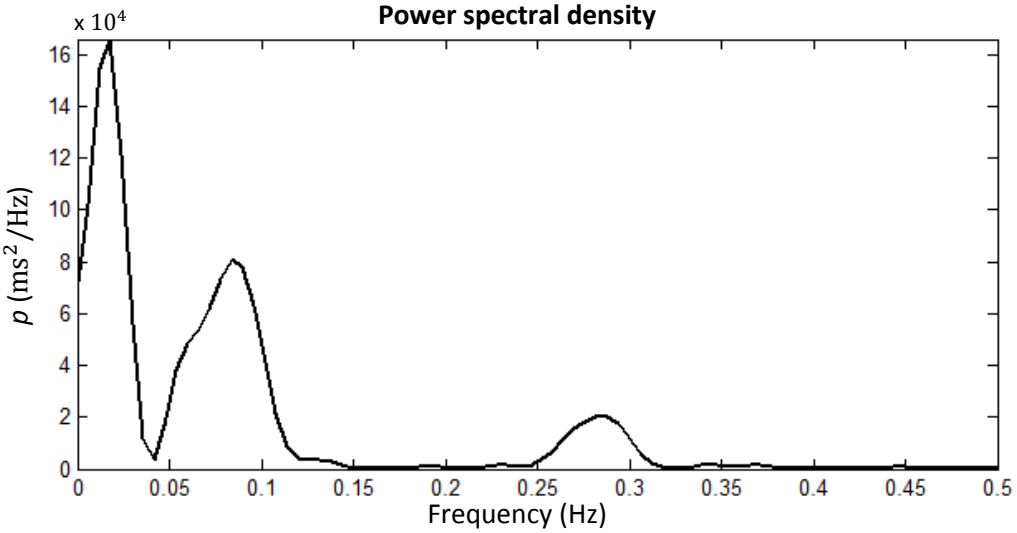

Figure 1.8: Example of power spectral density of HRV during sleep

The power spectral density can then be defined as:

$$S_{\mathrm{xx}}(\omega) = \lim_{T\to\infty} E[|\hat{x}_{\mathrm{T}}(\omega)|^2] \tag{1.5}$$

Where E denotes the expected value.

The power of the signal in a given frequency band $[\omega_1, \omega_1]$ can be calculated by integrating over positive and negative frequencies:

$$\int_{\omega_1}^{\omega_2} S_{\mathrm{xx}}(\omega) + S_{\mathrm{xx}}(-\omega)d\omega = F(\omega_2) - F(-\omega_2) \tag{1.6}$$

Where F is the integrated spectrum whose derivative is S_{xx}.

Applications:

Power spectral density as prognostic tool of HRV for patients with chronic heart failure (CHF) [26]**:**

Guzzetti et al. found that the power of the LF spectral component was significantly lower in the CHF patients compared to the control subjects. They concluded that spectral analysis methods of HRV have a prognostic value independently from time-domain measures.

Quantitative marker of autonomic dysfunction in patients with renal failure (RF) [27]**:**

Axelrod et al. found that the power spectrum in all frequencies was reduced in patients with RF. They concluded that spectral analysis of HRV makes it possible to quantitate autonomic dysfunction in patients who suffer from RF.

Assessing depth of Anesthesia [28]**:**

Toweill et al. assessed the depth of propofol anesthesia in patients by analyzing the response to painful stimuli in short-duration procedures. They found that the low-frequency power of the heart rate increased and concluded that power spectral analysis of HRV may be an accurate measure of depth of propofol anesthesia.

Stability and improvements:

Long-term spectral analysis may hide information which is contained in shorter term recordings. Therefore long-term and short-term analysis should be clearly distinguished. Physiological mechanisms of HRV can influence spectral analysis and should therefore be controlled. It was also suggested to perform statistical tests for stationarity of the signal before using spectral analysis. [10]

HRV triangular index and triangular interpolation of the RR interval histogram (TINN)

The HRV triangular index is the total number of all RR intervals divided by the height of the histogram of all RR intervals measured on a discrete scale with bins of 7.8125 ms. TINN (triangular interpolation of the RR interval histogram) can be described as the baseline width of the minimum square difference triangular interpolation of the highest peak of the histogram of all RR intervals [10].

Method:

As shown by the Task Force of the European Society of Cardiology and the North American Society of Pacing and Electrophysiology [10]:

To perform geometric measures on the RR interval histogram we have to construct a sample density distribution D. It assigns the number of equally long RR-intervals to each value of their lengths. Then the most frequent RR-interval length is established (maximum of the sample density distribution D). (Figure 1.9)

$$Y = D(X) \tag{1.7}$$

Calculation of HRV index:

$$HRV\ index = \frac{total\ number\ of\ all\ RR\ intervals}{Y} \tag{1.8}$$

Calculation of TINN:

We construct a multilinear function q with:

$$q(t) = \begin{cases} 0, & if\ t \leq N \\ 0, & if\ t \geq M \end{cases} \tag{1.9}$$

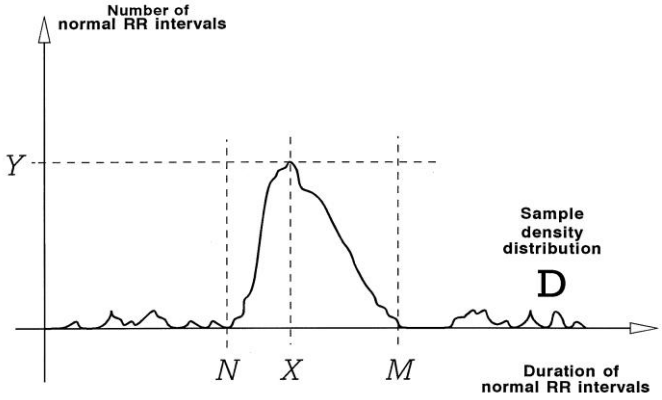

Figure 1.9: Sample density distribution of RR-intervals (D), where Y is the maximum of D and X is the most frequent RR-interval length. M and N are the upper and lower bounds [10].

and

$$q(X) = Y \tag{1.10}$$

such that

$$\int_0^{+\infty} (D(t) - q(t))^2 dt \tag{1.11}$$

is the minimum among all selections of all values N and M.

$$TINN = M - N \tag{1.12}$$

Applications:

HRV triangular index as measurement of clinical status and prognosis in patients with chronic congestive heart failure (CHF) [14]**:**

Wijbenga et al. found that patients with CHF who had a restrictive transmitral flow pattern had lower HRV index values compared to patients with CHF and a non-restrictive transmitral flow pattern. They also showed that a low HRV index and diminished left ventricular ejection fraction were the only independent predictors of the occurrence of cardiac death or heart transplantation. They concluded that the HRV index provides independent information on clinical status and prognosis in patients with chronic congestive heart failure.

Analysis of HRV in obese and eutrophic children [29]**:**

Vanderlei et al. investigated the autonomic modulation of eutrophic and obese children by applying geometric HRV analysis methods. Their results showed that TINN was reduced in obese children. They concluded that obese children presented changes in the autonomic nervous system characterized by decreases in parasympathetic activity and overall variability.

Prognosis of Type 2 Diabetic Autonomic Neuropathy [30]**:**

Tale et al. analyzed HRV signals of patients with Type 2 Diabetic Autonomic Neuropathy. The TINN values and other time and frequency domain values were significantly decreased in the diabetes mellitus group. They concluded that the reduction in parameters of HRV shows clinical expression of autonomic neuropathy in diabetes mellitus.

Poincare plots

Poincare plots portray the nature of RR interval fluctuations. Each RR interval is plotted as a function of the previous RR interval. The resulting graph provides a qualitative picture of both overall and beat-to-beat RR behavior. The shape of the plot is categorized into functional classes that indicate, for example, the degree of heart failure. [31]

Points above the line of identity (see Figure 1.10) indicate *RR* intervals that are longer than the preceding RR interval, whereas points below the line of identity indicate shorter *RR* intervals than the previous one. Accordingly, the dispersion of points perpendicular to the line of identity (width) reflects the short-term variability $SD1$. The dispersion of points along the axis of the line of identity (length) reflects the long-term variability $SD2$. [32]

Method:

Calculation of the two descriptors $SD1$ and $SD2$ [33]

We have a time series of RR-intervals

$$RR_{\mathrm{n}} = (RR_1, RR_2, \dots, RR_{\mathrm{N}-1}) \tag{1.13}$$

and the same time series shifted by 1:

$$RR_{\mathrm{n}+1} = (RR_2, RR_3, \dots, RR_{\mathrm{N}}) \tag{1.14}$$

$SD1$:

$$x_1 = \frac{RR_{\mathrm{n}} - RR_{\mathrm{n}+1}}{\sqrt{2}} \tag{1.15}$$

$$SD1 = \sqrt{Var(x_1)} \tag{1.16}$$

$SD2$:

$$x_2 = \frac{RR_{\mathrm{n}} + RR_{\mathrm{n}+1}}{\sqrt{2}} \tag{1.17}$$

$$SD2 = \sqrt{Var(x_2)} \tag{1.18}$$

Where Var d*enotes the* variance.

Furthermore we can calculate the ratio between $SD1$ and $SD2$ which seems to be a powerful predictor of post operative myocardial ischemia (see below). [34] There are various techniques for geometric analysis of Poincare plots. A common method is the ellipse fitting technique.

Ellipse fitting technique [16]**:**

To characterize the shape of the plot a set of axis - oriented with the line of identity - is defined. The axes of the Poincare plot (Figure 1.10) are related to the new set of axes by a rotation of $\theta = \frac{\pi}{4} rad$:

$$\begin{bmatrix} x_1 \\ x_2 \end{bmatrix} = \begin{bmatrix} cos\,\theta & -sin\,\theta \\ sin\,\theta & cos\,\theta \end{bmatrix} \begin{bmatrix} RR_{\mathrm{n}} \\ RR_{\mathrm{n}+1} \end{bmatrix} \tag{1.19}$$

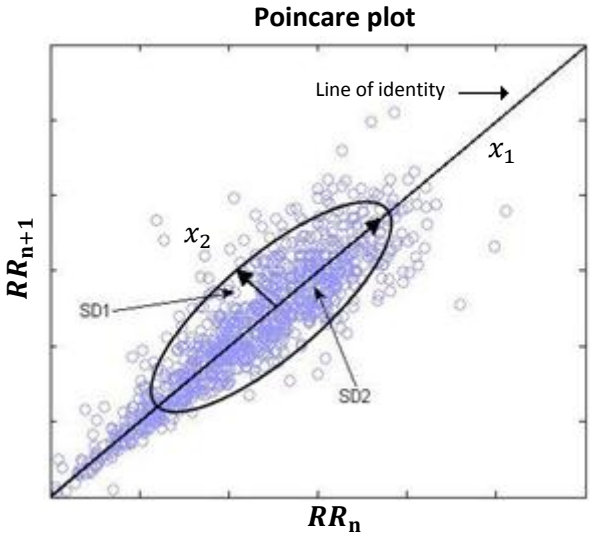

Figure 1.10: An example of Poincaré plot detailing the ellipse fitting process. The coordinate system x_1 and x_2 is established at 45° to the normal axis. The standard deviation of the distance of the points from each axis determines the width ($SD1$) and length ($SD2$) of the ellipse. RR_n and RR_{n+1} are the RR-interval series and its time shifted copy [35]

$SD1$ and $SD2$ can be related to standard HRV measures. For example to the standard deviation of successive differences of RR-intervals (SDSD): [16]

$$SD1^2 = Var(x_1) = Var\left(\frac{1}{\sqrt{2}}RR_n - \frac{1}{\sqrt{2}}RR_{n+1}\right) = \frac{1}{2}Var(RR_n - RR_{n+1}) = \frac{1}{2}SDSD^2 \qquad (1.20)$$

or the SDNN:

$$SD1^2 + SD^2 = 2SDNN^2 \qquad (1.21)$$

Both of those Indices are related themselves:

$$SD2^2 = 2SDNN^2 - \frac{1}{2}SDSD^2 \qquad (1.22)$$

Applications:

Poincare plots as predictor of post operative ischemia [34]**:**

The results of Laitio et al. showed an increased ratio between the short-term variability $SD1$ and the long-term variability $SD2$ of the first postoperative day in the univariate analysis of HRV. In the multivariate model, the increased ratio $SD1/SD2$ of the first post operative day was the most powerful independent predictor of all possible confounding variables for the occurrence of postoperative ischemia.

Assessment of the effect of endurance training on HRV [36]**:**

Mourot et al. stated that together with changes in HRV due to acute maneuvers or disease, the Poincare plot could discriminate altered HRV due to short- and/or long-term endurance training. The Poincare scatter grams were wider in the trained state. Standard deviations of the Poincare plot (especially $SD1$) correlated significantly with the main parameters of the time-domain and frequency-domain analyses, especially concerning the parasympathetic indicators. Their results suggested that the Poincare plot parameters as well as the width of the scatter gram could be considered as surrogates of time and frequency-domain analysis to assess training-induced changes in HRV.

Heart rate analysis in normal subjects of various age groups [37]**:**

$SD1/SD2$ shows the ratio of short interval variation to the long interval variation. Acharya et al. concluded that this ratio is higher in the case of child and old male subjects, indicating lesser *RR* variability in the short time. This ratio is reduced in the middle aged subjects, indicating higher *RR* variability.

Assessment of the level of sedation in sedated cardiac surgery patients [38]**:**

Korhonen et al. compared linear and nonlinear analysis of HRV in sedated cardiac surgery patients. Their results showed that $SD1$ was strongly related to the square root of the mean squared difference of successive RR intervals ($RMSSD$) and HF power. In addition, the standard deviation and *SD2* were strongly correlated. All the parameters except the ratios (*LF/HF* and $SD1/SD2$) correlated significantly with the mean *RR interval*. They confirm that the level of sedation modifies the HRV and hence HRV is a potential tool for the assessment of the level of sedation in critical care.

Stability and improvements:

To improve the quality of the RR data and the Poincare plot itself we can apply some pre-filtering. Filters also allow us to access the information on the sinus rhythm, which is usually mixed with some other information. Piskorsky et al. [33] applied a couple of filtering methods (annotation filter, square filter and quotient filter), showed the correct way of filtering data and presented a few results of not-filtering or even incorrect filtering. They also demonstrated how proper filtering helps to extract interesting information from the data. [33]
Kim et al. [39] studied effects of missing RR intervals on the Poincare analysis and came to the conclusion that the parameters $SD1$ and $SD2$ can be recommended for an accurate nonlinear HRV analysis with missing RR intervals. [39]

The standard descriptors $SD1$ and $SD2$ do not directly quantify the nonlinear temporal variations in the time series contained in the Poincare plot. When applied to data sets that form multiple clusters in a Poincare plot due to complex dynamic behaviors, the $SD1/SD2$ statistics yield mixed results. This is because the technique relies on the existence of a single cluster or a defined pattern. Therefore Karmakar et al. [35] proposed the complex correlation measure (*CCM*) to overcome the limitation of the standard descriptors and confirmed the hypothesis that *CCM* measures the temporal variation in the Poincare plot. [35]

1.2.2. Nonlinear analysis

It has been proposed that HRV can be better described through nonlinear analysis rather than linear analysis. There are various nonlinear methods to analyze HRV. Some of them quantify the fractal scaling characteristics or RR-interval series, some of them measure the likelihood through incremental comparisons between data patterns of a certain length and some of the methods measure sensitive dependence to initial conditions. Each method has its strengths and weaknesses:

	Advantages	**Disadvantages**
Detrended fluctuation analysis (DFA)	Can be applied to non-stationary time series [40]. Avoids the spurious detection of apparent long-range correlations that are an artifact of non-stationarity [40]. Could be used for on-line monitoring of changes in patient status in order to help surgeons diagnose patients in Surgical intensive care units more rapidly in the future [41].	It has been suggested to include at least 8000 data points. [40] It does not relate the derived parameters to specific neuro-autonomic control mechanisms. [40]
Lyapunov exponents (λ)	Discriminates correctly between chaos and non chaos [42]. Relatively robust to noise [42].	Misclassifies high-dimensional chaos [42]. Unreliable for small data sets [43]. Computationally intensive [43].
Approximate entropy (ApEn)	Robust against noise contamination below r. [44] ApEn is resistant to short strong transient interference. [45] It is applicable for stochastic, deterministic, and mixed processes. [46]	ApEn is dependent on the record length and is uniformly lower than expected for short records. [47] It lacks relative consistency (If ApEn of one data set is higher than that of another, it should, but does not, remain higher for all conditions. E.g. for different choices of m and r). [47] Outliers (missed beat detections, artifacts) may affect the entropy values. [17] It counts "self-matches" which leads to bias (improved in Sample Entropy (SampEn)) [17] Stationarity is required. [17]
Sample entropy (SampEn)	It does not count "self-matches" [17] SampEn provides a more reliable estimate of complexity of a signal compared to ApEn [9]	Stationarity is required [17] Higher pattern length requires an increased number of data points [17]
Multiscale entropy (MSE)	Accounts for the multiple time scales in biological signals [48] It yields consistent findings when applied to assess the complexity of cardiac interbeat intervals under healthy and pathologic conditions. [49] MSE is statistically independent from conventional linear measures (e.g. RMSSD, SDRR). [50]	In order to have a good statistical reliability at higher scales, the number of data points must be greater than 10000 [9]

Table 1.4: Nonlinear methods of analysis of HRV plus their advantages and disadvantages

Detrended fluctuation analysis (DFA)

The Detrended fluctuation analysis is a method that permits the detection of long-range correlations embedded in non-stationary time series and at the same time avoids the spurious detection of apparent long-range correlations that are an artifact of non-stationarity. [40]

Method:

Method as shown by Peng et al. [40]:

First, we have to integrate the RR interval time series (of total length N):

$$y(k) = \sum_{i=1}^{k} [RR(i) - RR_{\text{avg}}] \tag{1.23}$$

Where $y(k)$ is the k-th value of integrated series, $RR(i)$ denotes the i-th RR interval and RR_{avg} is the average RR-interval over the entire series.

Next the integrated time series is divided into boxes of equal length, n *(*$n \leq 11$ for short-term scaling, $n > 11$ for long-term scaling*)*. (Figure 1.11)

Then we detrend the integrated time series, $y(k)$, by subtracting the local trend, $y_{\text{n}}(k)$, in each box. The rootmean-square fluctuation of this integrated and detrended time series is calculated by

$$F(n) = \sqrt{\frac{1}{N}\sum_{k=1}^{N} [y(k) - y_{\text{n}}(k)]^2} \tag{1.24}$$

This computation is repeated over all time scales (box sizes) to provide a relationship between $F(n)$, the average fluctuation as a function of box size, and the box size n (I.e. the number of beats in a box

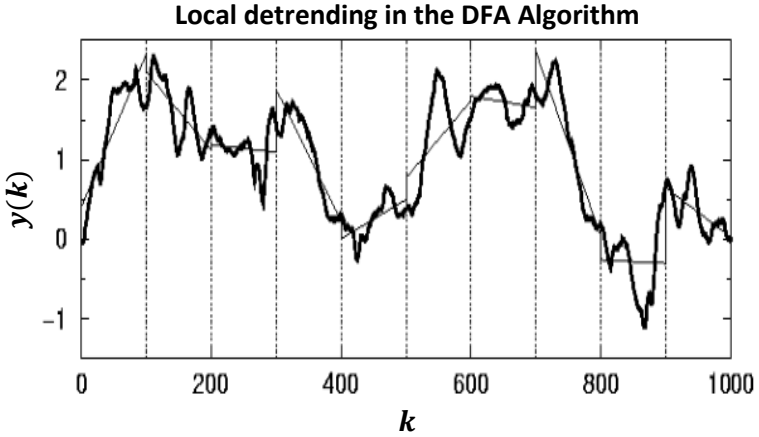

Figure 1.11: In each box of length n, a least-squares line is fit to the data (representing the trend in that box). The y coordinate of the straight line segments is denoted by $y_{\text{n}}(k)$*. The vertical dotted lines indicate the box size.* [40]

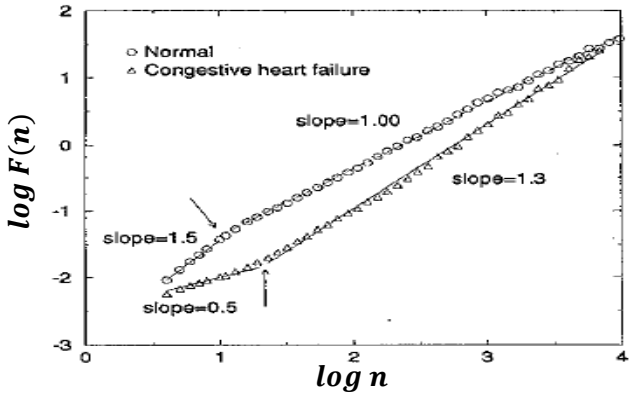

Figure 1.12: Plot of $\log F(n)$ vs. $\log n$. Arrows indicate "crossover" Points in scaling. [40]

which is the size of the window of observation). Typically, $F(n)$ will increase with box size n. A linear relationship on a double log graph indicates the presence of scaling. Scaling refers to the self-similarity of the HRV. From a general point of view, it corresponds to the fact that a certain scale-dependent quantity behaves as a power-law of the scale. Under such conditions, the fluctuations can be characterized by a scaling exponent α, the slope of the line relating $\log F(n)$, to $\log n$. (Figure 1.12)

We can distinguish between the short-term scaling index α_1 (computed for $n \leq 11$ samples) and the long-term scaling index α_2 (computed for $n > 11$).

α=0.5	White noise (If there are only short-term correlations, the initial slope may be different from 0.5, but a will approach 0.5 for large window sizes.) [7]
$0.5 < \alpha < 1$	Indicates persistent long-range power-law correlations such that a large (compared to the average) interbeat interval is more likely to be followed by large interval and vice versa.
$0 < \alpha < 0.5$	Indicates a different type of power law correlation such that large and small values of the time series are more likely to alternate.
$\alpha = 1$	Corresponds to $1/f$ noise.
$\alpha = 1.5$	Indicates Brown noise, the integration of white noise.

Table 1.5: Different ranges for scaling index α

Applications:

Comparison between healthy subjects and subjects with congestive heart failure (CHF) [40]**:**

Peng et al. applied DFA to the nonstationary heart beat time series from healthy subjects and those with severe heart disease (congestive heart failure). They showed that DFA is capable of identifying crossover behavior (change of dynamics when going from short to long time scales).

Prediction of progressive ventricular enlargement in dilated cardiomyopathy patients [51]**:**

Mahon et al. concluded, that the short-term scaling component (α_1) is abnormal in asymptomatic relatives of dilated cardiomyopathy patients who have left ventricular enlargement (LVE). In addition they state that (α_1) is a predictor of progressive ventricular enlargement in dilated cardiomyopathy patients.

Separation of sleep stages and identifying Sleep Apnea [52]**:**

Penzel et al. compared DFA to Spectral Analysis to determine the best method for the separation of sleep stages and sleep apnea severity. They concluded that changes in HRV are better quantified by the scaling analysis than by spectral analysis.

Analysis of short-term heart rate variability in late pregnant women [53]**:**

Yeh et al. found that late pregnant women have an elevated global scaling exponent, an elevated short-term scaling exponent and lower heart rate variability measures in the low and high frequency ranges than those of the healthy controls and 3 months after delivery. Their study suggested that the global and short term detrended fluctuation scaling exponents might be new and independent measures of heart rate variability in late pregnancy, in addition to the conventional time and frequency domain measures.

Distinguishing pathologic states in surgical intensive care units [41]**:**

The α index derived from the DFA method was applied to patients in a surgical intensive care unit (SICU). The results have shown that it can clearly distinguish pathologic states in the SICU from the healthy group and white noise signals. However, the variation of α in the SICU group was still too large.

Comparison between a group of patients with coronary heart disease and a healthy group [6]**:**

Krstacic et al. investigated the clinical and prognostic significance of nonlinear methods and to correlate the results of dynamic examinations between patients with coronary heart disease (CHD) and a healthy control group. They concluded that normal fractal properties of the RR interval dynamics are altered in patients with CHD, as estimated by the R/S and DFA methods.

Stability and improvements:

An interesting topic is the influence of preprocessed signals on the DFA algorithm. Gomes et al. applied two preprocessing algorithms (convolution of inverse interval function values with a rectangular window and cubic polynominal interpolation of inverse interval function values) on their data and concluded that preprocessing with those two methods do not significantly change the deterministic signature in the data, except for the index $\alpha 1$ with the method of convolution. [54]

Valencia et al. used an approximation of DFA based on symbolic dynamics for analyzing heart rate variability by means of RR series which are characterized by long-range correlations. This approach was compared with other different proposals that involve RR increment series, magnitude and sign of those RR increment series. It seems that an adequate symbolic transformation of the RR series allowed DFA scaling exponents to better identify different correlation properties between the studied cardiac risk groups. [55]

An important issue can be missing RR-interval data. Kim et al. have analyzed the effects of missing RR-interval data on nonlinear heart rate variability analysis. They used RR-interval tachograms with simulated missing data and actual missing data. Also they used some reconstruction methods including bootstrapping and several interpolation methods. Their conclusion was that the DFA may not be appropriate for accurate HRV analysis with missing data, since these parameters have relatively larger error values than time- or frequency-domain HRV parameters. However, the analysis of the long-term variation for nonlinear HRV values can be available through applying the rules for the reconstruction of the data obtained in their study. [39]

Lyapunov exponents (λ)

Lyapunov exponents quantify the sensitivity of the system to initial conditions, which is an important feature of chaotic systems and describes how small changes in the state of a system grow at an exponential rate and eventually dominate the behavior. Lyapunov exponents are defined as the long time average exponential rates of divergence of nearby states. If a system has at least one positive Lyapunov exponent, then the system is chaotic. (Figure 1.13) The larger the positive exponent, the more chaotic the system becomes (i.e., the shorter the time scale of system predictability). Lyapunov exponents will be arranged such *that* $\lambda_1 \geq \lambda_2 \geq \cdots \geq \lambda_n$, where λ_1 and λ_n correspond to the most rapidly expanding and contracting principal axes, respectively. Therefore, λ_1 may be regarded as an estimator of the dominant chaotic behavior of a system. [56]

Method:

Algorithm proposed by Wolf et al. [57] as shown by Acharya et al. [37]:

For a given the time series of RR-intervals ($RR(t)$) for m dimensional phase space with delay coordinate t, that is a point on the attractor is given by:

$$\{RR(t), RR(t+t), \dots, RR(t+(m-1)t)\} \tag{1.25}$$

We locate nearest neighbor to initial point:

$$\{RR(t_0), RR(t_0+t), \dots, RR(t_0+(m-1)t)\} \tag{1.26}$$

And denote the distance between these two points as $L(t_0)$. At a later time t_1, initial length $L(t_0)$ will evolve to length $L'(t_1)$. The mean exponential rate of divergence of two initially close orbits is characterized by

$$\lambda = \frac{1}{t_M - t_0} \sum_{k=1}^{M} log_2 \frac{L'(t_k)}{L'(t_{k-1})} \tag{1.27}$$

In an implementation of this program, the following set of numerical parameters has to be chosen:

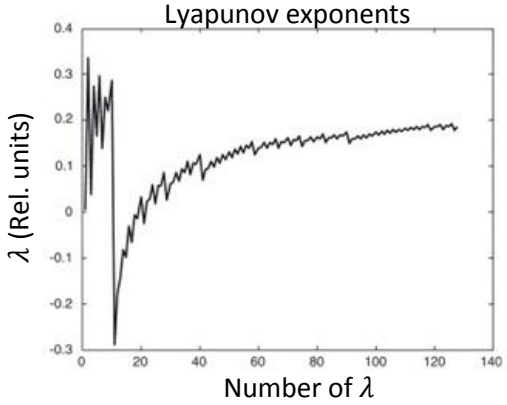

Figure 1.13: Lyapunov exponents (λ) of a typical normal ECG beat. Lyapunov exponents (y-axis) are plottet against the Number of Lyapunov exponents (x-axis) [58]

$$P = \{m, t, T, S_{\max}, S_{\min}, th_{\max}\} \quad (1.28)$$

where m *is the* embedding dimension, t the Delay, T the Evaluation time ($= t_{k+1} - t_{k-1}$), $S_{\max}$, $S_{\min}$ are maximum and minimum separations of replacement point respectively and $th_{\max}$ is the maximum orientation error.

According to Das et al. [59] an embedding dimension between 5 to 20 and a delay of 1 should be chosen when calculating LE for EEG data.

λ = Negativ	Implies that the orbits approach a common fixed point
λ =*Zero*	Orbits maintain their relative positions
λ =*Positiv*	Implies that the orbits are on a chaotic attractor

Table 1.6: Different ranges for lyapunov exponent λ

Applications:

Showing a clear distinction between the neutral and the arousal elicitation [60]**:**

The outcomes of Valenza et al. showed a clear switching mechanism between regular and chaotic dynamics when switching from neutral to arousal elicitation. The mean approximate entropy (ApEn, see below) decreased with statistical significance during arousal elicitation and λ became negative. They state that their results could be profitably exploited to improve the accuracy of emotion recognition systems based on HRV time series analysis.

Analysis of the mobile phone effect on heart rate variability [61]**:**

The results of Yilmaz et al. show that the LLE (Largest Lyapunov exponent) values increased slightly with higher electromagnetic fields produced by Mobile phones. This change indicates that the degree of chaos in the HRV signals increased at high electromagnetic fields compared to low level electromagnetic fields. They concluded that high level electromagnetic fields changed the complexity of the cardiac system behavior significantly.

Analysis of heart rate variability in Preterm and Term Neonates [62]**:**

Selig et al. concluded that preterm neonates have a less complex heart rate variability behavior than term neonates. The preterm neonates were significantly different from the term neonates, with $p < 0.0001$. The Lyapunov exponent of the term neonates was closer to one than the Lyapunov exponent of the preterm neonates.

Analysis of heart rate time series in Patients with major depression [63]**:**

Yeragani et al. suggested that major depression is associated with decreased cardiac vagal function and a relative increase in sympathetic function, which may be related to the higher risk of cardiovascular mortality in this group and illustrates the usefulness of nonlinear measures of chaos such as LLE in addition to the commonly used spectral measures.

Analysis of cardiac health [64]**:**

HRV signals can be used as reliable indicator of heart diseases. Acharya et al. have evaluated linear and nonlinear parameters and subjected the results to a t-*test* with more than 90 % confidence interval giving significant p-*values* in all cases. Correlation dimension, LLE and the scaling exponent α (see DFA) decrease as the RR interval decreases.

Stability and improvements:

The algorithm by Wolf et al. [57] fails to take advantage of all the available data because it focuses on one "fiducial" trajectory. A single nearest neighbor is followed and repeatedly replaced when its separation from the reference trajectory grows beyond a certain limit. Additional computation is also required because the method approximates the Gram-Schmidt procedure by replacing a neighbor with one that preserves its phase space orientation. [43]
Therefore Rosenstein et al. have presented a new method for calculating LLE from experimental time series, which can also be applied to small data sets. [43]

It has been controversial if HRV follows chaotic or stochastic behavior. Hu et al. tried to shed some light on the issue by characterizing heart rate variability by a scale-dependent Lyapunov exponent (SDLE). The SDLE is a multiscale complexity measure that is able to characterize deterministic chaos, noisy chaos, stochastic oscillations, random $1/f$ processes, random Levy processes, and complex time series with multiple scaling behaviors. [65]

Approximate entropy (*ApEn*)

Approximate Entropy (*ApEn*) is a family of statistic indexes which quantify different degrees of regularity in time series. [44] It represents the overall complexity and predictability of time series. [66] *ApEn* reflects the logarithmic likelihood that two sequences that are similar (within a tolerance r) for m points remain similar at the next point. [67] A low *ApEn* reflects a high degree of signal regularity while a random signal has relatively high *ApEn*.

Method:

Method by Pincus et al. [66] as shown by Al-Angari et al. [45]:

ApEn requires three input parameters:

$$ApEn(m, r, N) \tag{1.29}$$

where m is the embedded dimension of the vector to be formed (length of the vectors to be compared), r denotes the threshold that serves as a noise filter and N is the length of the RR-interval series.

Pincus et al. [66] used an embedded dimension of $m = 2$. The choice of r will be discussed under the stability section of the *ApEn* method.

Suppose we have an RR-interval series:

$$RR(n) = RR(1), RR(2), \dots RR(N) \tag{1.30}$$

The computation of $N - m + 1$ vectors (templates), each of size m, is done as follows:

$$X^{\mathrm{m}}(i) = [RR(i), RR(i+1), \dots RR(i+m-1)] \qquad i = 1, N-m+1 \tag{1.31}$$

The distance $d[X^{\mathrm{m}}(i), X^{\mathrm{m}}(j)]$ between each template and other templates (including itself) is computed as:

$$d[X^{\mathrm{m}}(i), X^{\mathrm{m}}(j)] = \max[|RR(i+k) - RR(j+k)|] \qquad k = 0, m-1 \tag{1.32}$$

For each template $X^{\mathrm{m}}(i)$, the number of matching templates $N^{\mathrm{m}}(i)$ which fulfill $d[X^{\mathrm{m}}(i), X^{\mathrm{m}}(j)] \leq r$) is found.

$$C_{\mathrm{r}}^{\mathrm{m}}(i) = \frac{N^{\mathrm{m}}(i)}{N-m+1} \tag{1.33}$$

$C_{\mathrm{r}}^{\mathrm{m}}(i)$ is the probability that any template $X^{\mathrm{m}}(j)$ matches $X^{\mathrm{m}}(i)$.

Next the natural logarithm of each $C_{\mathrm{r}}^{\mathrm{m}}(i)$ is taken and averaged over i:

$$\Phi^{\mathrm{m}}(r) = \frac{1}{N-m+1} \sum_{i=1}^{N-m+1} lnC_{\mathrm{r}}^{\mathrm{m}}(i) \tag{1.34}$$

By increasing the dimension to $m + 1$ and repeating previous steps to find $\Phi^{\mathrm{m}+1}(r)$, the value of the approximate entropy, for a finite length of data points N, is given by:

$$ApEn(m, r, N) = \Phi^{m}(r) - \Phi^{m+1}(r) \tag{1.35}$$

Applications:

Measurement of HRV complexity in healthy groups of different ages and different times of the day [68]**:**

Pikkujämsä et al. concluded that cardiac interbeat interval dynamics change markedly from childhood to old age in healthy subjects. Children show complexity and fractal correlation properties of RR interval time series comparable to those of young adults, despite lower overall heart rate variability. Compared with young adults, children showed similar complexity (*ApEn*) and fractal correlation properties of RR interval dynamics despite lower spectral and time-domain measures. Progressive loss of complexity (*ApEn*) was observed thereafter from middle age to old age.

Analysis of heart rate variability in patients with coronary heart disease [6]**:**

Krstacic et al. investigated the clinical and prognostic significance of nonlinear methods and correlated the results of dynamic examinations between patients with coronary heart disease (CHD) and a healthy control group. Their results were that patients with CHD had lower *ApEn* than the healthy control group.

Studying measures of heart rate dynamics after acute myocardial infarction [69]**:**

Perkiömäki et al. concluded that short-term fractal scaling properties of heart rate dynamics change to a more correlated direction and the complexity of heart rate behavior decreases from the acute phase to the predischarge period after AMI. However, the individual values of the short-term scaling exponent α_1 and *ApEn* are more stable over time than those of the conventional linear HRV measurements

HRV as a marker for the rheumatoid arthritis stage [70]**:**

Kamal found that the *ApEn* measure was reduced in patients with rheumatoid arthritis (RA) in comparison with the control group. The power spectra of patients with RA showed reduced high frequency value and increased low frequency value in comparison with control subjects. Additionally the *ApEn* measure was significantly reduced in RA patients who have had RA for a long time. Kamal concludes that *ApEn* may be a marker of RA stage.

Stability and improvements:

For a shorter time series it is better to choose the Sample Entropy method (*SampEn*) instead of the Approximate Entropy method (*ApEn*), because the number of samples does not affect the result of *SampEn* (see figure 1.14). [71]

Pincus et al. [66] used a selected threshold r between 0.1-0.25 times the standard deviation of the RR time series. In the following years a lot of authors used a value of r = 0.2 when applying *ApEn* to heart rate dynamics. It has been proposed that signals of faster dynamics are better analyzed with an r that maximizes *ApEn*. [72] Castiglioni et al. [73] have compared $r_{\max}$ (the r value that corresponds to the maximum *ApEn* value) to the values used until now and concluded that $r_{\max}$ is not incompatible with the traditionally recommended range when applying them to physiologic signals. However, they also state that small maneuvers (like change of posture from supine to sitting) do not have simple effects on *ApEn*. They suggest to quantify preliminary the whole *ApEn*(r) profile as a function of r to get a more complete picture and to verify preliminary how critical the choice of r can be in the quantification of *ApEn*. [73]

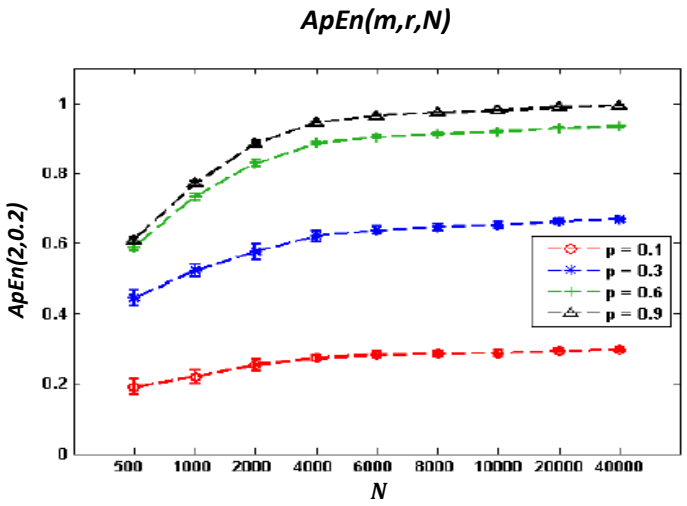

Figure 1.14: ApEn's dependence on the data length (N) with $m = 2$ *and* $r = 0.2 * sd$ [74]

Sample entropy (*SampEn*)

Richman and Moorman developed the Sample entropy method as an improvement to Approximate entropy (see above). [71] *SampEn* is similar to *ApEn*. *SampEn* does not count self-matches as comparisons within itself which will lower *ApEn* values so the signals are perceived to be more regular than they actually are. When estimating conditional probabilities, *SampEn* adopts a one template approach to find a match of length $m + 1$, whereas *ApEn* adopts a template-wise approach. [71]

Method:

By Richman and Moorman [71]as shown by Kim et al. [39]:

We need three input parameters:

$$SampEn(m, r, N) \tag{1.36}$$

where m is the embedded dimension of the vector to be formed (length of the vectors to be compared), r denotes the threshold that serves as a noise filter and N is the length of the sequence.

$$x_{\mathrm{m}}(i) = [RR_{\mathrm{i}}, \dots, RR_{\mathrm{i+m-1}}] \tag{1.37}$$

RR_i denote the different RR-intervals.

$$A_{\mathrm{i}}^{\mathrm{m}}(r) = \frac{the\ number\ of\ j \leq N - m (j \neq i)\ such\ that\ d[x_{\mathrm{m+1}}(i), x_{\mathrm{m+1}}(j)] \leq r}{N - m + 1} \tag{1.38}$$

where $d[x_{\mathrm{m}}(i), x_{\mathrm{m}}(j)]$ is the distance between the vectors $x_{\mathrm{m}}(i)$ and $x_{\mathrm{m}}(j)$

$$A^{\mathrm{m}}(r) = \frac{1}{N - m} \sum_{i=1}^{N-m} A_{\mathrm{i}}^{\mathrm{m}}(r) \tag{1.39}$$

$$B_{\mathrm{i}}^{\mathrm{m}}(r) = \frac{the\ number\ of\ j \leq N - m (j \neq i)\ such\ that\ d[x_{\mathrm{m}}(i), x_{\mathrm{m}}(j)] \leq r}{N - m + 1} \tag{1.40}$$

$$B^{\mathrm{m}}(r) = \frac{1}{N - m} \sum_{i=1}^{N-m} B_{\mathrm{i}}^{\mathrm{m}}(r) \tag{1.41}$$

Finally we can compute the *SampEn*:

$$SampEn(m, r, N) = -ln\left[\frac{A^{\mathrm{m}}(r)}{B^{\mathrm{m}}(r)}\right] \tag{1.42}$$

Applications:

Detection of obstructive sleep apnea Syndrome [45]**:**

The results of Al-Angari et al. showed that complexity of HRV was significantly different between normal and obstructive sleep apnea groups and they state that analysis of HRV might be a useful way to detect sleep apnea without using a polysomnopraphic study.

Study of Heart rate complexity prior to the onset of atrial fibrillation [7]**:**

Tuzcu et al. used *SampEn* for complexity analysis. Their results showed that the *SampEn* of RR-intervals was significantly reduced in the pre-Atrial Fibrillation period compared with the Atrial Fibrillation period. There was a significant decreasing trend in the entropy towards the onset of Atrial Fibrillation using linear mixed models.

Analysis of heart rhythm following cardiac transplantation [75]**:**

Tuzcu et al. concluded that system complexity decreases in patients who have undergone heart transplantation. Patients who underwent heart transplantation showed significant decrease in entropy as assessed by *SampEn*. This can be related to loss of the neural modulation of heart rate. Their limited number of transplanted patients do not seem to support presence of cardiac re-innervation.

Characterization of heart rate variability loss with aging and heart failure [76]**:**

Goya-Esteban et al. characterized HRV loss with aging by *SampEn*. They were able to obtain a good representation of the HRV loss for CHF condition as well as a steady decrease of *SampEn* with a fixed threshold value r. They achieved higher discrimination than with an r value given as a percentage of the standard deviation of each data series.

Identifying diabetic patients with cardiac autonomic neuropathy [77]**:**

Khandoker et al. concluded that *SampEn* of HRV could have potential in identifying asymptomatic cardiac autonomic neuropathy (CAN). Their results showed that the *SampEn* values found in CAN group were lower, which could be a practical diagnostic and prognostic marker.

Stability and improvements:

SampEn is less dependent on the data length than *ApEn* (Figure 1.15), although it has higher standard deviation for low number of samples. [74]

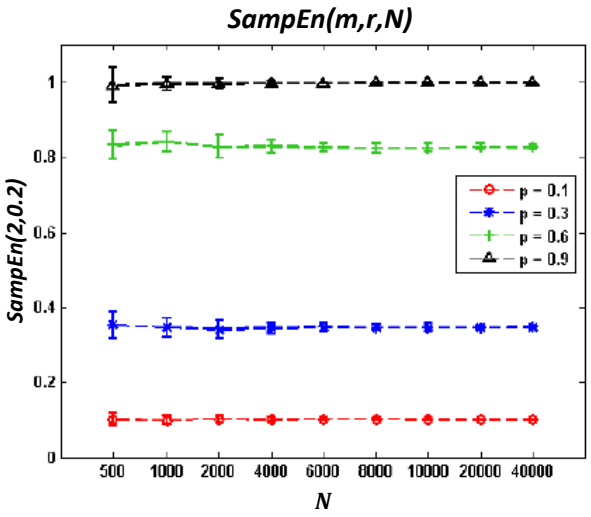

Figure 1.15: SampEn's dependence on the data length (N) with $m = 2$ *and* $r = 0.2 * sd$ [74]

Multiscale entropy (MSE)

Multiscale entropy is an indicator or the regularity of the signal at different time scales. MSE is based on the observation that the output of complex systems is far from extremes of either perfect regularity or complete randomness. Instead, the signals generally reveal structures with long-range correlations on multiple spatial and temporal scales. These multiscale features, ignored by conventional entropy calculations, are explicitly addressed by the MSE method. [48]

Method:

As shown by Costa et al. [49]:

We have a one dimensional-discrete time series of RR-intervals with a total number (N) of RR-intervals:

$$\{RR_1, \dots, RR_i, \dots, RR_N\} \tag{1.43}$$

From that time series we construct a coarse-grained time series determined by the scale factor τ :

$$y_{\mathrm{j}}^{(\tau)} = \frac{1}{\tau \sum_{i=(j-1)\tau+1}^{j\tau} RR_{\mathrm{i}}} 1 \leq j \leq \frac{N}{\tau} \tag{1.44}$$

For a scale of 1, the time series $\{y^{(1)}\}$ is the original time series. The length of the coarse-grained time series is equal to the length of the original time series divided by the scale factor τ . (Figure 1.16)

Then we calculate an entropy measure (e.g. *SampEn* or *ApEn*) for each coarse grained time series, which can be plotted as a function of the scale factor τ . (Figure 1.17)

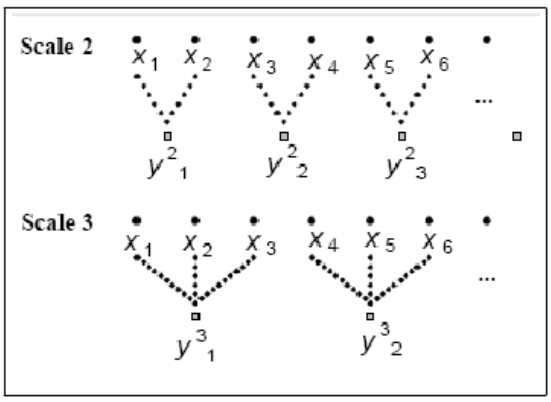

Figure 1.16: Coarse-graining procedure for scales 2 and 3 [78]

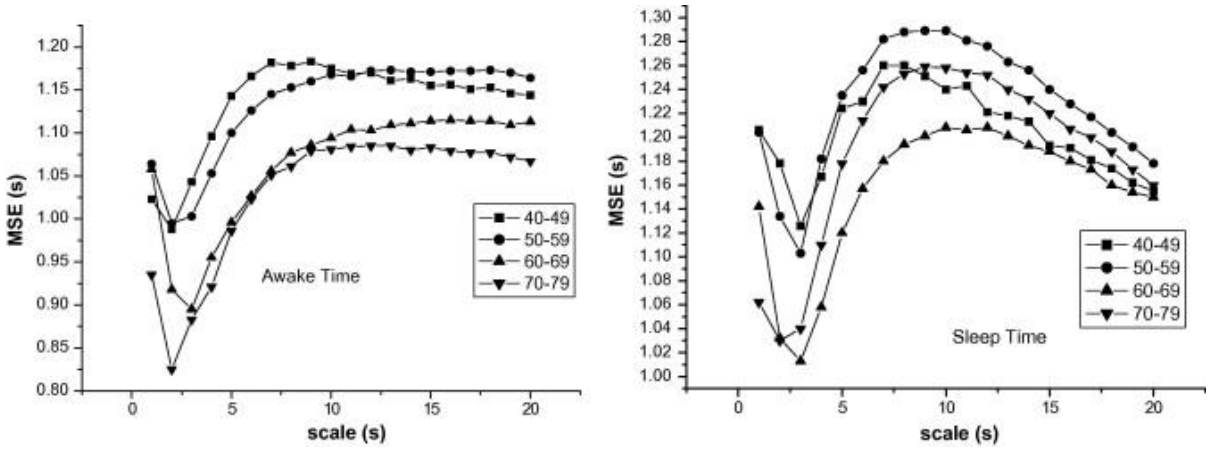

Figure 1.17: Plot of MSE average signature with $m = 2, r = 0.15$ *(from ApEn and/or SampEn). Awake and sleep period considering different age groups of non-healthy patients* [79]

Applications:

Comparison of HRV between healthy subjects, subjects with congestive heart failure and subjects with atrial fibrillation [48]**:**

Costa et al. applied multiscale entropy to cardiac interbeat interval time series of healthy subjects, those with congestive heart failure and those with atrial fibrillation. They concluded that under pathologic conditions, the structure of the time series variability may change in two different ways. One dynamical route towards disease is associated with loss of variability and the emergence of regular patterns (e.g. heart failure). The other dynamical route is associated with more random types of outputs (e.g. atrial fibrillation). In both cases, MSE reveals decrease in system complexity.

Prediction of hospital mortality in trauma patients [80]**:**

Norris et al. showed that nonsurvivors show lower SampEn at each scale factor and therefore lower MSE. Survivors had higher *SampEn* values, indicating more variability of HR and fewer consistent repeating patterns. This effect was consistent when MSE was computed across various durations of HR data. They concluded that MSE of the heart rate within hours of hospital admission predicts death occurring days later and that complexity may be a new physiological biomarker of the outcome.

Detection of subtle abnormalities in cardiovascular control in young patients with diabetes mellitus type1 [50]**:**

Trunkvalterova et al. concluded that MSE analysis of spontaneous HR and Blood pressure oscillations is able to detect subtle abnormalities in cardiovascular control in young patients with diabetes mellitus, supporting the concept of complexity loss. The values of *SampEn* in diabetes mellitus patients were significantly reduced on coarse-grained signals (scales 2 and 3). They suggest that complexity is mostly reduced on scales covering Respiratory Sinus Arrhythmia, which is in accordance with the parasympathetic dysfunction in diabetes mellitus.

Indication of fetal distress associated with the presence of a pathological condition at birth [81]**:**

Ferrario et al. applied the *ApEn* and *SampEn* estimators to fetal heart rate signals on both single and multiple scales for an early identification of fetal sufferance antepartum. Their results showed that the *ApEn* index significantly distinguishes suffering fetuses from normal fetuses between the 30th and the 35th week of gestation. They state that MSE entropy values are reliable indicators of the fetal distress associated with the presence of a pathological condition at birth.

Stability and improvements:

Multiscale entropy suffers from two limitations: 1. The artificial MSE reduction due to the coarse graining procedure. [82] 2. The introduction of spurious MSE oscillations due to the suboptimal procedure for the elimination of the fast temporal scales. The MSE approach eliminates fast temporal scales (e.g. short-term neural regulation carried out by the autonomic nervous system) in order to focus progressively on slower time scales (e.g. vasomotor control, chemoreflex regulation and thermoregulation). [83]

Valencia et al. [83] proposed a refined method of the MSE in order to avoid these limitations. The method is called Refined Multiscale Entropy (RMSE) and it offers a way to resolve the two shortcomings that produce the MSE dependence on variance and on the shape of the power spectrum of the considered series. [83]

1.3. Sleep

Sleep is an important topic in the lives of human beings because it is necessary for survival. Other than its general known function of revitalizing the human body sleep can also be associated with various pathologic conditions. Therefore sleep has been subject of studies for many of years. It can be described as state of rest which normalizes physiological parameters destabilized during the day. [1] From a practical point of view falling asleep can be promoted by lying down relaxed in a comfortable thermal environment, warm drinks, hypnotic suggestions of warmth, autogenic training, switching off lights or sleep medicine. [84] It is composed of different cycles of REM (Rapid eye movement) and NREM (Non-rapid eye movement) phases, with NREM consisting of shallow to deep sleep stages. Those cycles of sleep vary in human beings of different age groups. In children and young people cycles of about 2 hours duration each can be observed. Especially children exhibit a lot of deep sleep and a lot of REM phases, while elders have an increased amount of shallow sleep. Elders also experience more nocturnal awakenings leading to fragmented sleep and therefore to poorer sleep quality. [1] The deterioration of deep sleep with aging can be seen in table 1.7:

Sleep phases/stages	Young adults (about 25 years)	Elderly persons (about 80 years)
Awake	< 5 %	14 %
REM	25 %	18 %
NREM Stage 1	4 %	8 %
NREM Stage 2	50 %	54 %
NREM Stage 3	6 %	4 %
NREM Stage 4	13 %	2 %

Table 1.7: Relative durations of sleep phases and stages for young adults and elderly persons [1]

Sleep is tightly coupled to the circadian rhythm. Circadian rhythms have an impact on biochemical, physiological and psychological parameters. For example the stress hormone cortisol is produced in the second half of the night to prepare the body for waking up. Another example is the hormone melatonin which is activated by darkness and causes drowsiness, and lower body temperature.

1.3.1. Sleep stages

The characterization of sleep which is widely used today was originally introduced by Rechtschaffen and Kales [85]. It consists of different stages and phases such as an awake phase, a REM phase and several NREM phases (S1-S4). 2007 the American Acedemy of Sleep Medicine (AASM) proposed new guidelines for sleep scoring where they combined sleep stages S3 and S4 [86]. There are some significant differences between conventional sleep scoring and the new AASM standard and thus new normative data still has to be established [87]. Therefore we decided to use the sleep scoring method by Rechtschaffen and Kales. Different sleep stages can be visualized in so called Somnograms or Hypnograms. (Figure 1.18)

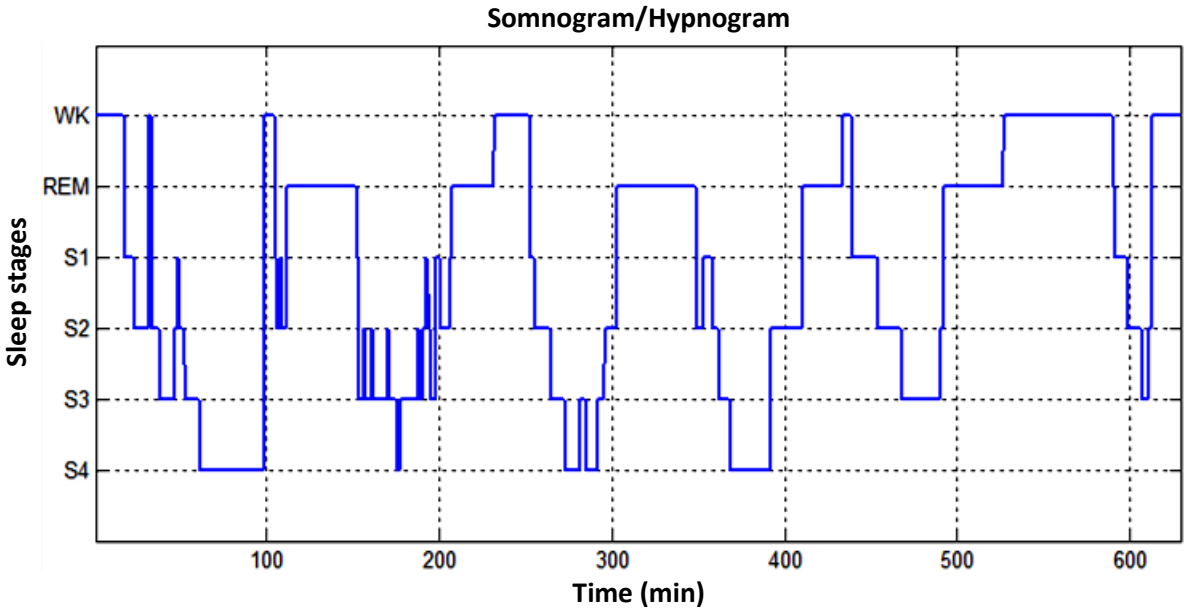

Figure 1.18: Somnogram/Hypnogram showing different sleep stages (Awake, REM, S1-S4) over time in minutes (Dataset nr. 10)

Each sleep phase has its own purpose. REM sleep is accompanied by a heightened mental activity which includes counteracting daily life's wearing effects like realistic rehearsals of threatening events, memorable dreaming and processing/saving implicit memory tasks. NREM sleep corresponds to revitalization of the body and plays an important role in processing of explicit memory tasks. Sleep stages can be classified by Polysomnography (PSG) by measuring different physiological signals using multiple measuring and recording devices [1]:

	Electroencephalogram (EEG) Brain activity	**Electrooculogram (EOG) Eye movements**	**Electromyogram (EMG) Muscle tension**	**Electrocardiogram (ECG) Heartbeats**
Awake	Relatively fast alpha and beta waves	Normal eye movement	High muscle tension	
REM		Rapid eye movements	Nearly absent muscle tension	Accelerated heartbeat
S1	Reduction of alpha waves, increase of theta waves	Slow eye movements	Vanishing muscle tension	
S2	Theta waves, upcoming delta waves	No eye movements	Decreasing muscle tension	
S3	Domination of delta waves (up to 50 %) and increased amplitude	No eye movements	Further decreasing muscle tension	
S4	Domination of delta waves > 50 %	No eye movements	Low muscle tension	

Table 1.8: Sleep stages and their physiological relations

1.3.2. Sleep and HRV

In general HRV is increased during sleep states as compared with the awake state indicating increased restorative effects of the body. HRV is highest during REM sleep and decreases with increasing sleep depth. During sleep we can identify different frequencies of the power spectral density of the consecutive RR-intervals corresponding to different physiological phenomena and therefore also to different sleep stages [1]:

Very low frequency (VLF) **Humoral activity**	**Low frequency (LF)** **Sympathetic activity**	**High frequency (HF)** **Parasympathetic activity**
0.01-0.06 Hz	0.06-0.15 Hz	0.15-0.4 Hz
Very slow oscillations in the rhythmogram most likely influenced by thermoregulation, humoral and metabolic regulation, circardian variations and blood pressure regulation	Slow oscillations in the rhythmogram influenced by arterial blood pressure oscillations in terms of baroreflex (resonance phenomenon in the control loop of the baroreflex involving sympathetic nervous system (SNS) and parasympathetic nervous system (PNS))	Mainly characterized by respiratory sinus arrhythmia (relatively rapid respiratory modulation of RR-intervals) which is mediated by the PNS

Table 1.9: Frequency ranges of HRV and their physiological relations

In healthy humans the LF frequency components dominate during REM sleep, while on the other side there is a HF dominance during NREM sleep. (Figure 1.19)

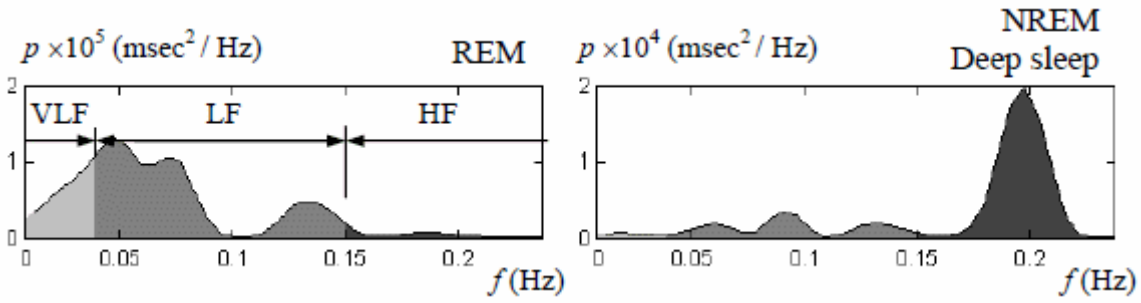

Figure 1.19: Power spectral density of HRV during REM and deep NREM sleep. It shows different frequency bands (Hz) of HRV (VLF, LF and HF) [1]

With depth of sleep HF components increase compared to shallow sleep stages. (Figure 1.20)

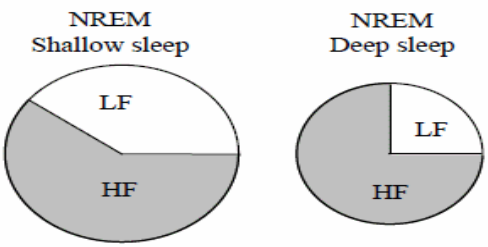

Figure 1.20: Relative distribution of LF and HF components during deep and shallow NREM sleep. [1]

1.3.3. Sleep and pathologic conditions

There are many disorders of sleep patterns of human beings. Some of them are serious enough to interfere with normal physical, mental and emotional functioning. Different types of sleep disorders such as Dyssomnias (sleep disorders characterized by either hypersomnia or insomnia) and Parasomnias (disorders that involve abnormal and unnatural movements, behaviors, emotions, perceptions and dreams in connection with sleep) have been identified. [88] Some of the sleep disorders which have a pathologic impact are for example:

Duration of sleep and mortality [89]:

Kripke et al. analyzed the data of 1.1 million men and women from 30 to 102 years of age. The best survival was found among those who slept 7 hours per night. Patients who slept 8 hours or more experienced significantly increased mortality hazard. The same was valid for patients who slept 6 hours or less. The increased risk exceeded 15 % for those reporting more than 8.5 hours or less than 4.5 or 3.5 hours of sleep.

REM sleep behavior disorder (RBD) as marker of neurodegenerative diseases [90]:

The skeletal muscle tone is usually reduced during REM sleep, preventing the acting out of dreams. In RBD the skeletal muscle remains active during dreaming, resulting in vocalization and sometimes violent activity of arms and legs. Many patients insure themselves or their bed partners while dreaming that they are defending themselves against an attack. Studies have shown that neurologically normal RBD patients have reduces striatal dopamine activity, suggesting that they may be in the pre-symptomatic stages of Parkinson's disease. These insights may provide a way of identifying patients with a high risk of developing serious neurologic disease and therefore perhaps allowing preventive therapies to be administered in the future.

Obstructive sleep apnea [91]:

Gastaut et al. documented the sleep of patients with obesity hypoventilation and found that they had repetitive episodes of upper-airway obstruction terminated by brief arousals that in turn fragmented nocturnal sleep, obstructive sleep apnea (OSA). It has been determined that OSA produces sleep fragmentation and daytime sleepiness. OSA is a common condition affecting men and women. Epidemiologic studies have confirmed that obesity remains one of the major risk factors for OSA. It can also be associated with the hypertension, along with an increased prevalence of coronary heart disease, heart failure and stroke.

2. Methodology

In order to get an RR-interval series it is necessary to detect R-peaks of the QRS-complex of ECG recordings. ECG recordings contain a lot of artifacts which have an effect on R-peak detection algorithms. Therefore it was necessary to preprocess ECG signals and remove those artifacts. Our gained RR-interval series contained outliers which had to be removed manually. With a clean RR-interval series it was possible to calculate spectrum weighted mean frequencies of all spectrums of HRV which are the basis of our HRV based sleep estimation. After considering some options and parameters we were able to compare our estimation of sleep stages to the sleep stages recorded by conventional PSG.

2. 1. Data

For our study we acquired 22 sets of sleep data from Giedrius Varoneckas, Professor at the Institute of Psychophysiology and Rehabilitation, Kaunas University of Medicine, Lithuania. The data was stored in the EDF file format and contained multiple channels such as for example ECG, EEG, EOG and EMG channels. We extracted the ECG channel and stored it in the ASCII file format. The ECG data was recorded with a sampling rate of 2000 Hz. Additionally we acquired the corresponding somnogram data stored as text files which contained an assessment of the current sleep stage (Awake, REM, S1,S2,S3,S4) every 30 seconds during the period of sleep. Somnograms were detected by the means of standard PSG evaluation software (ALICE-4 Respironics) and then reassessed visually by an expert.
Our datasets contained healthy subjects, subjects suffering from insomnia or parasomnia and subjects with sleep apnea:

Dataset number	Diagnosis	Dataset number	Diagnosis
1	Insomnia	12	Sleep apnea/Insomnia
2	Insomnia	13	Insomnia
3	Insomnia	14	Insomnia
4	Insomnia	15	Insomnia
5	Insomnia	16	Insomnia
6	Insomnia	17	Insomnia
7	Healthy	18	Insomnia
8	Healthy	19	Insomnia
9	Healthy	20	Insomnia
10	Healthy	21	Insomnia
11	Healthy/Parasomnia	22	Insomnia

Table 2.1: Used datasets and their pathologic conditions

2. 2. ECG preprocessing

We used the software MATLAB for our analysis. In order to ensure a good automated R-peak detection we removed some common artifacts of the recorded ECG signals such as baseline drift and noise. (Figure 2.1) We tried different filters for the removal of those artifacts. After a comparison we chose to use a moving average filter with a span of 1000 points for the removal of the baseline drift by using the MATLAB's smooth function. Once we had the signal without baseline drift, we removed noise artifacts by filtering our ECG signal with MATLAB's filter function by using an Nth order lowpass digital butterworth filter with a filter order of $N = 2$ and a cut-off frequency of $Wn = 0.025$.

a)

b)

c)

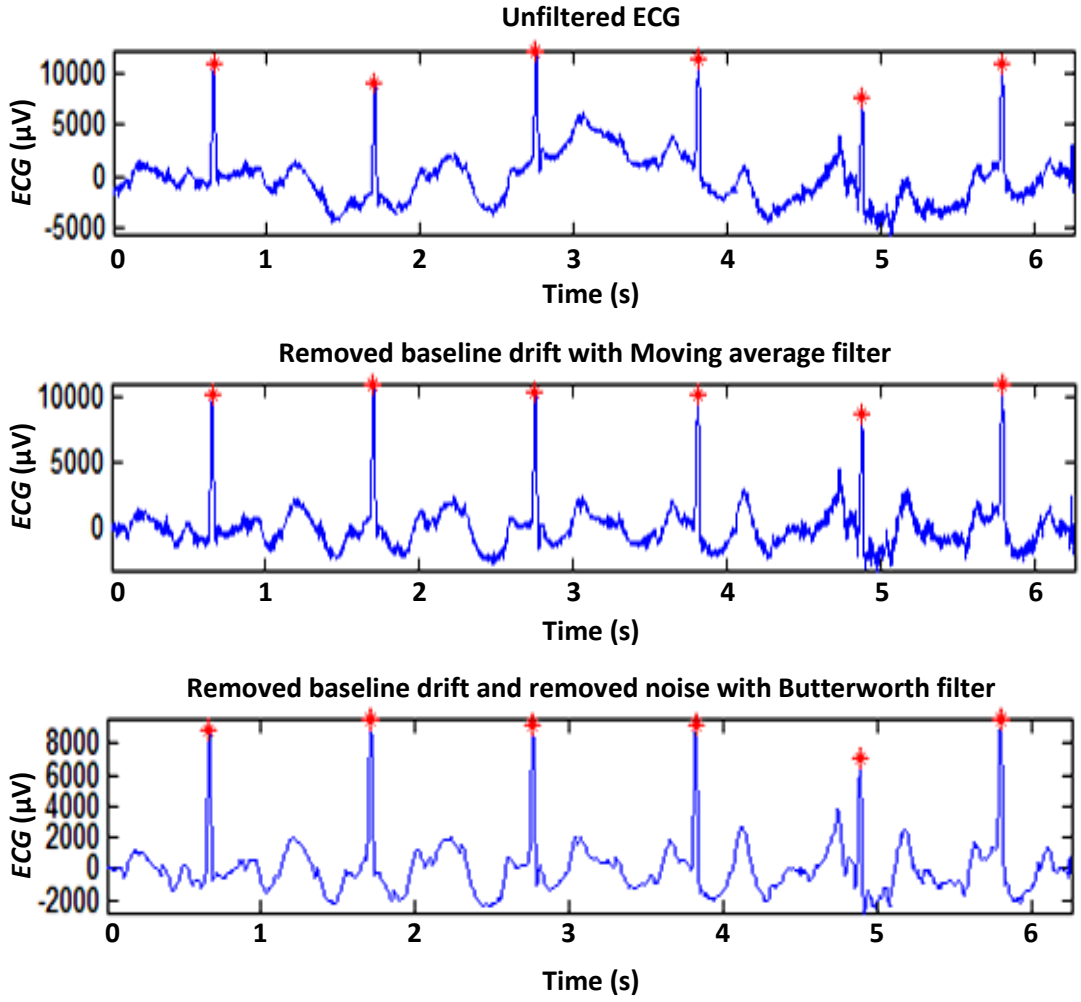

Figure 2.1: Preprocessing steps from the raw ECG signal to the clean one in order to ensure good R-peak detection. a) Raw ECG signal with noise and baseline drift. b) The baseline drift of the ECG was removed with an algorithm using a moving average filter. c) The noise of the ECG signal was removed by using a Butterworth filter.

2. 3. R-peak detection and correction of RR-intervals

To identify R-peaks of the ECG data we used an R-peak detection algorithm developed by the Vienna University of technology. Even though the R-peak detection algorithm worked really well, some R-peaks were missed or falsely identified due to ectopic beats and strong noise (e.g. movement artifacts) in some parts of the ECG signals. (Figure 2.2) We compared and corrected each RR-interval series manually. Ectopic beats and false R-peak detections were removed from our RR-interval series. (Figure 2.3) For further analysis it was important to preserve the information of the exact point in time when the individual RR-intervals were detected.

RR-intervals before manual correction:

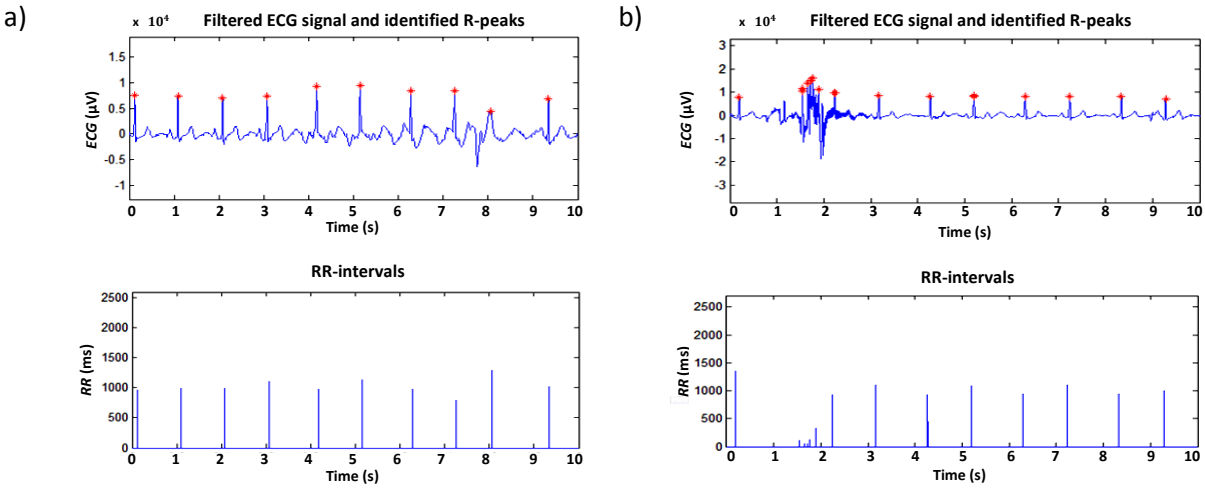

Figure 2.2: Filtered ECG signal (top) and its corresponding RR-interval series (bottom) containing artifacts which have to be corrected in order to use PSD correctly. a) ECG with falsely identified R-peak (ectopic beat) and RR-interval series. b) ECG with falsely identified R-peaks due to movement artifacts and RR-interval series.

RR-intervals after manual correction:

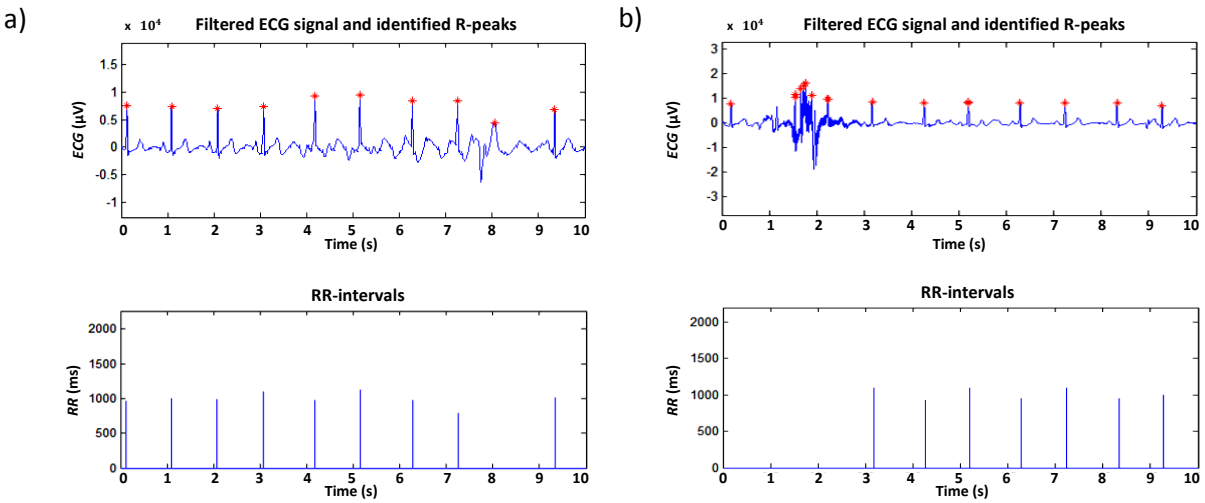

Figure 2.3: ECG (top) and corresponding corrected RR-interval series (bottom) a) Removed RR-interval (ectopic beat). b) Removed RR-intervals originating from movement artifacts.

2. 4. Spectrum weighted mean frequencies

As shown by Kaniusas et al. [2]:

Since the established sequence of RR-intervals represents an irregularly time-sampled signal, the sequence was linearly interpolated with a frequency of F_1 = 3 Hz. The value of F_1 was chosen to be higher than the highest instantaneous heart rate and sufficiently high that the Nyquist frequency ($= \frac{F_1}{2} = 1.5$ Hz) of the HRV-spectrum is not within the frequency range of interest (i.e., up to 0.5 Hz).

The values of the power spectral density (p) were estimated in absolute units (ms^2/Hz) using intervals of 60 seconds (180 points) with zero overlap, applying Hamming smoothing and zero padding up to 512 points. Thus the resulting frequency resolution of p was about 0.006 Hz (=$F_1/512$). i.e. sufficiently fine to estimate p in the lowest humoral band.

Spectrum-weighted frequencies f_W were assessed according to:

$$f_W = \int_{f\,\min}^{f\,\max} f \cdot \mathrm{d}A \Big/ \int_{f\,\min}^{f\,\max} \mathrm{d}A = \int_{f\,\min}^{f\,\max} f \cdot p \cdot \mathrm{d}f \Big/ \int_{f\,\min}^{f\,\max} p \cdot \mathrm{d}f \qquad (2.1)$$

where f is the frequency, $f_{\min}$ and $f_{\max}$ are the lower and upper bounds of the relevant frequency range, respectively, and A is the area encompassed by p. It can be derived from Eq. 2.1 that f_{W} represents the frequency of the center of A in the given frequency range [$f_{\min}$, $f_{\max}$]. The values of f_{W} were assessed for different frequency ranges:

Total ($f_{\mathrm{W}}^{\mathrm{t}}$):	0.01-0.5 Hz
Humoral ($f_{\mathrm{W}}^{\mathrm{h}}$):	0.01-0.06 Hz
Sympathetic ($f_{\mathrm{W}}^{\mathrm{s}}$):	0.06-0.15 Hz
Parasympathetic ($f_{\mathrm{W}}^{\mathrm{p}}$):	0.15-0.4 Hz

The chosen ranges are widely accepted for HRV analysis in the clinical and research fields, and correspond to a particular physiological activity or sleep stage. Spectrum weighted mean frequencies of HRV can be seen in figure 2.4.

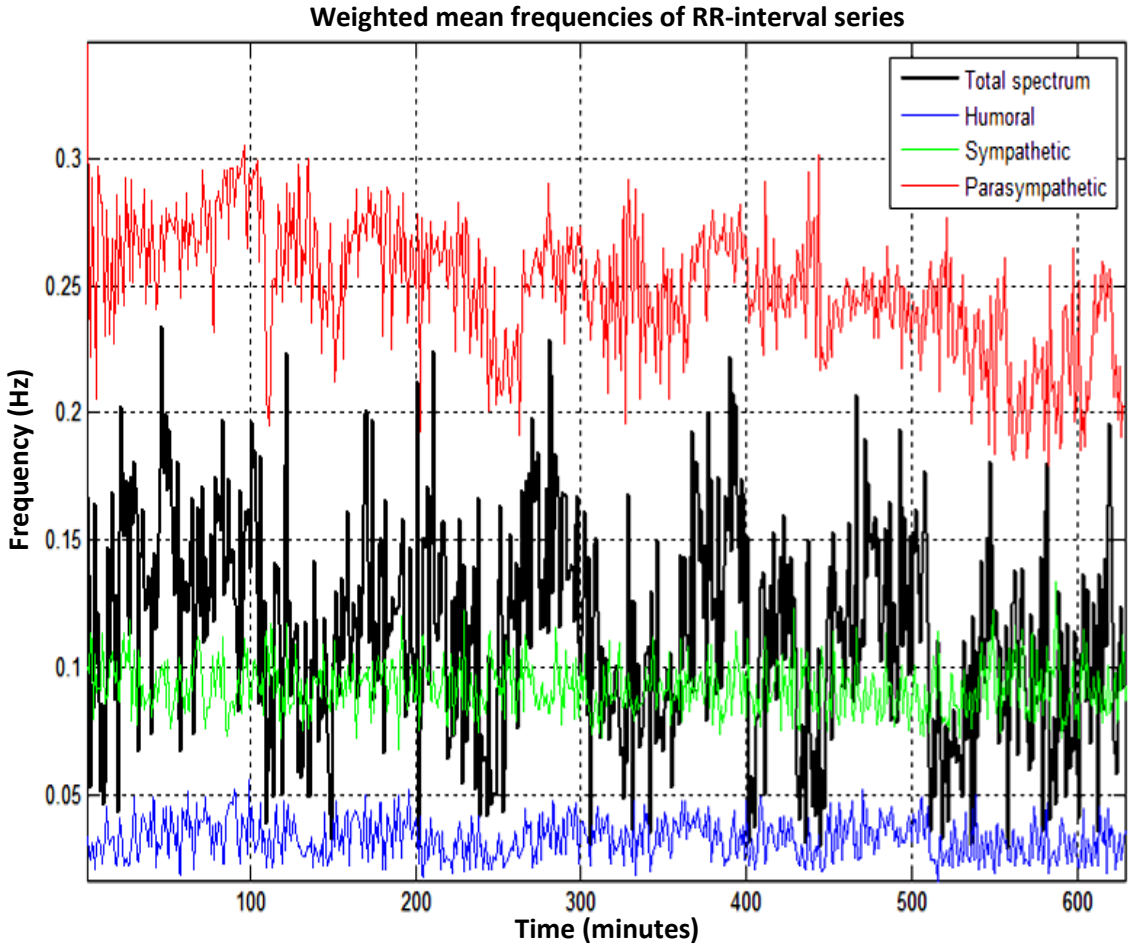

Figure 2.4: Weighted mean frequencies of RR-interval series containing different frequency ranges of HRV $f_{\mathrm{W}}^{\mathrm{t}}$(black trace), $f_{\mathrm{W}}^{\mathrm{h}}$(blue trace), $f_{\mathrm{W}}^{\mathrm{s}}$(green trace) and $f_{\mathrm{W}}^{\mathrm{p}}$ (red trace). (Dataset nr. 10)

2. 5. Comparison of weighted mean frequencies with sleep stages

For further analysis we only used the weighted mean frequencies of the total spectrum f_{W}^{t} (black trace in figure 2.4). To analyze the correlation between $f_{\mathrm{W}}^{\mathrm{t}}$ and acquired somnograms recorded by conventional PSG we processed both signals and considered different options on how to improve the correlation between them. The signals were rescaled into relative units and filtered with the same filter parameters. After rescaling we inverted $f_{\mathrm{W}}^{\mathrm{t}}$ and considered combining sleep stages, the removal of sleep stages of short period of time and different smoothing procedures.

2. 5. 1. Inversion of signal and relative units

We inverted $f_{\mathrm{W}}^{\mathrm{t}}$ to get a better visual assessment of the correlation between f_{W}^{t} and the different sleep stages of the somnogram. We chose to compare two different ways of signal inversion. The Inversion $f_{\mathrm{Winv}}^{\mathrm{t}}$ was calculated by:

$$f_{\mathrm{Winv}}^{\mathrm{t}} = f_{\mathrm{W}}^{\mathrm{t}} * (-1) \qquad (2.2) \qquad\qquad f_{\mathrm{Winv}}^{\mathrm{t}} = 1/f_{\mathrm{W}}^{\mathrm{t}} \qquad (2.3)$$

To compare the weighted mean frequencies to the somnograms we rescaled the signals to fit them between 0 and 1. To rescale the frequencies we calculated the new frequency $f_{\mathrm{Winv_{rel}}}^{\mathrm{t}}$:

$$f_{\mathrm{Winv,rel}}^{t} = \frac{f_{\mathrm{Winv}}^{\mathrm{t}} - \min\left(f_{\mathrm{Winv}}^{\mathrm{t}}\right)}{\max\left(f_{\mathrm{Winv}}^{\mathrm{t}}\right) - \min\left(f_{\mathrm{Winv}}^{\mathrm{t}}\right)} \qquad (2.4)$$

For better view-ability in Figure 2.5 and 2.6, $f_{\mathrm{Winv,rel}}^{t}$ was filtered by creating a filter kernel with fir1 using MATLAB. We used an Nth order filter of $N = 8$ and a cut-off frequency of $Wn = 0.1$. The filter uses a Hamming window of the length $N + 1$ and the normalized gain at Wn is -6 dB.

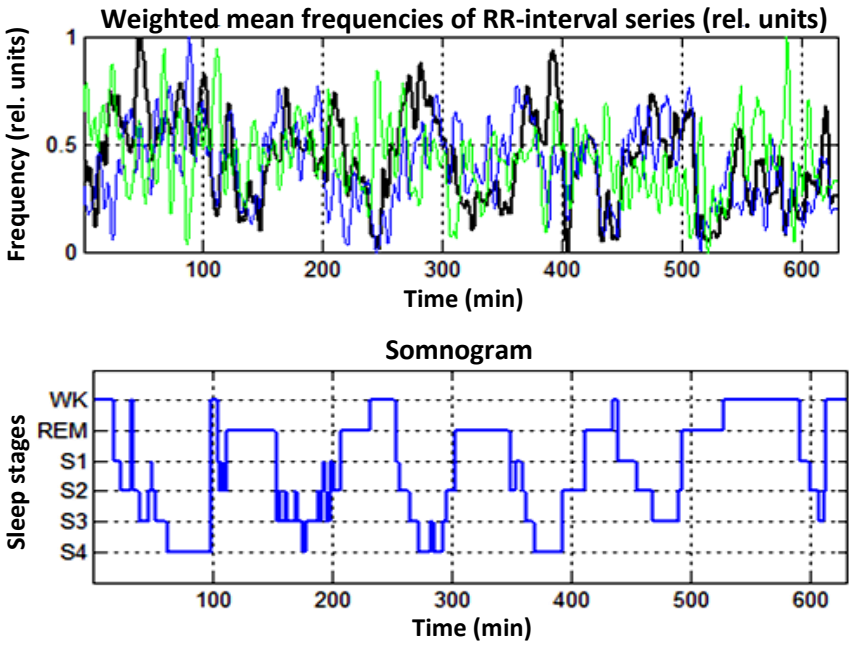

Figure 2.5: The diagram on top shows rescaled weighted mean frequencies of total spectrum of HRV f_{W}^{t} (black), humoral (blue), sympathetic (green) filtered with fir1 ($N = 8$, $Wn = 0.1$) and corresponding somnogram (blue) over time in minutes (bottom). (Dataset nr. 10)

a) b)

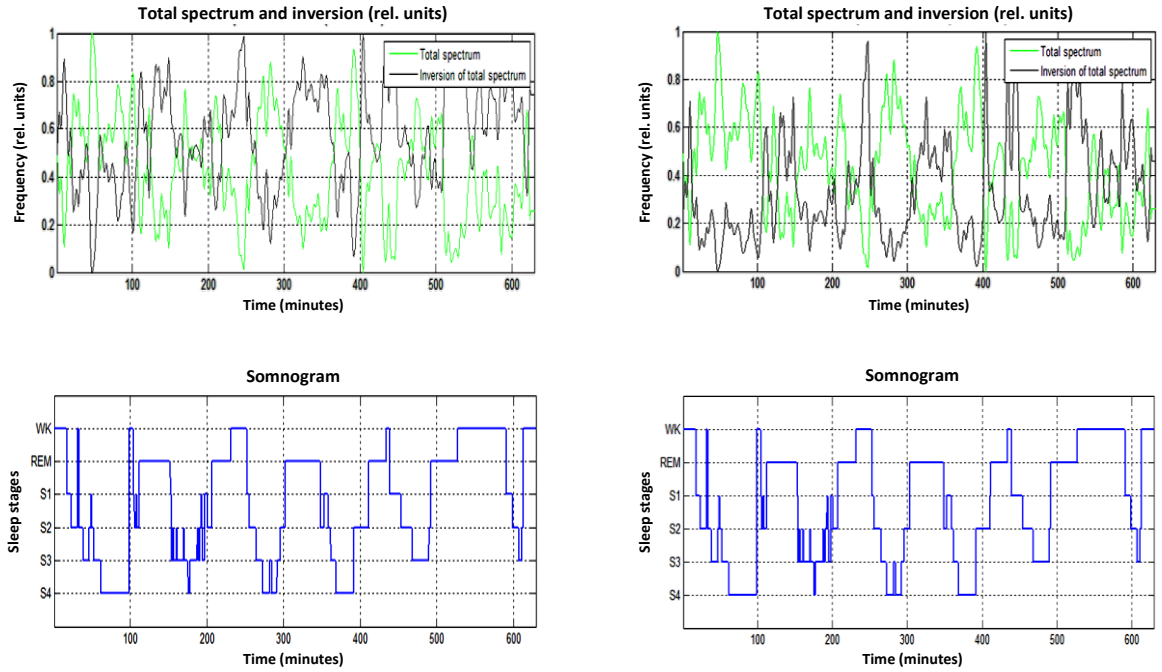

Figure 2.6: Weighted mean frequency of total spectrum f_{W}^{t} (green trace), its inversion (a: $f_{\mathrm{W}}^{\mathrm{t}} * (-1)$ and b: $1/f_{\mathrm{W}}^{\mathrm{t}}$) (black trace) filtered with fir1 (N=8, Wn=0.1) are shown on top and corresponding somnograms (blue trace) are shown in the bottom diagram. (Dataset nr. 10)

After a comparison we decided to use $f_{\mathrm{Winv}}^{\mathrm{t}} = f_{\mathrm{W}}^{\mathrm{t}} * (-1)$ as inversion method for further analysis.

2. 5. 2. Removal of sleep stages of short duration

We removed sleep stages of short periods of time (e.g. 1-3minutes) to get a “smoother” somnogram in order to achieve an improved correlation between the sleep stages and the weighted mean frequencies of the RR-interval data sets. (Figure 2.7) If a sleep stage lasts shorter than a specified range of minutes the value of the sleeps stage gets set to the value of the previous stage.

a)

b)

c)

d)

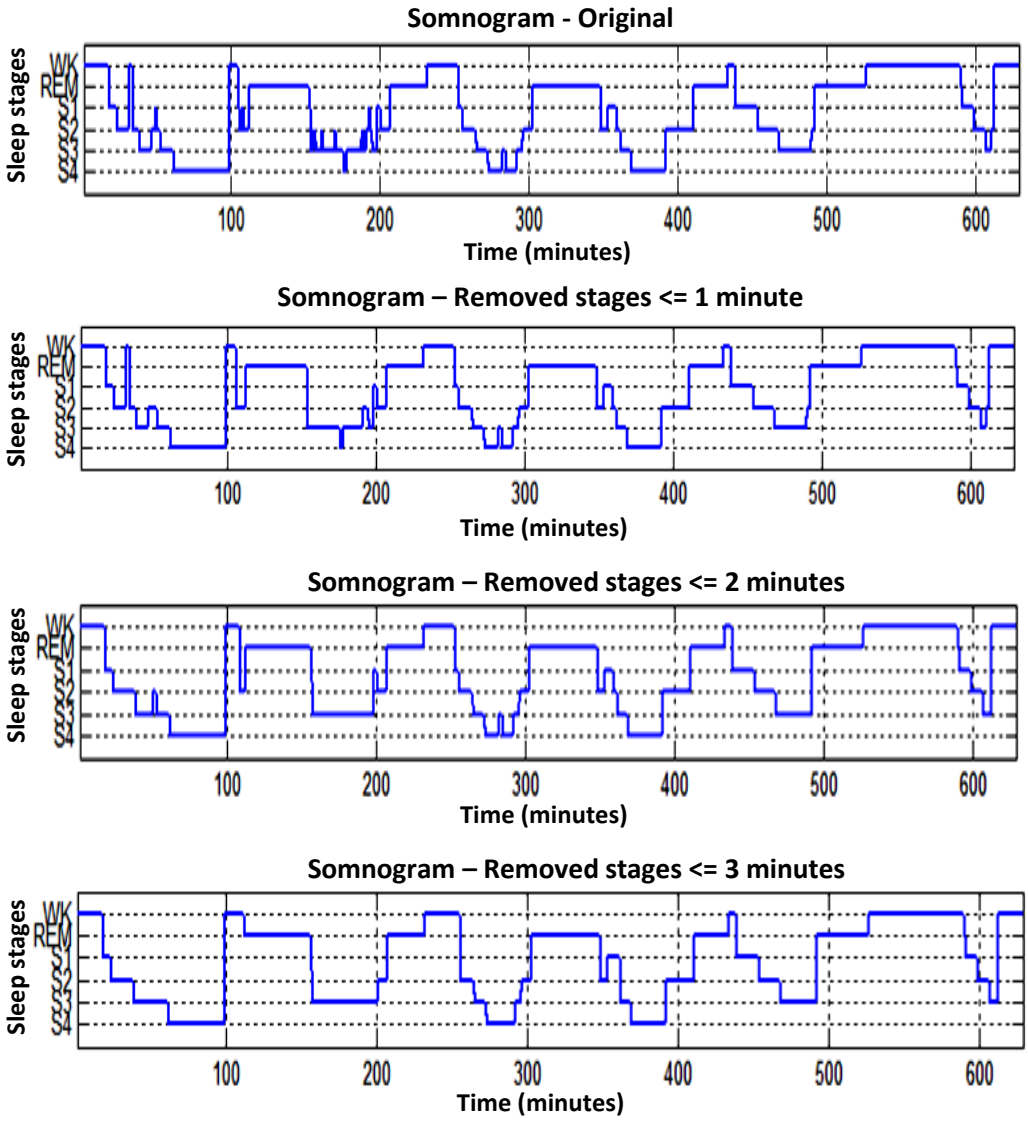

Figure 2.7: Comparison of somnograms with removed sleep stages of different periods of time. a) Original somnogram b) Removed sleep stages <= 1 minute c) Removed sleep stages <= 2 minutes, d) Removed sleep stages <= 3 minutes. (Dataset nr. 10)

2. 5. 3. Combining sleep stages

We also analyzed how the correlation between $f^{t}_{\mathrm{Winv,rel}}$ and the somnograms change if we combine different sleep stages. (Figure 2.8) Stages which lasted a short period of time were removed, as shown in the chapter above, before combining the different stages. 2007 the American Academy of Sleep Medicine provided new guidelines on sleep scoring where they combined S3 and S4 to a single stage. Therefore for one part we combined only S3 and S4 while the combination of WK+REM, S1+S2 and S3+S4 was our other choice of combination method.

a)

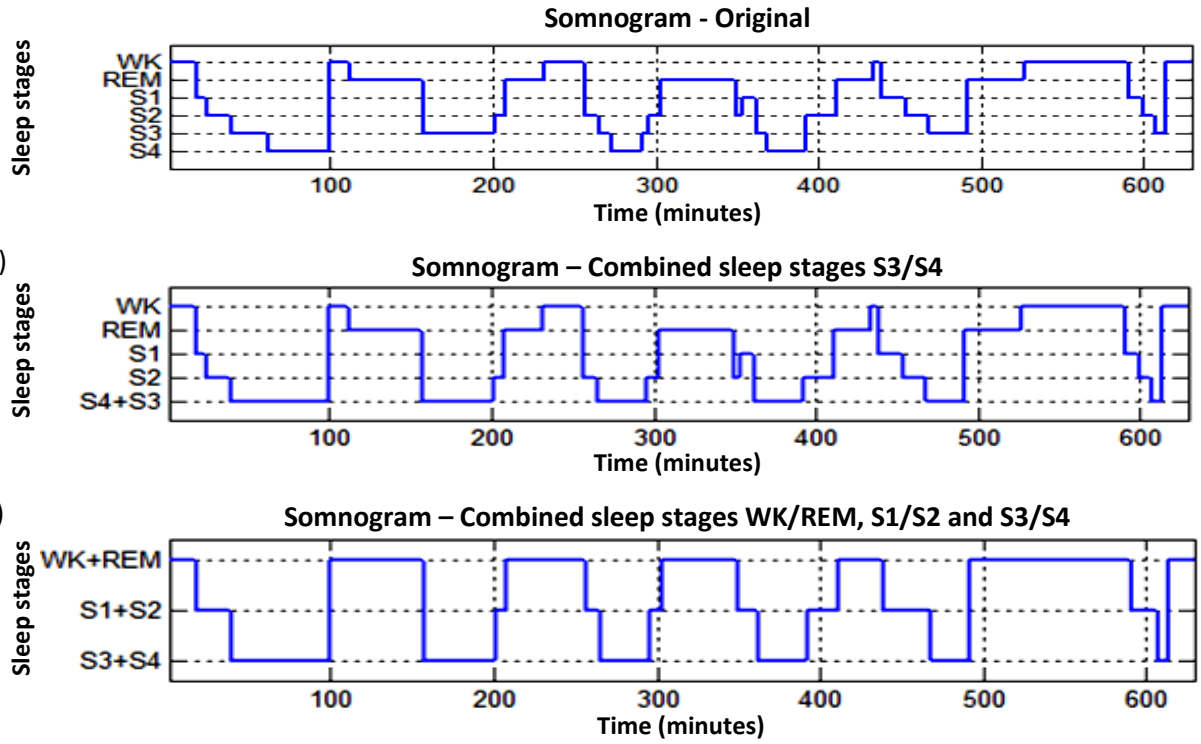

Figure 2.8: Combination of sleep stages. a) Original sleep stages after removal of stages of short period of time. b) Combination of S3 and S4 c) Combination of WK+REM, S1+S2 and S3+S4. (Dataset nr. 10)

2. 5. 4. Smoothing procedures

To compare $f^{\mathrm{t}}_{\mathrm{Winv,rel}}$ to the sleep stages of the somnograms we filtered both signals with the same filter. We used the MATLAB function fir1 to design our filters with different parameters. Fir1 designs an Nth order low pass filter with a cut-off frequency Wn. It uses a Hamming window of length $N + 1$. The cut-off frequency Wn must be between $0 < Wn < 1.0$ with 1.0 corresponding to half the sample rate. The normalized gain of the filter at Wn is -6 dB. We added values before and after the signal to eliminate the delay of the signal caused by the filter's settling time in order to preserve length and timing of the signal.

Comparison of signals using different filter orders N:

The higher the filter order N and therefore the window length of the hamming window, the smoother both signals get, but the more detail they lose. (Figure 2.9)

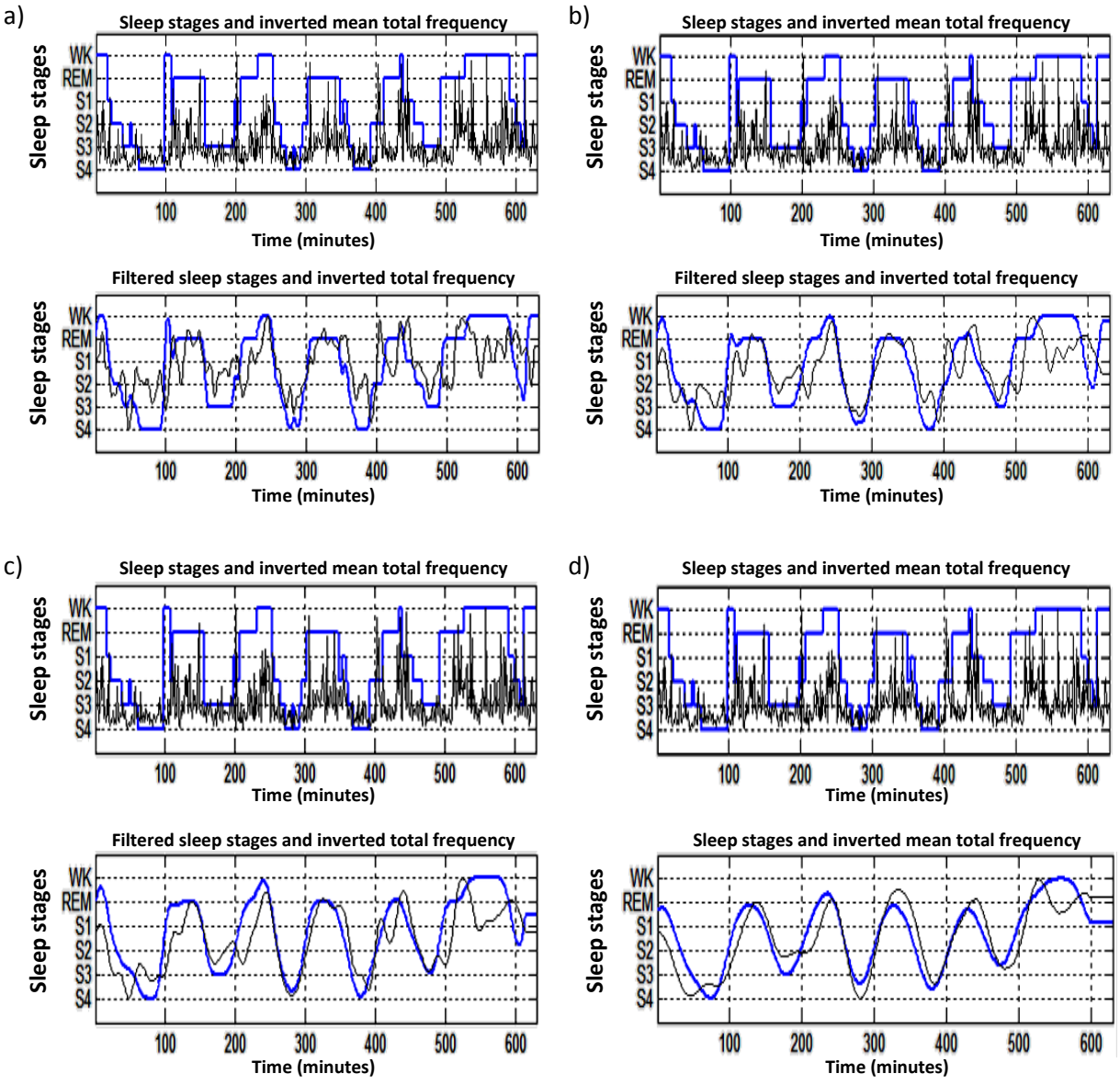

Figure 2.9: Original Sleep stages and $f^{\mathrm{t}}_{\mathrm{Winv,rel}}$ (top) compared to filtered version by using different filter orders. (bottom) N. Wn = 0.01, a) N=10, b) N = 20, c) N= 30, d) N=60. (Dataset nr. 10)

Comparison of signals using different cut-off frequencies Wn:

With a relatively high value of Wn we can see that there is still a lot of noise left especially in the HRV signal $f^{t}_{\mathrm{Winv,rel}}$, whereas with a lower value of Wn noise gets weaker. (Figure 2.10)

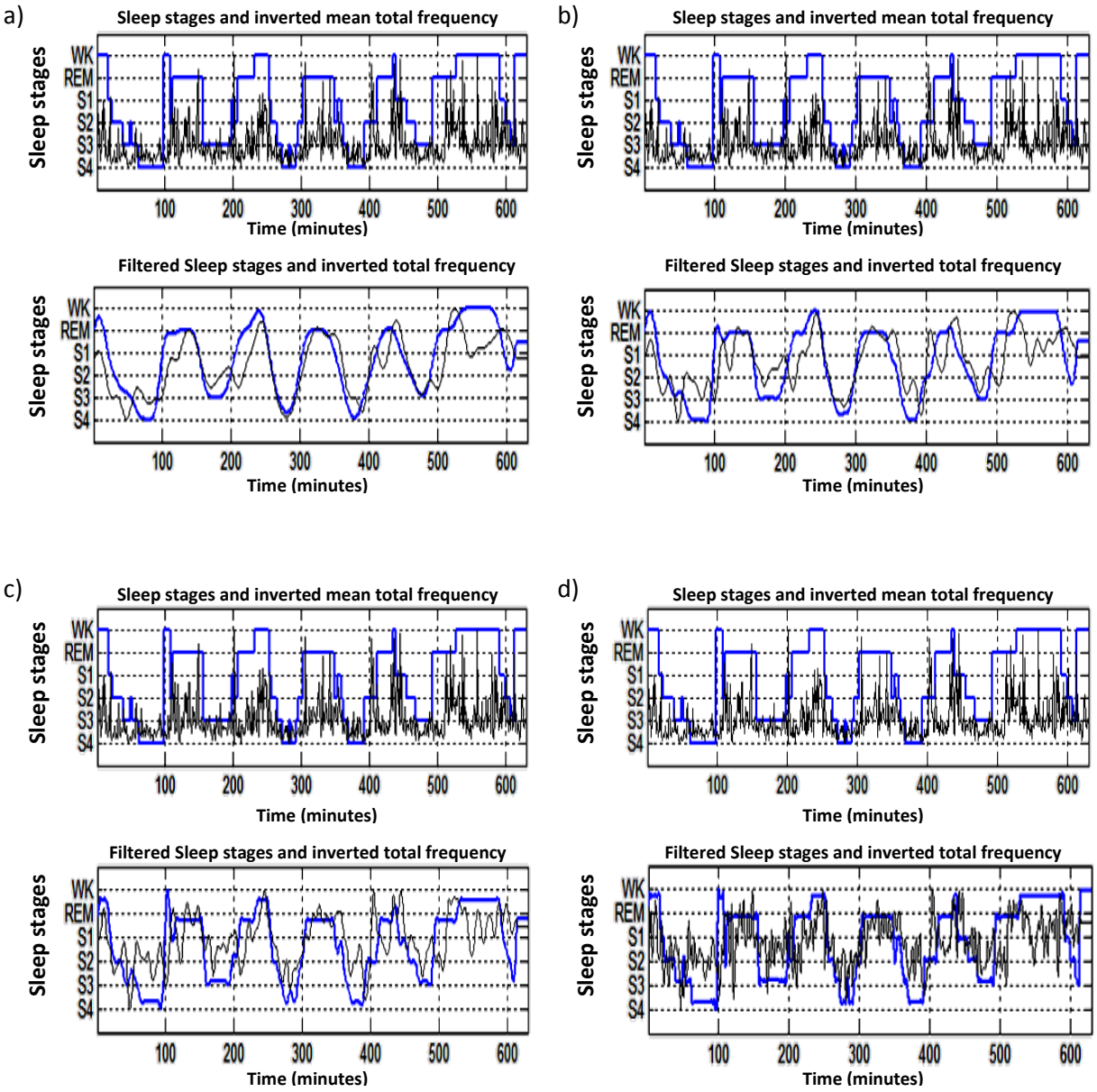

Figure 2.10: Original Sleep stages and $f^{t}_{\mathrm{Winv,rel}}$ (top) compared to filtered version by using different cut-off frequencies Wn. (bottom) N = 30 a) Wn = 0.01, b) Wn = 0.1, c) Wn = 0.2, d) Wn = 0.5. (Dataset nr. 10)

3. Results

We analyzed the 22 datasets we acquired with the different parameters shown above (Removal of short sleep stages of different duration, combining multiple sleep stages, using different filter orders N and using different cut-off frequencies (Wn)) and created plots of their cross-correlation coefficients r and their corresponding histograms. To investigate how the different choices of individual parameters we used influenced each single dataset we also visualized the influence with Box plots and multivariable charts.

3. 1. Correlations

The cross-correlation coefficient r (with $-1 \leq r \leq 1$) specifies the correlation between sleep stages of the somnograms and our HRV based sleep estimation $f^{\mathrm{t}}_{\mathrm{Winv,rel}}$.

Negative correlation	No correlation	Positive correlation
$r = -1$	$r = 0$	$r = 1$

Table 3.1: Ranges of cross-correlation coefficient r

3.1.1. Influence of different parameters on correlations

Removal of sleep stages of short duration:

The removal of sleep stages of short periods of time did not alter our results significantly. The cross-correlation coefficients r of some datasets alter in a very small range. The histograms just show small shifts of distribution of r. (Figure 3.1)

a)

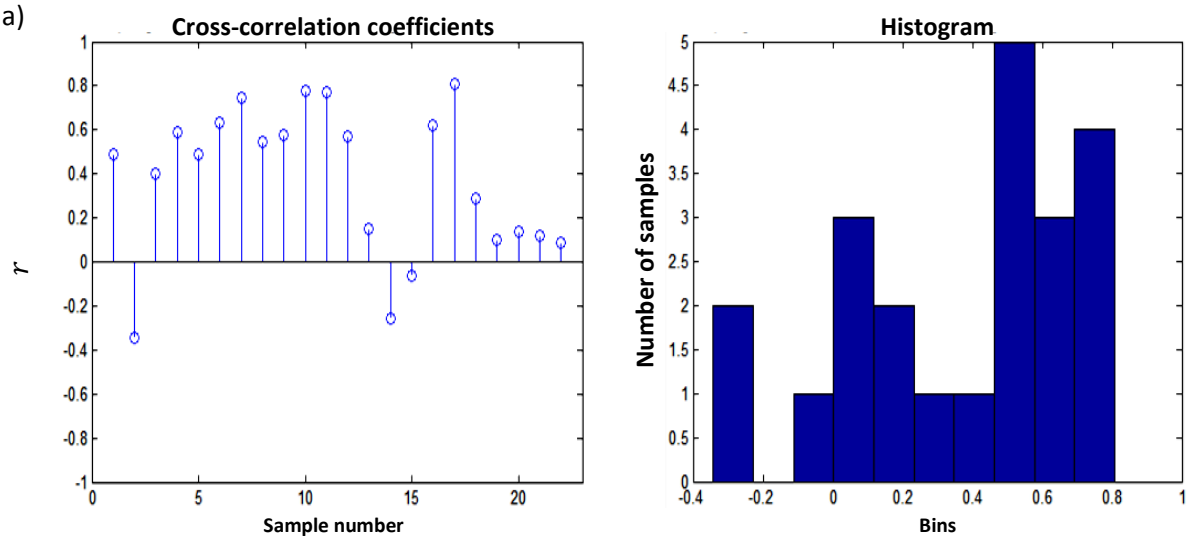

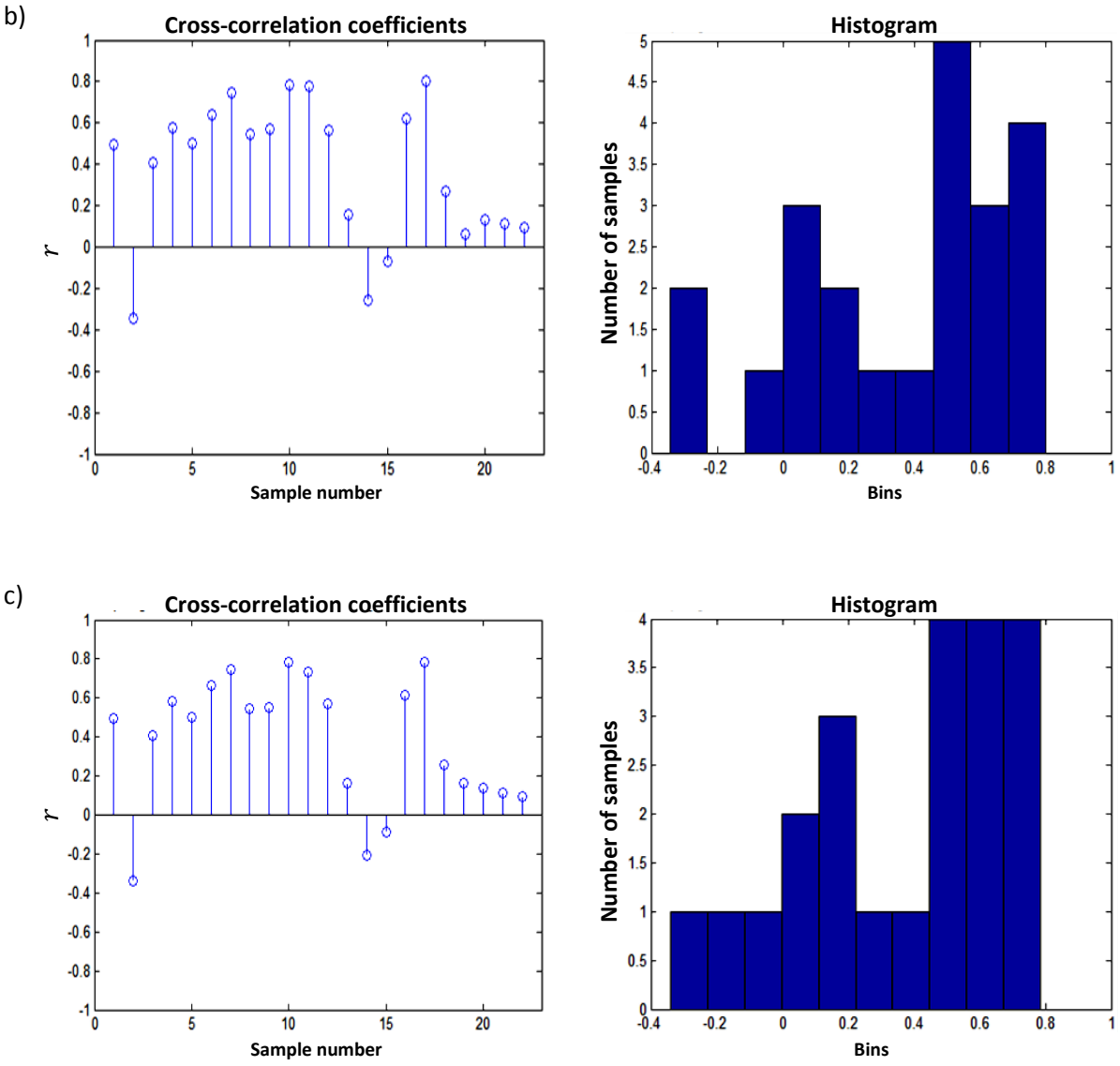

Figure 3.1: Comparison of cross-correlation coefficients r of sample datasets and histograms with removed sleep stages <= a) 1 minute b) 2 minutes c) 3 minutes.

Combination of sleep stages:

The combination of sleep stages seemed to influence our correlations and the distribution of r in the corresponding histograms. Whereas the combination of Wake+REM, S1+S2, S3+S4 (figure 3.2c) strengthens the correlation, the combination of only S3+S4 (figure 3.2b) weakens it significantly in a lot of cases. (Figure 3.2)

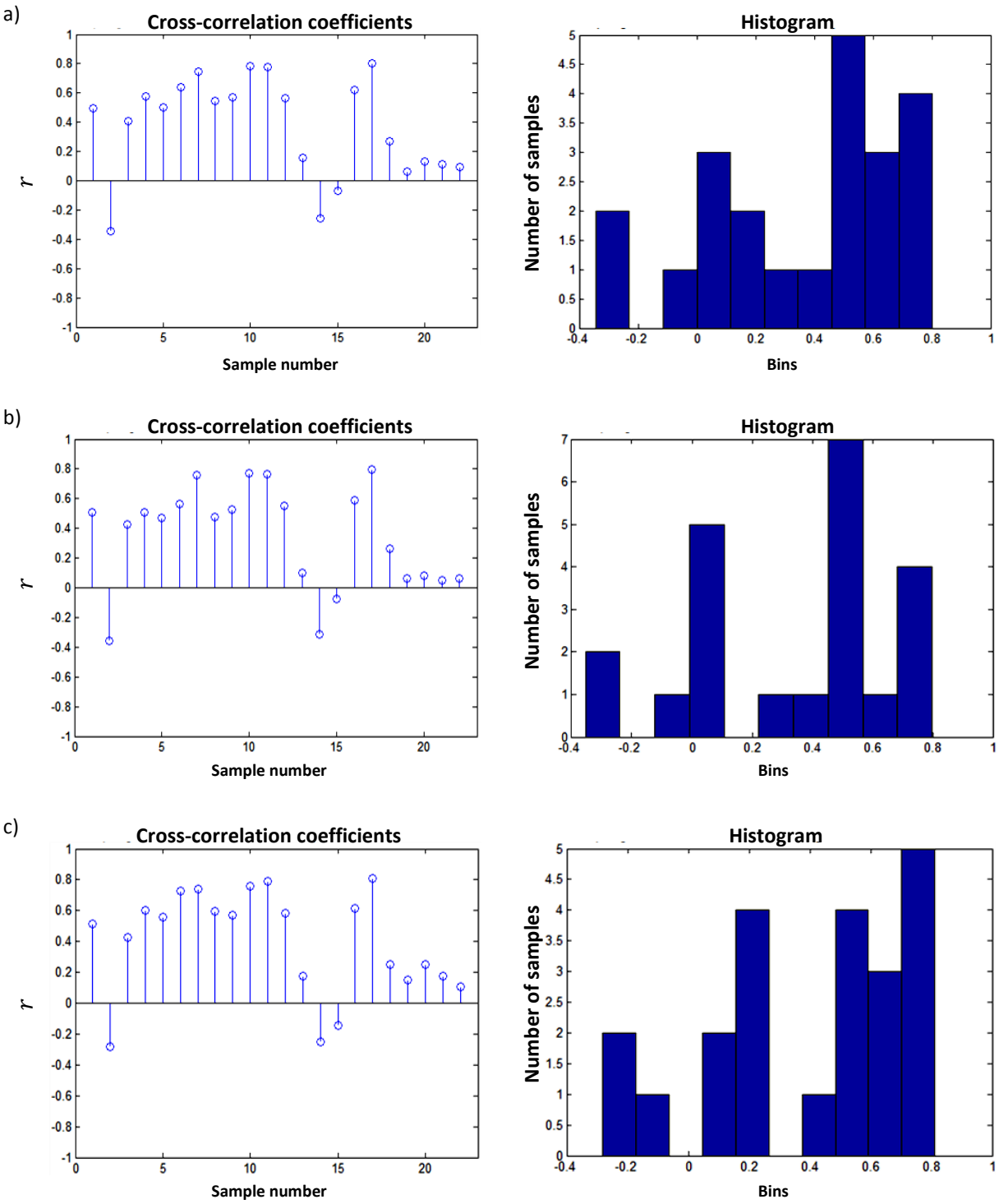

Figure 3.2: Comparison of cross-correlation coefficients r and histograms with combined sleep stages a) Not combined, b) S3 and S4 combined, c) WAKE and REM, S1 and S2, S3 and S4 combined

Different filter Orders N:

In general, a higher value of the filter order N improves the correlation of our sleep stages and our HRV based sleep evaluation. Both signals get "smoother" by increasing the filter order. Therefore there is also a loss of detail. (Figure 2.9)

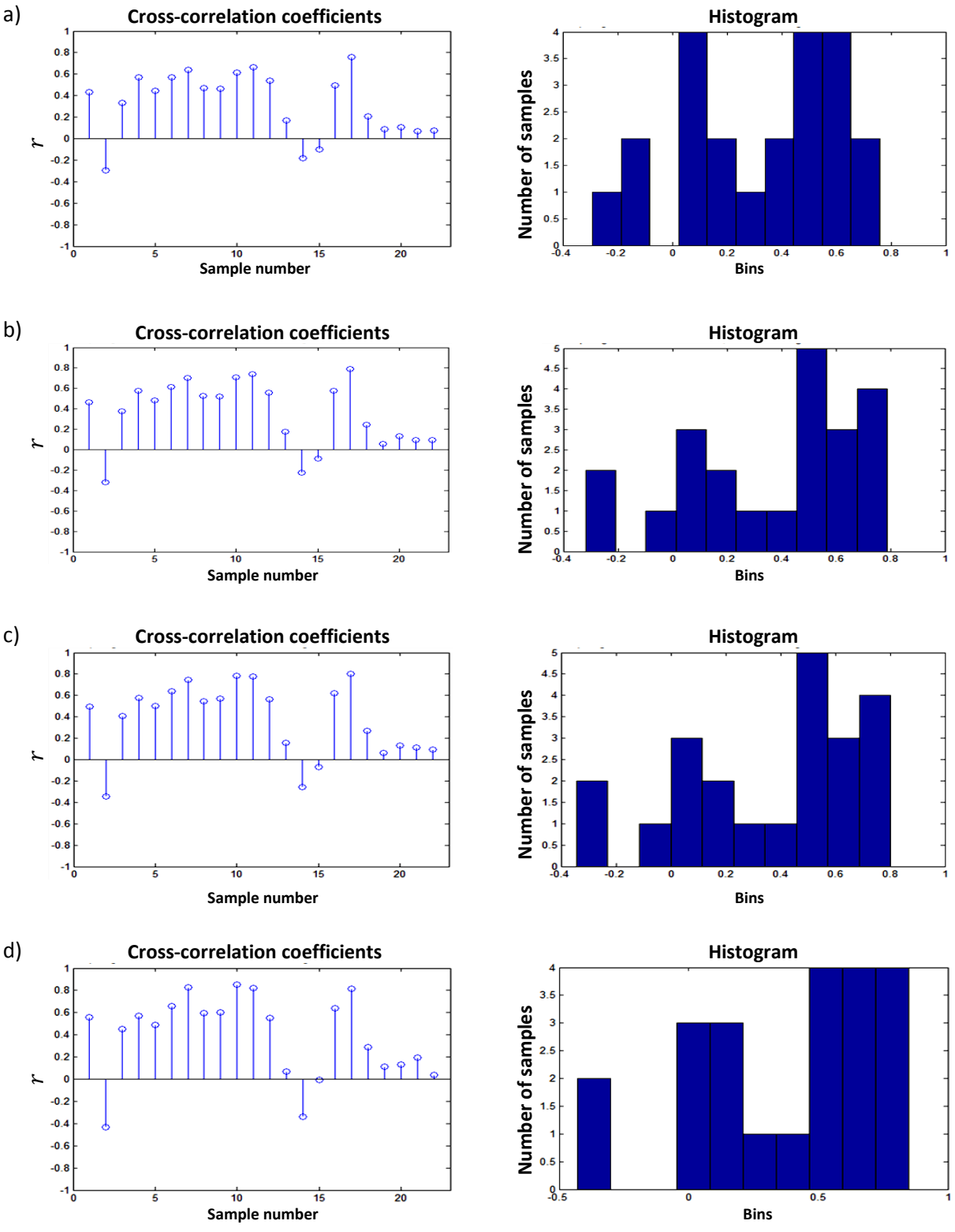

Figure 3.3: Comparison of cross-correlation coefficients r and histogram of different filter orders N a) N = 10, b) N = 20, c) N = 30 and d) N = 60

Different cut-off frequencies Wn:

In our datasets smaller cut-off frequencies in general resulted in higher correlations of sleep stages and our HRV based sleep estimation. With a relatively high value Wn there is still a lot of noise left especially in the HRV signal $f^{t}_{\mathrm{Winv,rel}}$ (Figure 2.10d) where as the noise is almost canceled out completely with a smaller value of Wn (Figure 2.10a) thus leading to different distributions of r seen in the histograms (Figure 3.4a-d).

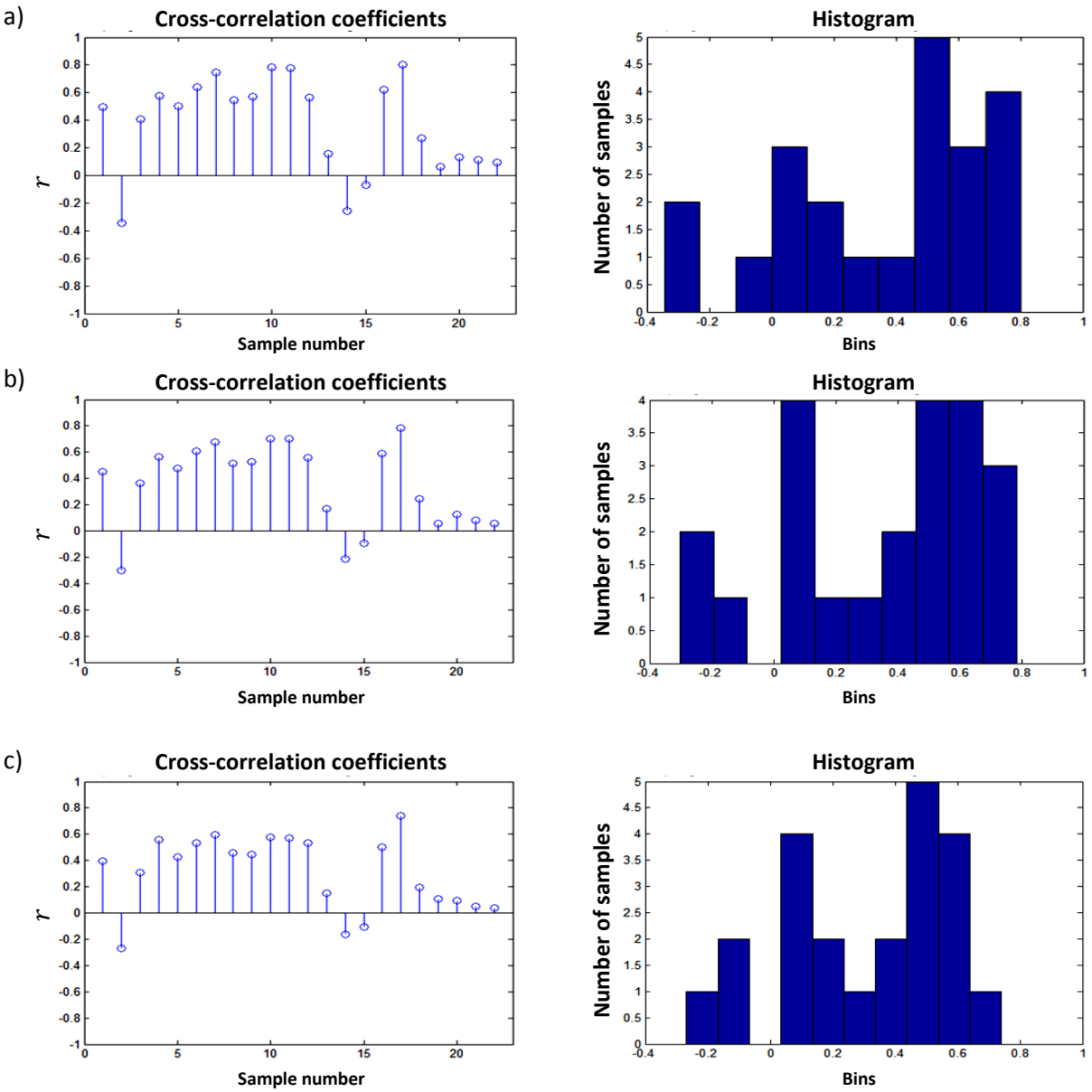

d)

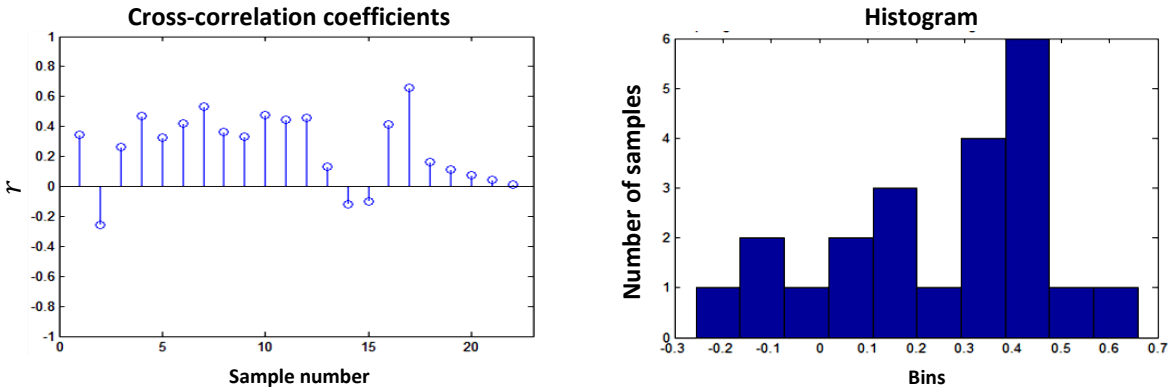

Figure 3.4: Comparison of cross-correlation coefficients r and histograms of different cut-off frequencies Wn a) Wn = 0.01, b) Wn = 0.1, c) Wn = 0.2 and d) Wn = 0.5

Boxplots and Multivariable charts

Box plots contain multiple statistical descriptors such as the median (red line), outliers (stars), first and third quartile (upper and lower box borders) and whiskers (lines outside the boxes) extending to the value which is the most extreme data value that is not an outlier. Multivariable charts visualize different parameters by assigning a different symbol to each option.

Different filter orders *N*:

Higher filter orders strengthened the correlation in most cases. It seems that datasets that have relatively higher correlation compared to datasets with a low correlation (around zero) especially increase with a choice of a higher filter order N. (Figure 3.5 and 3.6)

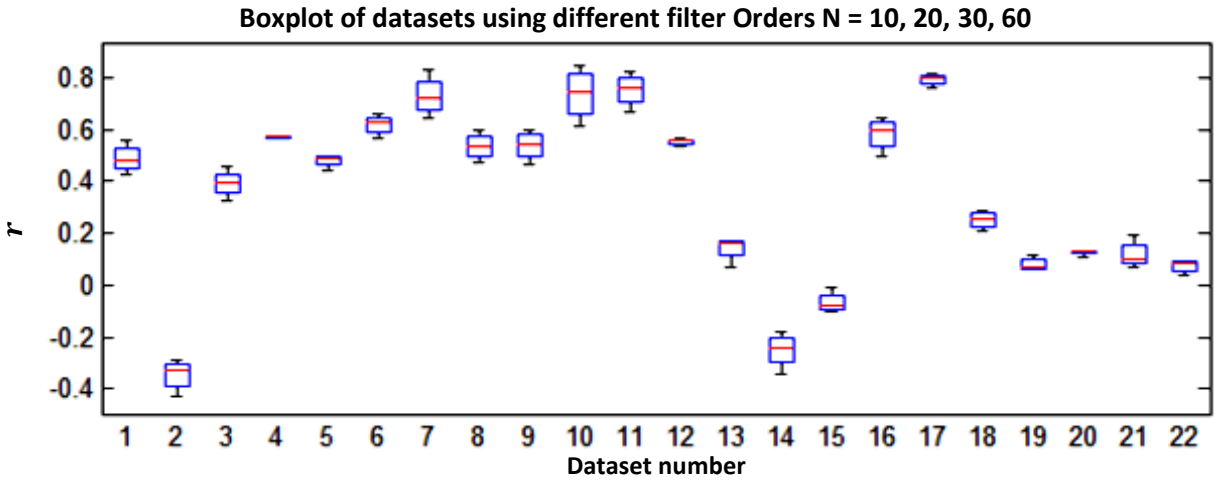

Figure 3.5: Box plot of 22 datasets using varying filter orders N = 10, 20, 30, 60. Wn=0.01, removed sleep stages <=2 minutes, sleep stages not combined.

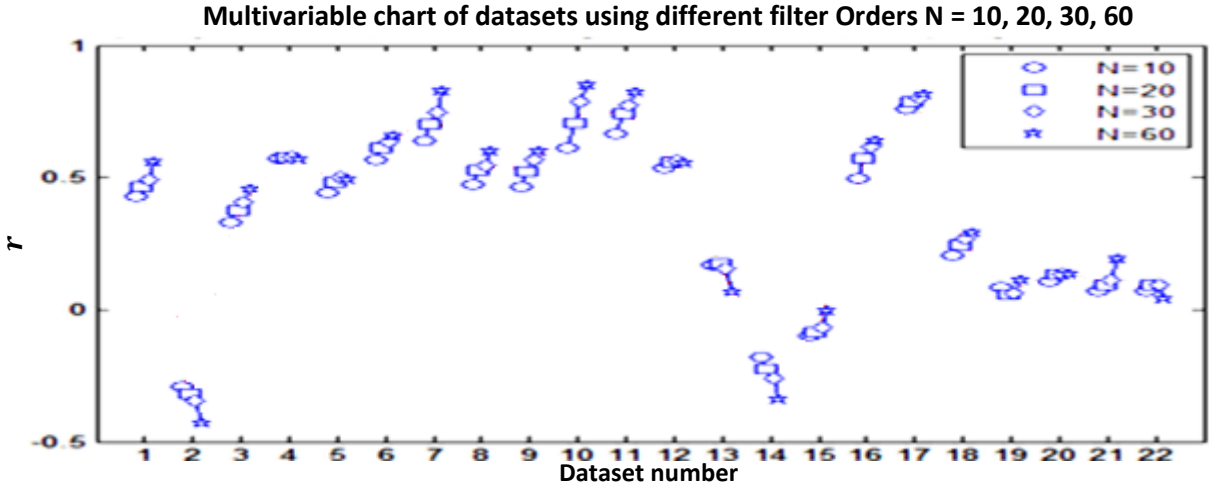

Figure 3.6: Multivariable chart of 22 datasets using varying filter orders N = 10, 20, 30, 60. Wn=0.01, removed sleep stages <=2 minutes, sleep stages not combined.

Different cut-off frequencies Wn:

Higher values of Wn generally weakened the correlation. Datasets where the correlation is relatively higher especially seemed to be influenced by the variation of cut-off frequencies, whereas datasets which did not correlate too well did not experience a big change in the cross-correlation coefficients r (Figure 3.8).

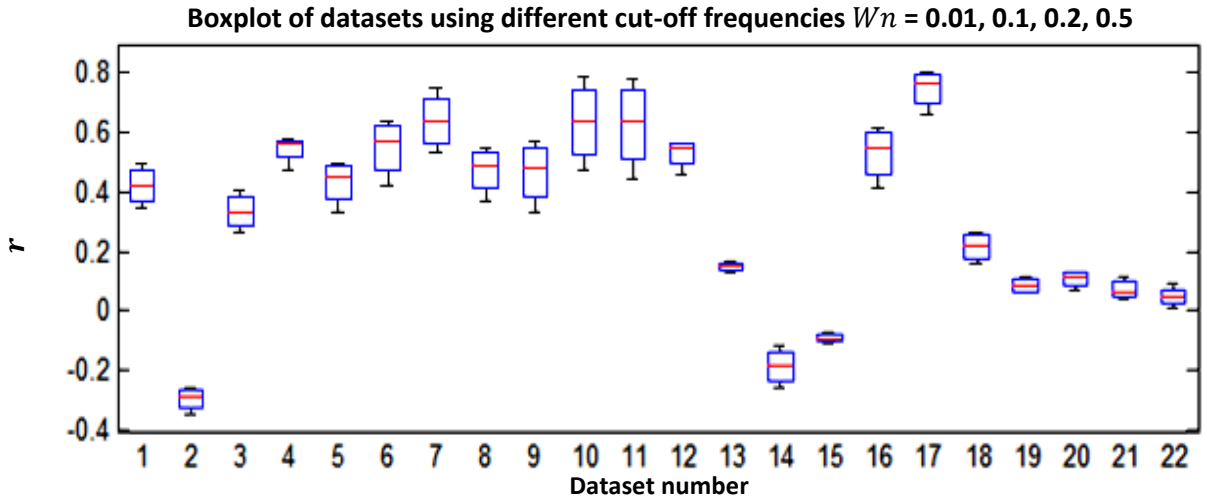

Figure 3.7: Box plot of 22 datasets using different cut-off frequencies Wn = 0.01, 0.1, 0.2, 0.5. N = 30, Removed stages <= 2 minutes, sleep stages not combined.

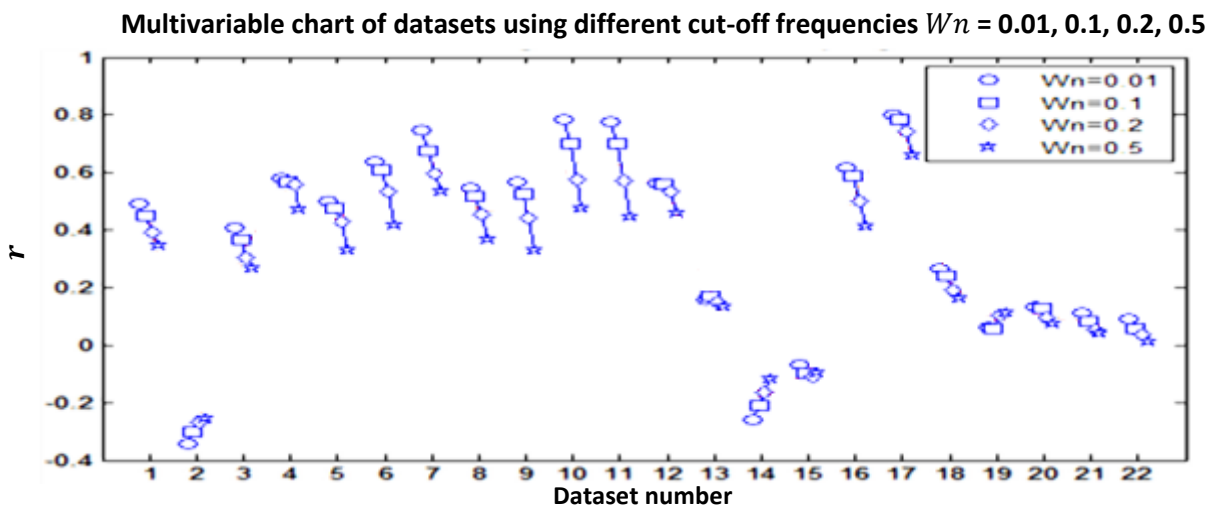

Figure 3.8: Multivariable chart of 22 datasets using different cut-off frequencies Wn = 0.01, 0.1, 0.2, 0.5. N = 30, Removed stages <= 2 minutes, sleep stages not combined.

Combination of sleep stages:

The multivariable chart (Figure 3.10) shows clearly that the combination of sleep stages S3+S4 weakens the correlation in most datasets, whereas the method of combining Wk+REM, S1+S2, S3+S4 improves most of them. It has to be considered that there is a loss of information when combining different sleep stages.

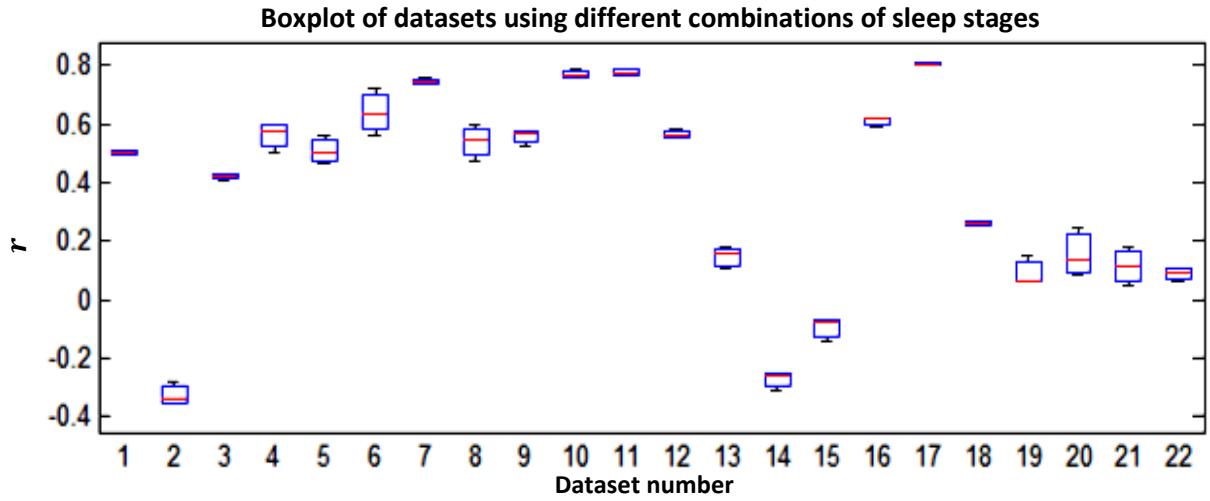

Figure 3.9: Box plot of 22 datasets using different combinations of sleep stages: Not combined, S3+S4, Wake + REM S1+S2 S3+S4. N = 30, Wn = 0.01, removed stages <= 2 minutes

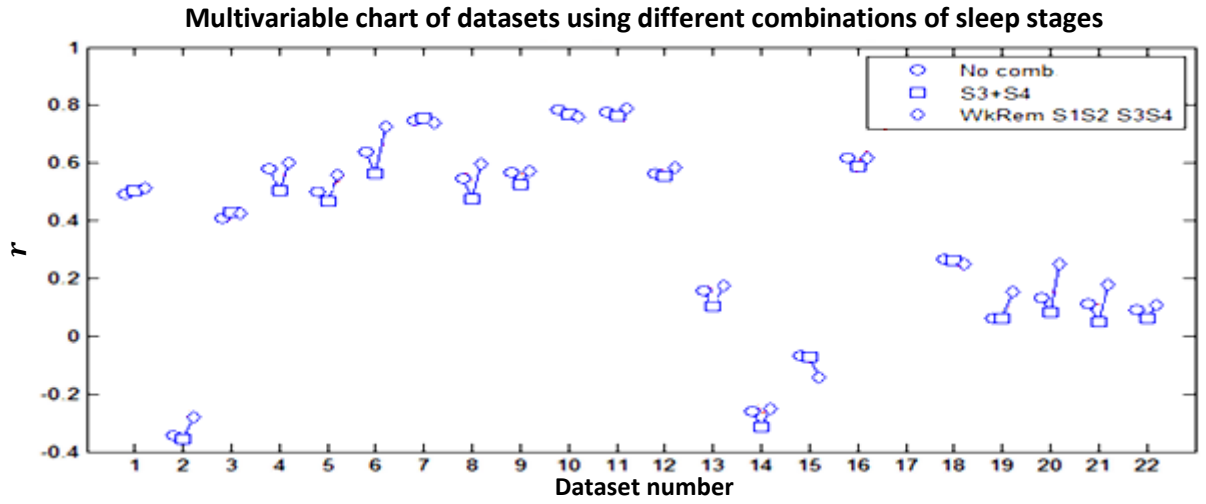

Figure 3.10: Multivariable chart of 22 datasets using different combinations of sleep stages: Not combined, S3+S4, Wake + REM S1+S2 S3+S4. N = 30, Wn = 0.01, removed stages <= 2 minutes

Removal sleep stages of duration

The box plot shows that there is no significant change of the correlation between somnograms and our HRV based sleep estimation (Figure 3.11). Only one dataset experiences a slightly better correlation by removing sleep stages of duration shorter or equal to three minutes (Figure 3.12).

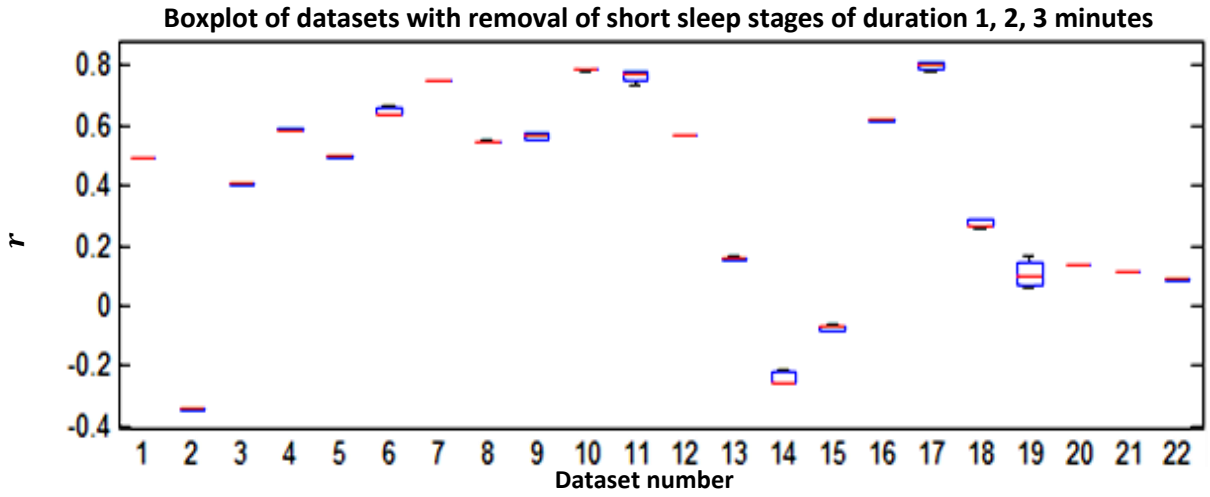

Figure 3.11: Box plot of 22 datasets with removal of short sleep stages of duration 1, 2 and 3 minutes. N = 30, Wn = 0.01, sleep stages not combined

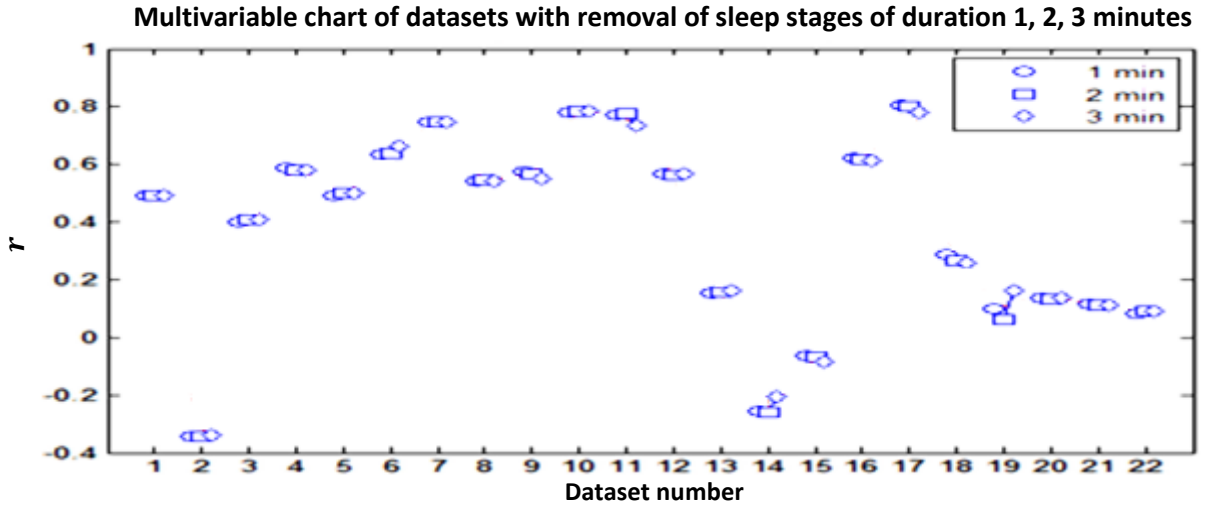

Figure 3.12: Multivariable chart of 22 datasets with removal of short sleep stages of duration 1, 2 and 3 minutes. N = 30, Wn = 0.01, sleep stages not combined

Different Inversion methods:

$$f^{t}_{Winv} = f^{t}_{W} * (-1) \qquad (3.1)$$

$$f^{t}_{Winv} = \frac{1}{f^{t}_{W}} \qquad (3.2)$$

In most cases the negation of f^{t}_{W} (equation 3.1) worked better than the inversion method in equation 3.2. (Figure 3.14)

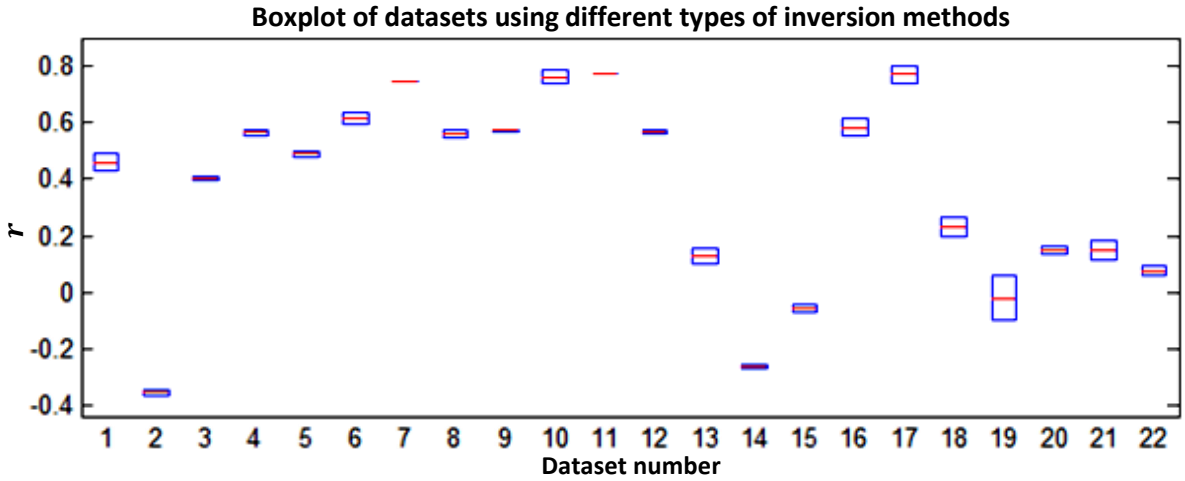

Figure 3.13: Box plot of 22 datasets using different types of inversion methods: $f^{t}_{Winv} = f^{t}_{W} * (-1)$ and $f^{t}_{Winv} = 1/f^{t}_{W}$. N = 30, Wn = 0.01, sleep stages not combined, removed stages <= 2 minutes

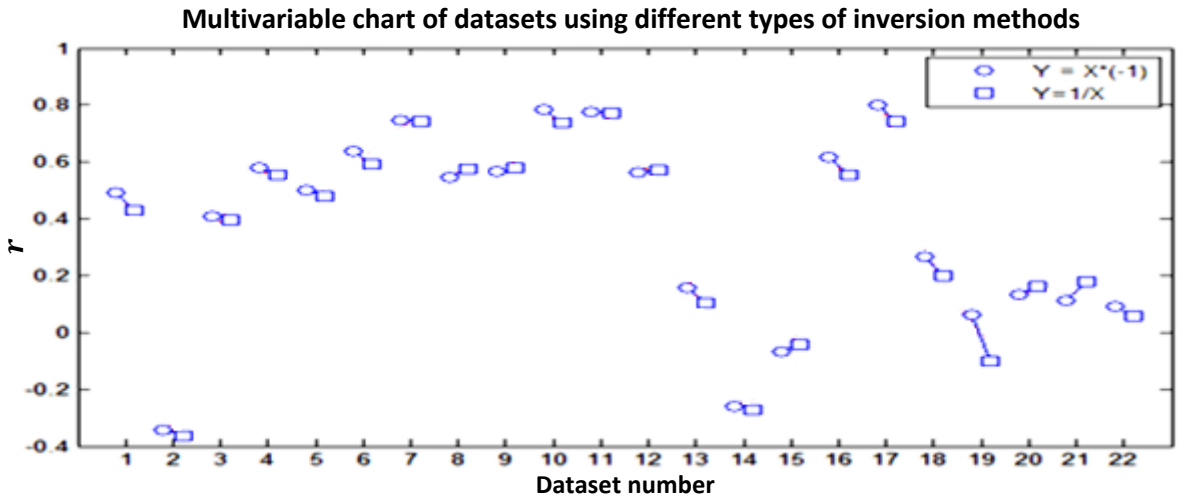

Figure 3.14: Multivariable chart of 22 datasets using different types of inversion methods: $f^{t}_{Winv} = f^{t}_{W} * (-1)$ and $f^{t}_{Winv} = 1/f^{t}_{W}$. N = 30, Wn = 0.01, sleep stages not combined, removed stages <= 2 minutes

3.1.2. Good versus weak correlations

After evaluating the different parameters we chose to use a filter order of $N = 30$, a cut-off frequency of $Wn = 0.01$, removal of sleep stages <= 2 minutes and no combination of sleep stages in order to achieve high correlations and not lose too much detail of our signals. A lot of HRV datasets showed a really good correlation with their corresponding somnograms recorded by conventional PSG. (Figure 3.15) It seemed like our HRV based sleep evaluation worked especially well with semi-periodic somnograms.

Examples of good correlations:

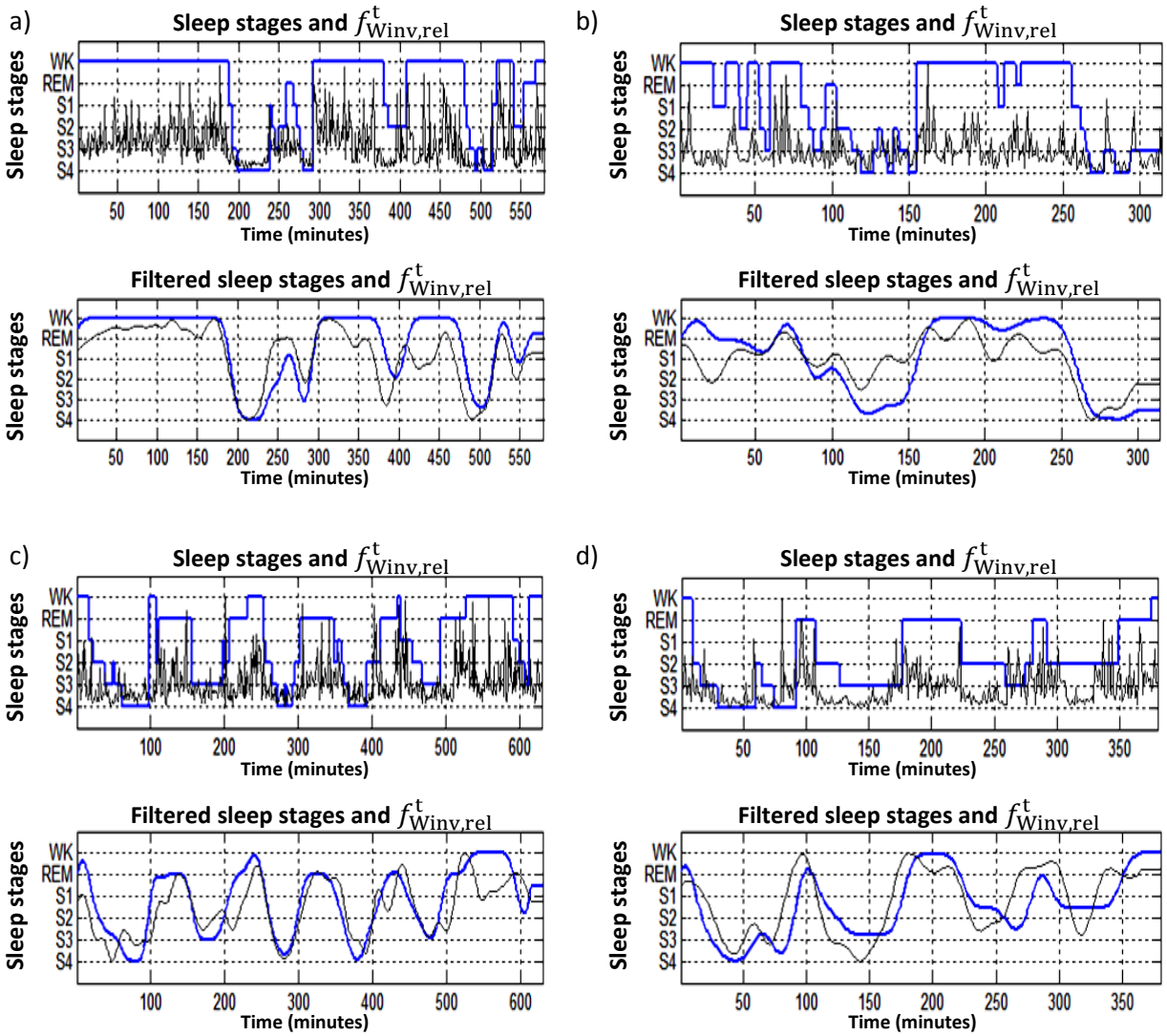

Figure 3.15: Examples of datasets with high cross-correlation coefficients of a) $r = 0.8298$ *(Dataset nr. 17) b)* $r = 0.77579$ *(Dataset nr.11) c)* $r = 0.78582$ *(Dataset nr. 10) and d)* $r = 0.7473$ *(Dataset nr. 7). The parameters we chose were: N* = 30, Wn = 0.01, removal of sleep stages <= 2 minutes and no combination of sleep stages.

Examples of weak correlations:

There were also some somnograms which did not correlate very well at all with our sleep prediction method. (Figure 3.16) Most of them were either fragmented, or did not have a lot of sleep phases with long periods of being awake.

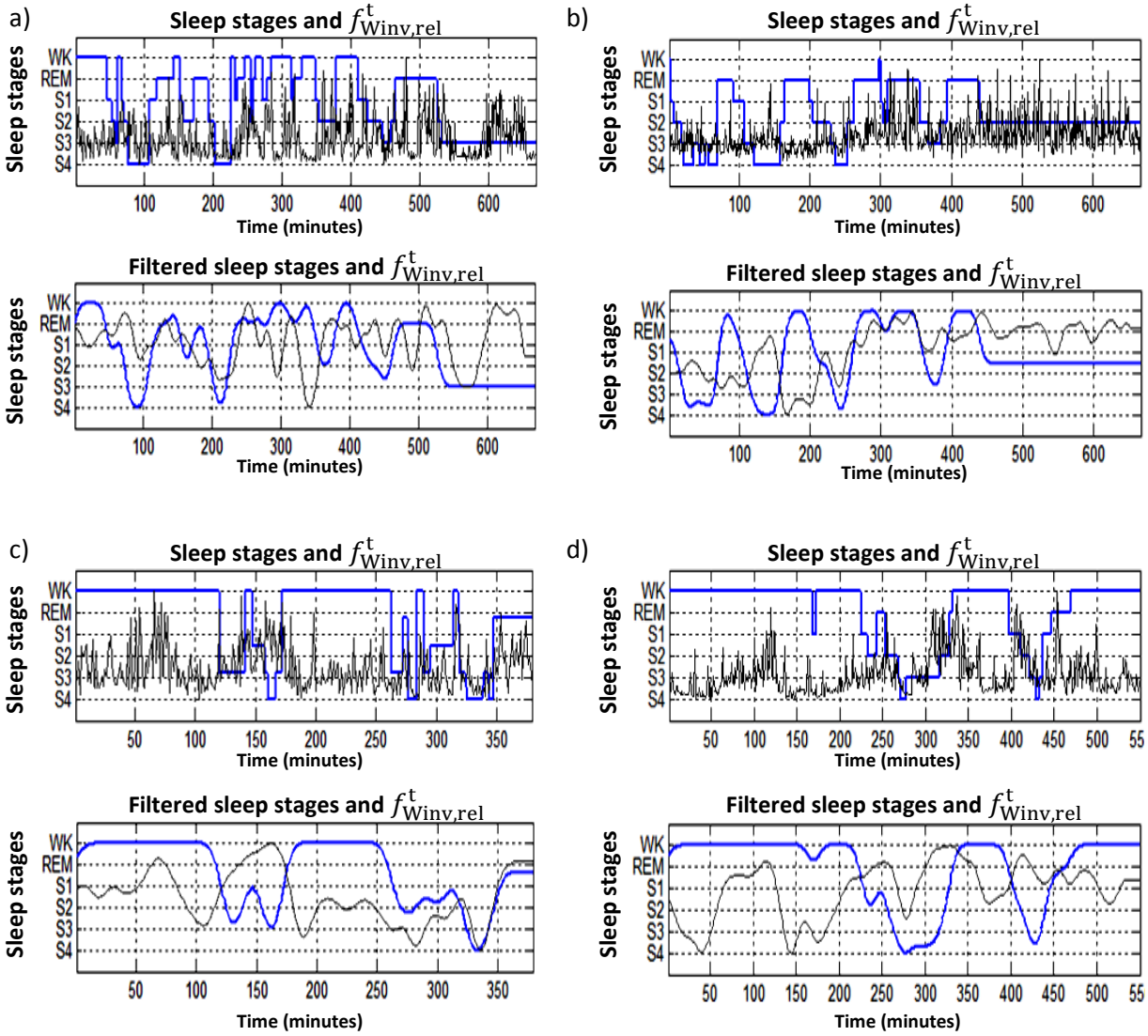

Figure 3.16: Examples of datasets with low (around zero) cross-correlation coefficients a) $r = 0.091562$ *(Dataset nr. 22) b)* $r = 0.1132$ *(Dataset nr. 21) c)* $r = 0.059796$ *(Dataset nr. 19) and d)* $r = -0.34408$ *(Dataset nr. 2). The parameters we chose were:* N = 30, Wn = 0.01, removal of sleep stages <= 2 minutes and no combination of sleep stages.

3.1.3. Association with pathologic conditions

After examining our results we tried to determine which datasets showed good correlations and which ones did not correlate very well. Datasesets 7 to 11 originated from healthy subjects. Subject 12 was suffering from sleep apnea and the rest of the datasets were suffering from insomnia. Healthy subjects showed relatively high correlations (about 0.6 to 0.8) while subjects with insomnia showed mixed results (good correlations, no correlations and negative correlations). (Figure 3.17)

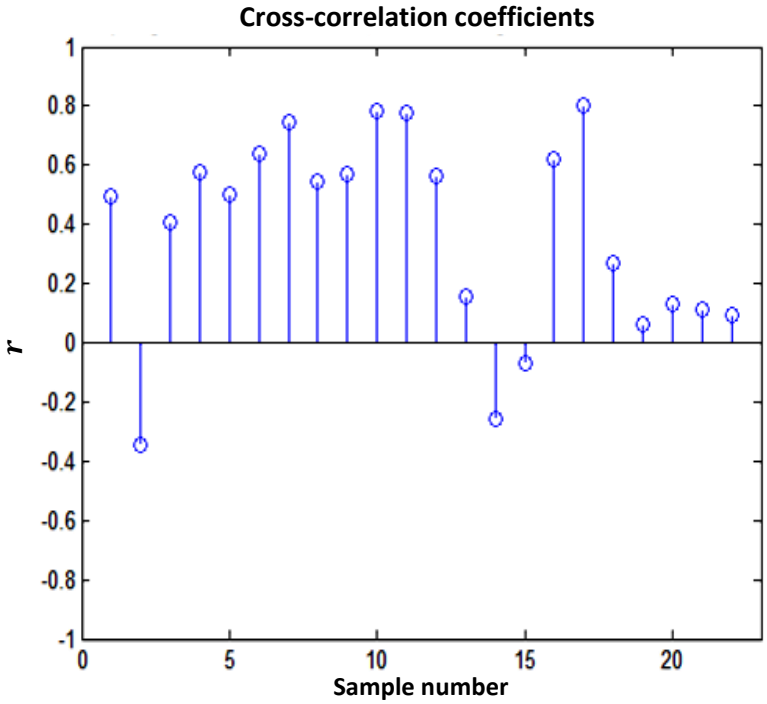

Figure 3.17: Comparison of cross-correlation coefficients of different datasets. The parameters we used were: No combination of sleep stages, removed sleep stages <= 2 minutes, $Wn = 0.01$ *and* $N = 30$

3. 2. Influence of ECG preprocessing on the results

In order to ensure a good R-peak detection the raw ECG Signals had to be filtered. When filtering a signal it is possible that the R-peaks are subjected to a certain amount of delay depending on the filter parameters. To gain knowledge about how ECG preprocessing influences our output signal we made a comparison between our filtered signal and its unfiltered counterpart. (Figure 3.18)

For the removal of the baseline drift we used a moving average filter. We compared the timing of R-peaks of the raw signal to the signal with removed baseline drift. The peaks showed no signs of delay. To filter out the noise we used a Butterworth filter with a filter order N = 2 and a cut-off frequency of Wn = 0.025. As example we used a dataset which was not too noisy in order to still ensure a good R-peak detection. Both datasets were corrected manually after automated R-peak detection:

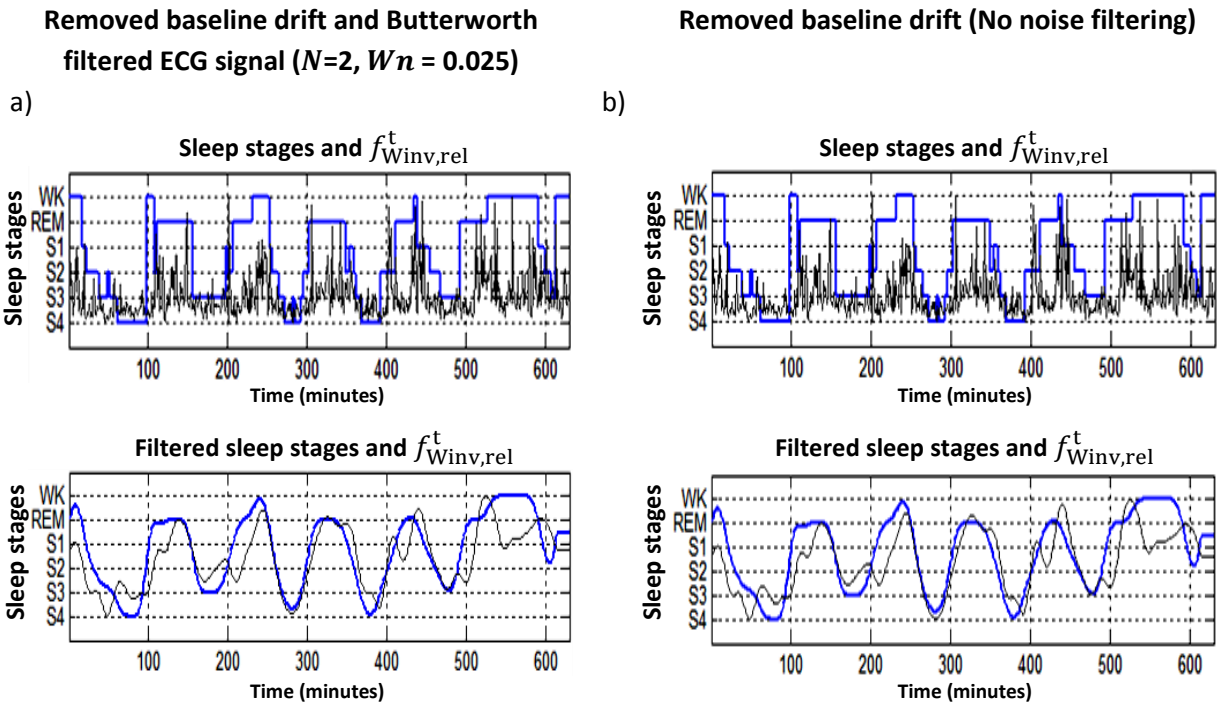

Figure 3.18: Comparison sleep stages and $f^{t}_{Winv,rel}$ originating from filtered and unfiltered ECG data. Unfiltered sleep stages and $f^{t}_{Winv,rel}$ can be seen on top, while our filtered results can be seen on the bottom. (Dataset nr. 10)

One peak is slightly higher, but that can be related to small differences of the R-peak detection or the manual correction. The overall signal and the cross-correlation coefficients did not change significantly (Filtered ECG: $r = 0.78582$, Unfiltered ECG: $r = 0.78367$) and so we concluded that the ECG preprocessing methods we used did not significantly influence our results.

4. Conclusions

Sleep is an important topic in the lives of human beings because it is necessary for survival. Other than its general known function of revitalizing the human body sleep can also be associated with various pathologic conditions. The standard method of evaluating sleep quality is PSG. Due to the use of multiple recording devices it is not accessible for everybody and has to be performed in a highly technical, medical environment. It is desirable to reduce the amount of applied devices in order to gain accessibility. There is a close relation between HRV and activity of the ANS, especially during sleep when ambient factors do not dominate. Therefore it might be possible to evaluate sleep using HRV as reflection of the human brain. Our goal was to asses a new method to estimate different sleep stages by using ECG as a single biosignal instead of the multiparametric analysis of the traditional PSG in order simplify the process of sleep evaluation.

For our analysis we compared somnograms of 22 datasets recorded by PSG with our HRV based sleep estimation. As method we used spectrum weighted mean frequencies of the total spectrum of HRV to estimate different stages of sleep. Our results showed that the HRV-based sleep estimation provides a better sleep prediction in semi-periodic somnograms than fragmented somnograms. The combination of sleep stages (Wake+REM, S1+S2, S3+S4) seems to improve the HRV-based estimation of somnograms, whereas the combination of only S3+S4 seems to weaken this estimation in most cases. The removal of sleep stages with the duration of only a few minutes does not seem to alter our results significantly. We found that the negation of the weighted mean frequency ($-f_w^t$) tends to yield better sleep prediction than its inversion ($1/f_{\mathrm{W}}^{\mathrm{t}}$). We also show that ECG preprocessing methods we used do not significantly influence our results.

We conclude that HRV can be used to assess sleep quality in many cases, especially in rather healthy somnograms. However, further research is needed to improve sleep prediction in fragmented somnograms.

5. Literature

[1] E. Kaniusas, „Biomedical Signals and Sensors 1: Linking Physiological Phenomena and Biosignals," *Springer-Verlag,* 2012.

[2] E. Kaniusas, A. Podlipskyte, A. Alonderis und G. Varoneckas, „Relation in-between autonomic cardiovascular control and central nervous system activity during sleep using spectrum-weighted frequencies," *Vibromechanika. Journal of Vibroengineering,* 2010.

[3] P. E. Inc., „http://droualb.faculty.mjc.edu," Pearson Education Inc. , [Online]. Available: http://droualb.faculty.mjc.edu/Course%20Materials/Physiology%20101/Chapter%20Notes/Fall%202011/chapter_13%20Fall%202011.htm.

[4] H. M., „Wikipedia - Electrical conduction system of the heart," [Online]. Available: http://en.wikipedia.org/wiki/File:Electrical_conduction_system_of_the_heart.svg.

[5] A. Atkielsky, „Wikipedia - QRS," [Online]. Available: http://en.wikipedia.org/wiki/QRS.

[6] G. Krstacic, A. Krstacic, M. Martinis, E. Vargovic, A. Knezevic, A. Smalcelj, M. Jembrek-Gostovic, D. Gamberger und T. Smuc, „Non-linear analysis of heart rate variability in patients with coronary heart disease," *Computers in Cardiology,* pp. 673-675, 2002.

[7] V. Tuzcu, S. Nas, T. Börklü und A. Ugur, „Decrease in the heart rate complexity prior to the onset of atrial fibrillation," *Europace ,* pp. 398-402, 2006.

[8] S. C. Malpas, „Neural influences on cardiovascular variability: possibibilities and pitfalls," *American Journal of Physiology,* pp. H6-H20, 2002.

[9] M. V. Kamath, M. A. Watanabe und A. R. Upton, Heart Rate Variability (HRV) Signal Analysis: Clinical Applications, CRC Press Taylor & Francis Group, 2012.

[10] Task Force of the European Society of Cardiology and the North American Society of Pacing and Electrophysiology, „Heart rate variability. Standards of measurement, physiological interpretation, and clinical use.," *European Heart Journal,* 17 March 1996.

[11] A. J. Seely und P. T. Macklem, „Complex systems and the technology of variability analysis," *Critical Cre,* pp. R367-R384, 2004.

[12] U. R. Acharya, K. P. Joseph, N. Kannathal, C. M. Lim und J. S. Suri, „Heart rate variability: a review," *International Federation for Medical and Biological Engineering,* November 2006.

[13] R. Furlan, S. Guzzetti, W. Crivellaro, S. Dassi, M. Tinelli, G. Baselli, S. Cerutti, F. Lombardi, M. Pagani und A. Malliani, „Continous 24-hour assessment of the neural regulation of systemic arterial ressure and RR variabilities in ambulant subjects," *Circulation,* pp. 537-547, 1990.

[14] J. Wijbenga, A. Balk, S. Meij, M. Simoons und M. Malik, „Heart rate variability index in

congestive heart failure: relation to clinical variables and prognosis," *European Heart Journal,* pp. 1719-1724, 1998.

[15] A. C.-C. Yang, „Poincare Plots: A Mini-Review," http://www.physionet.org/events/hrv-2006/yang.pdf, 2006.

[16] M. Brennan, M. Palaniswami und P. Kamen, „Do Existing Measures of Poincare Plot Geometry Reflect Nonlinear Features of Heart Rate Variability?," *IEEE TRANSACTIONS ON BIOMEDICAL ENGINEERING, VOL. 48, NO. 11,,* pp. 1342-1347, 2001.

[17] A. Voss, S. Schulz, R. Schroeder, M. Baumert und P. Caminal, „Methods derived from nonlinear dynamics for analysing heart rate variability," *Philosophical Transactions of the Royal Society A: Mathematical, Physical and Engineering Sciences,* pp. 277-296, 2009.

[18] S. Balanescu, A. Corlan, M. Dorobantu und L. Gherasim, „Prognostic value of heart rate variability after acute myocardial infarction," *Medical Science Monitor,* pp. 307-315, 2004.

[19] A. Sajadieh, O. W. Nielsen, V. Rasmussen, H. O. Hein, S. Abedini und J. F. Hansen, „Increased heart rate and reduced heart-rate variability are associated with subclinical inflammation in middle-aged and elderly subjects with no apparent heart disease," *European Heart Journal,* 2003.

[20] R. M. Carney, R. D. Saunders, K. E. Freedland, P. Stein, M. W. Rich und A. S. Jaffe, „Association of depression with reduced heart rate variability in coronary artery disease," *The American Journal of Cardiology,* pp. 562-564, September 1995.

[21] D. Chamchad, H. Djaiani, H. Jung, L. Nakhamchik, J. Carroll und J. C. Horrow, „Nonlinear heart rate variability analysis may predict atrial fibrillation after coronary artery bypass grafting.," *International Anesthesia Research Society,* pp. 1109-1112, November 2006.

[22] D. D. McManus, J. Lee, O. Maitas, N. Esa, R. Pidikiti, A. Carlucci, J. Harrington, E. Mick und K. H. Chon, „A novel application for the detection of an irregular pulse using an iPhone 4S in patients with atrial fibrillation," *Heart Rhythm,* pp. 315-319, March 2013.

[23] R. Carney, K. Freedland, P. Stein, J. Skala, P. Hoffman und A. Jaffe, „Change in Heart Rate and Heart Rate Variability during treatment for depression in patiens with coronary heart disease," *Psychosomatic medicine,* pp. 639-647, September 2000.

[24] P. Mork, J. Nilsson, H. Loras, R. Riva, U. Lundberg und R. Westgaard, „Heart rate variability in fibromyalgia patients and healthy controls during non-REM and REM sleep: a case-control study," *Scandinavian Journal of Rheumatology,* 2013.

[25] F. Rieke, W. Bialek und D. Warland, „Spikes: Exploring the Neural Code".*Computational Neuroscience.*

[26] S. Guzzetti, S. Mezzetti, R. Magatelli, A. Porta, G. De Angelis, G. Rovelli und A. Malliani, „Linear and non-linear 24 h heart rate variability in chronic heart failure," *Autonomic Neuroscience:*

Basic and Clinical, pp. 114-119, 2000.

[27] S. Axelrod, M. Lishner, O. Oz, J. Bernheim und M. Ravid, „Spectral analysis of fluctuations in heart rate: an objective evaluation of autonomic nervous control in chronic renal failure," *Nephron,* 1987.

[28] D. Toweill, W. Kovarik, R. Carr, D. Kaplan, S. Lai, S. Bratton und B. Goldstein, „Linear and nonlinear analysis of heart rate variability during propofol anesthesia for short-duration procedures in children," *Pedriatric Critical Care Med,* July 2003.

[29] L. C. M. Vanderlei, C. M. Pastre, I. F. Freitas Junior und M. F. de Godoy, „Geometric Indexes of Heart Rate Variability in Obese and Eutrophic Children," *Sociedae Brasileira de Cardiologia,* November 2009.

[30] S. Tale und T. Sontakke, „Time-Frequency Analysis of heart Rate Variability Signal in prognosis of Type 2 Diabetic Autonomic Neuropathy," *International Conference on Biomedical Engineering and Technology,* 2011.

[31] M. Woo, W. Stevenson, D. Moser, R. Trelease und R. Harper, „Patterns of beat-to-beat heart rate variability in advanced heart failure," *Am Heart J,* pp. 123:704-707, 1992.

[32] P. Kamen, H. Krum und A. Tonkin, „Application of the Poincare plot to heart rate variability: A new measure of functional status in heart failure," *Aust NZ J Med,* pp. 25: 18-26, 1995.

[33] J. Piskorsky und J. Guzik, „Filtering Poincare plots," *Computational Methods in Science and Technology 11,* pp. 39-48, 2005.

[34] T. T. Laitio, T. H. Mäkikallio, H. V. Huikuri, E. S. Kentala, P. Uotila, J. R. Jalonen, H. Helenius, J. Hartiala, S. Yli-Mäyry und H. Scheinin, „Relation of heart rate dynamics to the occurrence of myocardial ischemia after coronary artery bypass grafting," *American Journal of Cardiology,* pp. 1176-1181, 2002.

[35] C. K. Karmakar, A. H. Khandoker, J. Gubbi und M. Palaniswami, „Complex Correlation Measure: a novel descriptor for Poincaré plot," *BioMed Eng OnLine (BioMedical Engineering OnLine),* p. 17, 2009.

[36] L. Mourot, M. Bouhaddi, S. Perrey, J.-D. Rouillon und J. Regnard, „Quantitative Poincare plot analysis of heart rate variability: effect of endurance training," *European Journal of Applied Physiology,* pp. 79-87, 2004.

[37] U. Acharya, N. Kannathal, O. Sing, L. Ping und T. Chua, „Heart rate analysis in normal subjects of various age groups," *BioMedical Engineering OnLine,* July 2004.

[38] I. Korhonen, L. Mainardi, H. Yppärilä und T. Musialowicz, „Comparison of linear and non-linear analysis of heart rate variability in sedated cardiac surgery patients," *Engineering in Medicine and Biology Society, 2001. Proceedings of the 23rd Annual EMBS International Conference of the*

IEEE, pp. 496-499, 2001.

[39] K. K. Kim, Y. Baek und K. Park, „Effect of missing RR-interval data on nonlinear heart rate variability analysis," *ComputMethodsProgramsBiomed (Computer methods and programs in biomedicine),* pp. 210-218, 2012.

[40] C. K. Peng, S. Havlin, H. E. Stanley und A. L. Goldberger, „Quantification of scaling exponents and crossover phenomena in nonstationary heartbeat time series," *Chaos (Woodbury, N.Y.), vol. 5,* pp. 82-87, 1995.

[41] R.-G. Yeh, J.-S. Shieh, Y.-Y. Han, Y.-J. Wang und S.-C. Tseng, „Detrended fluctuation analyses of short-term heart rate variability in surgical intensive care units," *Biomedical Engineering: Applications, Basis and Communications,* 2006.

[42] K. Vibe, J.-M. Vesin und E. Pruvot, „Chaos and heart rate variability," *Engineering in Medicine and Biology Society,* pp. 1481-1482, 1995.

[43] M. Rosenstein, J. Collins und C. Luca, „A practical method for calculating largest Lyapunov exponents from small data sets," *Physica D 65,* pp. 117-134, 1993.

[44] M. G. Signorini, R. Sassi, F. Lombardi und S. Cerutti, „Regularity patterns in heart rate variability signal: The approximate entropy approach," *Proceedings of the 20th Annual International Conference of the IEEE Engineering in Medicine and Biology Society Vol. 20, No 1,* 1998.

[45] H. M. Al-Angari und A. V. Sahakian, „Use of Sample entropy Approach to Study Heart Rate Variability in Obstructive Sleep Apnea Syndrome," *IEEE Transactions on Biomedical Engineering Vol. 54 No. 10,* 2007.

[46] S. Pincus, „Assessing serial irregularity and its implications for health.," *Annals New York Academy of Sciences,* pp. 954:245-267, 2001.

[47] R. K. Sunkaria, „Recent Trends in Nonlinear Methods of HRV Analysis: A Review," *World Academy of Scieence, Engineering and Technology 51,* 2011.

[48] M. Costa, A. L. Goldberger und C.-K. Peng, „Multiscale entropy analysis of biological signals," *The American Physical Society Phys. Rev. E,* 2005.

[49] M. Costa, A. L. Goldberger und C.-K. Peng, „Multiscale Entropy Analysis of Complex Physiologic Time Series," *Comput. Cardiol. vol 29,* pp. 137-140, 2002.

[50] Z. Trunkvalterova, M. Javorka, I. Tonhajzerova, J. Javorkova, Z. Lazarova, K. Javorka und M. Baumert, „Reduced short-term complexity of heart rate and blood pressure dynamics in patients with diabetes mellitus type 1: multiscale entropy analysis," *Physiological Measurement volume 29 Nr. 7,* pp. 817-828, 2008.

[51] N. Mahon, A. Hedman, M. Padula, Y. Gang, I. Savelieva, J. Waktare, M. Malik, H. Huikuri und W. McKenna, „Fractal correlation properties of R-R interval dynamics in asymptomatic relatives of

patients with dilated cardiomyopathy," *European Journal of Heart Failure,* pp. 151-158, 2002.

[52] T. Penzel, J. Kantelhardt, L. Grote, J. Peter und A. Bunde, „Comparison of detrended fluctuation analysis and spectral analysis for heart rate variability in sleep and sleep apnea," *IEEE Trans. Biomed. Eng. (IEEE Transactions on Biomedical Engineering),* p. 1143–1151, 2003.

[53] R.-G. Yeh, J.-S. Shieh, G.-Y. Chen und C.-D. Kuo, „Detrended fluctuation analysis of short-term heart rate variability in late pregnant women," *Autonomic Neuroscience,* p. 122–126, 2009.

[54] M. Gomes, H. Guimaraes, A. Ribeiro und L. Aguirre, „Does preprocessing change nonlinear measures of heart rate variability?," *Computers in biology and medicine,* pp. 481-494, 2002.

[55] J. Valencia, M. Vallverdu, R. Schroeder, A. Voss, I. Cyganiewicz, R. Vasques, A. Luna und P. Caminal, „Detrended fluctuation analysis of heart rate by means of symbolic series," *Computers in Cardiology,* pp. 405-408, 2009.

[56] M. Owis, A. Abou-Zied, A. Youssef und Y. Kadah, „Study of Features Based on Nonlinear Dynamical Modeling in ECG Arrhythmia Detection and Classification," *Biomedical Engineering, IEEE Transactions on,* pp. 733-736, 2002.

[57] A. Wolf, J. Swift, L. Swinney und J. Vastano, „Determining Lyapunov exponent from a time series," *Physica D,* pp. 285-317, 1985.

[58] E. Übeyli und G. Inan, „Detection of electrocardiographic changes in partial epileptic patients using Lyapunov exponents with multilayer perceptron neural networks," *Engineering Applications of Artifical Intelligence,* pp. 567-576, 2004.

[59] A. Das, P. Das und A. Roy, „Aplicability of Lyapunov Exponent in EEG Data Analysis," *Complexity International,* 2002.

[60] G. Valenza, P. Allegrini, A. Lanata und E. Scilingo, „Dominant Lyapunov exponent and approximate entropy in heart rate variability during emotional visual elicitation," *Frontiers in Neuroengineering,* 2012.

[61] D. Yilmaz und M. Yildiz, „Analysis of the Mobile Phone Effect on the Heart Rate Variability by Using the Largest Lyapunov Exponent," *Journal of Medical Systems,* pp. 1097-1103, 2010.

[62] F. Selig, E. Tonolli, E. Silva und M. Godoy, „Heart rate variability in Preterm and Term Neonates," *Arq. Bros. Cardiol. vol. 96 no.6,* 2011.

[63] V. Yeragani, K. Rao, R. Smintha, R. B. Pohl, R. Balon und K. Srinivasan, „Diminished Chaos of Heart Rate Time Series in Patients with Major Depression," *Biological Psychiatry Volume 51,* 2002.

[64] R. Acharya, N. Kannathal und S. M. Krishnan, „Comprehensive analysis of cardiac health using heart rate signals," *Physiol. Meas. (Physiological Measurement),* p. 1139–1151, 2004.

[65] J. Hu, J. Gao und W.-w. Tung, „Characterizing heart rate variability by scale-dependent Lyapunov exponent," *American Institute of Physics,* 2009.

[66] S. Pincus, „Approximate entropy as a measure of system complexity," *Proc. Natl Acad. Sci.,* 1991.

[67] Z.-D. Deng, C.-S. Poon, N. M. Arzeno und E. Katz, „Heart Rate Variability in Pediatric Obstructive Sleep Apnea," *Proceedings of the 28th IEEE EMBS Annual International Conference,* 2006.

[68] S. M. Pikkujamsa, T. H. Makikallio, L. B. Sourander, I. J. Raiha, P. Puukka, J. Skytta, C.-K. Peng, A. L. Goldberger und H. V. Huikuri, „Cardiac Interbeat Interval Dynamics From Childhood to Senescence: Comparison of conventional and New Measures Based on Fractals and Chaos Theory," *American Heart Association,* 1999.

[69] J. Perkiömäki, Z. W, R. J, D. S, M. C, D. P, K. M und A. Bayes de Luna, „Fractal and complexity measures of heart rate dynamics after acute myocardial infarction," *The American Journal of Cardiology,* pp. 777-781, 2001.

[70] A. Kamal, „Assessment of autonomic function in patients with rheumatoid arthritis using spectral analysis and approximate entropy method," *Neurosciences Vol.12(2),* pp. 136-139, 2007.

[71] J. S. Richman und J. R. Moorman, „Physiological time-series analysis using approximate entropy and sample entropy," *American Journal of Physiology - Heart and Circulatory Physiology,* 2000.

[72] S. Lu, X. Chen, J. Kanters, I. Solomon und K. Chon, „Automatic selection of the threshhold value R for approximate entropy," *IEEE Trans Biomed Eng,* 2008.

[73] P. Castiglioni und M. Die Rienzo, „How the Threshold "R" Influences Approximate Entropy Analysis of Heart-Rate Variability," *Computers in Cardiology,* pp. 35:561-564, 2008.

[74] R. Goya Esteban und J. L. R. Alvarez, „Heart Rate Variability Characterization Using Entropy Measures," *Universidade do Porto,* 2008.

[75] V. Tuzcu und S. Nas, „Sample entropy analysis of heart rhythm following cardiac transplantation," *Systems, Man and Cybernetics 2005 IEEE International Conference,* pp. 198-202, 2005.

[76] R. Goya-Esteban, J. Marques de Sa, J. Rojo-Alvarez und O. Barquero-Perez, „Characterization of Heart Rate Variability Loss with Aging and Heart Failure Using Sample Entropy," *Computers in Cardiology,* pp. 35:41-44, 2008.

[77] A. H. Khandoker, H. F. Jelinek und M. Palaniswami, „Identifying diabetic patients with cardiac autonomic neuropathy by heart rate complexity analysis," *Biomedical Engineering Online,* 2009.

[78] M. Costa, P. C.-K, A. L. Goldberger und J. M. Hausdorff, „Multiscale entropy analysis of human gait dynamics.," *Physica A,* pp. 53-60, 2003.

[79] E. Tejera, J. Nieto-Villar und I. Rebelo, „Unexpected heart rate variability complexity in the aging process of arrhytmic subjects," *Communications in Nonlinear Science and Numerical Simulation,* pp. 1858-1863, 2010.

[80] P. R. Norris, S. M. Anderson, J. M. Jenkins, A. E. Williams und J. A. Morris, „HEART RATE MULTISCALE ENTROPY AT THREE HOURS PREDICTS HOSPITAL MORTALITY IN 3,154 TRAUMA PATIENTS," *Shock Inury, Inflammation, and Sepsis: Laboratory and Clinical Approaches,* pp. 27-22, 2008.

[81] M. Ferrario, M. Signorini, G. Magenes und S. Cerutti, „Comparison of Entropy-Based Regularity Estimators: Application to the Fetal Heart Rate Signal for the Identification of Fetal Distress," *Biomedical Engineering, IEEE Transactions on,* pp. 119-125, 2006.

[82] V. Nikulin und T. Brismar, „Comment on multiscale entropy analysis of complex physiologic time series," *Phys. Rev. Lett. vol 92,* 2004.

[83] J. Valencia, A. Porta, M. Vallverdu, F. Claria, R. Baranowski, E. Orlowska-Baranowska und P. Caminal, „Refined Multiscale Entropy: Application to 24-h Holter Recordings of Heart Period Variability in Healthy and Aortic Stenosis Subjects," *IEEE Trans. Biomed. Eng. (IEEE Transactions on Biomedical Engineering),* p. 2202–2213, 2009.

[84] K. Kräuchi, „Physiological review: The thermophysiological cascade leading to sleep initiation in relation to phase of entrainment," *Sleep Medicine Reviews 11,* pp. 439-451, 2007.

[85] A. Rechtschaffen und A. Kales, „A manual of standardized terminology, techniques and scoring system for sleep stages of human subjects," *National Institutes of Health Publication, Bethesda Maryland,* 1968.

[86] C. Iber, A.-I. S, A. Chesson und S. Quan, „The AASM manual for the scoring of sleep and associated events: rules, terminology, and technical specification," *Westchester, IL,* 2007.

[87] D. Moser, P. Anderer, G. Gruber, S. Parapatics, E. Loretz, M. Boeck und G. Kloesch, „Sleep Classification According to AASM and Rechtschaffen & Kales: Effects on Sleep Scoring Parameters," *Sleep,* 2009.

[88] Anonymous, „Wikipedia - sleep disorder," [Online]. Available: http://en.wikipedia.org/wiki/Sleep_disorder.

[89] D. Kripke, L. Garfinkel, D. Wingard, M. Klauber und M. Marler, „Mortality associated with sleep duration and insomnia," *Arch Gen Psychiatry,* 2002.

[90] J. W. Shepard, D. Buysse, A. Chesson, W. Dement, R. Goldberg, C. Guilleminault, C. Harris, C. Iber, E. Mignot, M. Mitler, K. Moore, B. Phillips, S. Quan, R. Rosenberg und T. Roth, „History of the Development of Sleep Medicine in the United States," *J Clin Sleep Med,* pp. 61-82, Janury 2005.

[91] H. Gastaut, C. Tassinari und B. Duron, „Polygraphic study of the episodic diurnal and nocturnal (hypnic and respiratory) manifestations of the Pickwickian syndrome," *Brain Res,* 1965.